THESIS APPROVAL

GRADUATE SCHOOL, KASETSART UNIVERSITY

Doctor of Philosophy (Food Science)

DEGREE

Food Science | Food Science and Technology

FIELD | **DEPARTMENT**

TITLE: Structure-Forming Processes of Solidified Physically Refined Rice Bran Oil

NAME: Miss Natchanok Nukit

THIS THESIS HAS BEEN ACCEPTED BY

(Associate Professor Parichat Hongsprabhas, Ph.D.) **THESIS ADVISOR**

(Associate Professor Siree Chaiseri, Ph.D.) **THESIS CO-ADVISOR**

(Assistant Professor Masubon Thongngam, Ph.D.) **THESIS CO-ADVISOR**

(Professor Jochen Weiss, Ph.D.) **THESIS CO-ADVISOR**

(Assistant Professor Wannee Jirapakkul, Ph.D.) **DEPARTMENT HEAD**

APPROVED BY THE GRADUATE SCHOOL ON _____

(Associate Professor Gunjana Theeragool, D.Agr.) **DEAN**

THESIS

STRUCTURE-FORMING PROCESSES OF SOLIDIFIED PHYSICALLY REFINED RICE BRAN OIL

NATCHANOK NUKIT

A Thesis Submitted in Partial Fulfillment of
the Requirements for the Degree of
Doctor of Philosophy (Food Science)
Graduate School, Kasetsart University
2014

Natchanok Nukit 2014: Structure-Forming Processes of Solidified Physically Refined Rice Bran Oil. Doctor of Philosophy (Food Science), Major Field: Food Science, Department of Food Science and Technology. Thesis Advisor: Associate Professor Parichat Hongsprabhas, Ph.D. 127 pages.

This research investigated the characteristics of solidified rice bran oil (RBO) using different oleogelators, namely high-temperature melting fat, self-assembled surfactants and carbohydrate polymers. The RBO oleogel could hold liquid oil phase at the temperature above melting temperature of RBO (-)30 - 5 °C up to 90 °C depending on the oleogelators used and proper aging process. Using commercial mono, di-acylglycerol (MDG) (mainly palmitic esterified) and crude wax as the source of rice bran wax (RBW) could stabilize the structure of RBO-RBW oleogel at 22 °C for more than 24 h. The mechanisms involved in stabilizing gel network were due to the ability of self-assembled of commercial MDG as well as fat crystal network of RBW, which resulted in the increased storage modulus, the increased viscoelastic transition temperature and the prolonged time for gel to change from elastic to viscous behavior. The ethyl cellulose (EC) network, however, could stabilize RBO-EC oleogel due to interactions between polymer and RBO to form of three-dimensional network. Raising concentration of EC from 2.5 to 3.25% increased storage modulus of RBO-EC oleogel. Such RBO-EC and RBO-RBW-EC oleogels could retain RBO and spices when the gel was used as pork marinade at 2 °C for 2 days by preventing salt and spice sedimentation. The RBO-EC and RBO-RBW-EC oleogels could withstand the temperature at 90 °C and further prevented sedimentation of salt and spices. Overall, the insights in the roles of different oleogelators in the formation of physically refined RBO oleogel could help forming solidified lipid structure holding liquid oil between 22 to 90 °C.

_____ _____ ___/___/___

Student's signature Thesis Advisor's signature

ACKNOWLEDGEMENTS

It would not have been possible to write this doctoral thesis without the help and support of the kind people around me, to only some of whom it is possible to give particular mention here. Firstly, I would like to express the deepest appreciation to my thesis advisor, Associate Professor Parichat Hongsprabhas who gave her time, talents and specialized knowledge to advise me. She has high patience for practice me in regard to research. Without her guidance and persistent help this dissertation would not have been possible. Secondary, I would sincerely like to thank my thesis committee; Associate Professor Siree Chaiseri and Assistant Professor Masubon Thongngam for their suggestions and their good advice. I gratefully thank Professor Jochen Weiss for good supports, advice and help given to me for doing research in Germany. Moreover, I would like to sincerely thank Dr. Monika Gibis and Mr. Kurt Herrmann for helping me to do research and always gave encouragement to me.

I am greatly indebted to Commission on Higher Education for financial supports. I am also greatly indebted to Surin Bran Oil Company for kind supports the raw materials and kindness of Mr. Prasert Setwipattanachai and Mrs. Petcharat Setwipattanachai. I would like to thank Department of Food Science and Technology, Faculty of Agro-Industry, Kasetsart University for providing the opportunity to study here. I am grateful to all staff, all my friends and all graduated students for supporting of my research work and gave encouragement to me. In addition, I would like to thank all members of Food Structure and Functionality Laboratories and Thai friends in Germany for taking care of me and the warm welcome when I was in Germany.

Finally, I appreciate my grandmother and my father who always gave encouragement when they were alive and they are always in my mind. I am especially appreciated my mother, my family and Mr. Wutthilers Meeprathom who give me love. They have always supported me and continuing encouragements.

Natchanok Nukit

June 2014

TABLE OF CONTENTS

LIST OF TABLES

LIST OF TABLES (Continued)

LIST OF TABLES (Continued)

LIST OF TABLES (Continued)

LIST OF TABLES (Continued)

LIST OF TABLES (Continued)

LIST OF FIGURES

LIST OF FIGURES (Continued)

LIST OF FIGURES (Continued)

STRUCTURE-FORMING PROCESSES OF SOLIDIFIED PHYSICALLY REFINED RICE BRAN OIL

INTRODUCTION

The structure of many fat products is based on the three-dimensional network of high melting crystalline triacylglycerol hard stock, which provides functional properties such as hardness, viscosity, plasticity, and spreadability to the products. (Roger, 2009; Wassell *et al*., 2010). Unfortunately, the high melting temperature lipids contain saturated and/or *trans* fatty acids, which are related to negative health implications by increasing low density lipoprotein cholesterol, risks of cardiovascular diseases and developing type II diabetes mellitus (Roger, 2009). Many methods have been tried to reduce *trans* fatty acid in fat product including modification of hydrogenation process, interesterification of mixed fats, genetic engineering of oil seeds and fractionation of tropical oils; e.g. coconut oil, palm kernel and palm oil. However, *trans* and saturated fat still remain in fat products and fat-containing food products. Some methods require chemical reactions and may pose health threats for the increase in risks of cardiovascular diseases (Trani *et al*., 2006).

The oleogel is one of the alternative methods in modifying the characteristics of liquid oil to those of hard stock. The oleogel is a bi-continuous colloidal system composed of liquid organic phase and oleogelator (Vazquez *et al*., 2007). The liquid organic phase can be organic solvent, mineral oil, or vegetable oil; while the oleogelator is the lipid-soluble material entrapping bulk liquid organic phase (Dassanayake *et al*., 2011). The structures of oleogel can be divided into 3 groups. The first group is crystal particle of lipid molecule family, such as wax or surfactant having low hydrophile-lipophile-balance (HLB). The second group has been proposed as crystalline fibers, self-assembled fibrillar network (SAFIN) of self-assembled molecules such as phytosterol and oryzanol. The self-assembled fibrillar network can hold the liquid oil within its three-dimensional structure. The last group is defined as polymeric strands of carbohydrate polymer, such as ethyl cellulose (EC),

which can form a network entrapping liquid oil (Roger, 2009; Bruno *et al*., 2011; Marangoni and Garti, 2011).

Rice bran oil (RBO) is considered as nutritious oil that contains many beneficial phytochemicals such as γ-oryzanol, tocotrienols, tocopherols and phytosetrols (Prasad, 2006). RBO contains cholesterol-lowering compounds, particularly phytosterols, which could reduce the risks of coronary heart diseases (Van Hoed *et al*., 2006). They are triterpenes having similar structure as cholesterol (Bot and Agterof, 2006). The γ-oryzanols are antioxidants found in rice and not in other plant sources. They are mixtures of ferulate esters of triterpene alcohol and phytosterols. The major components of γ-oryzanol are cycloartenyl ferulate, 24-methylenecycloartanyl ferulate and campesteryl ferulate (Patel and Naik, 2004).

Edible oil refining processes are classified into 2 categories: chemical and physical refining processes. The main differences between both processes include procedures in removal of free fatty acid (FFAs). Chemical neutralization by caustic soda (NaOH) has been used in chemical refining process. In physical refining, only high-vacuum deodorization step is used to remove the FFAs (Verhe *et al*., 2006). The disadvantage of chemical refining process is the major loss of major bioactive compounds due to removal or being destroyed. Most of minor constituents such as mono, di-acylglycerol, sterols and γ-oryzanol were concentrated in the soapstock after neutralization, which are sold as animal feed in Thailand. However, these phytochemicals are concentrated in deodorizer distillate during physical refining process (Gunawan and Ju, 2009). Physical refining process could retain high phytochemical contents in refined RBO than does chemical refining process. From previous investigation, physically refined RBO contained γ-oryzanol around 0.86% and major phytosterols around 0.89% (Sawadikiat and Hongsprabhas, 2014); while chemically refined RBO contained γ-oryzanol and major phytosterols around 0.25% and 0.86%, respectively (Sawadikiat *et al*., 2014).

Such high contents of γ-oryzanol and phytosterols in RBO may offer the possibility in the formation of nanofibril structure of self-assembled γ-oryzanol and phytosterol holding liquid oil as described by Bot and Agterof (2006) and Bot *et al*. (2008). Sawalha *et al*. (2011) proposed that the oleogels could be formed in the presence of γ-oryzanol and sitosterol at the ratio of 60:40 respectively. Such oleogel could withstand the temperature of 340 K (67 °C). Not only the γ-oryzanol and phytosterol self-assembled structure, rice bran wax (RBW) could also offer crystalline network and the formation of olive oil oleogel due to their high melting point range of 78 -81 °C (Dassanayake *et al*., 2011).

Based on the chemical composition of physically RBO itself, as well as potential use of RBW as oleogelators, the ability to form solidified RBO was investigated. This research hypothesized that the three-dimensional network of complex structure of crystalline fat network, self-assembled amphiphiic molecules, and/or carbohydrate polymers could be formed upon proper aging temperature for RBO containing different oleogelators. The characteristics of oleogel formed by different mechanisms induced by various oleogelators could be designed by choosing the complex structure appropriate for the end uses or applications.

OBJECTIVES

1. To investigate the influences of aging process on thermophysical properties of RBO in the presence of high temperature melting fat, mono, di-acyl glycerol obtained from molecular distillation of RBO deodorizer distillate, in comparison with the commercial surfactant (mainly mono, di-palmityl glycerol),

2. To investigate the influences of rice bran wax (RBW) and commercial surfactants mono, di-acyl glycerol (MDG) and/or sucrose palmitate (SP) on thermo-physical properties of solidified refined RBO at temperature above melting temperature of RBO,

3. To investigate the influence of ethyl cellulose (EC) and RBW concentrations in structure-forming process and rheological behaviors of RBO oleogel, and

4. To explore the potential use of RBO oleogel in pork steak marinade before and after grilling at 260°C.

LITERATURE REVIEW

1. Rice bran oil and its co-products during refining process

1.1 Refining process of rice bran oil

Rice bran oil (RBO) is nutritious oil since it contains many health - promoting components such as γ-oryzanol, tocotrienols, tocopherols, phytosetrols, etc, (Orthoefer, 2005). The γ-oryzanol and phytosterols have ability to lower blood cholesterol by reducing the LDL cholesterol and increasing HDL cholesterol (Patel and Naik, 2004). Therefore, they can prevent the risks of heart diseases. Tocotrienols and tocopherols are vitamin E active compounds and are important antioxidants in body tissue. They could also prevent coronary heart diseases and cancer (Orthoefer, 2005; Prasad, 2006).

The oil refining processes can be divided into 2 methods; i.e. physical refining process and chemical refining process. Physical refining process of crude rice bran oil is composed of five steps. The first refining step is degumming, which involves the removal of phospholipids, gums and metals from crude rice bran oil by heating crude oil at 90 °C-100 °C and then adding 10% phosphoric acid (w/v in water) to obtain 0.2 wt% acid in crude oil. The mixture was warmed to 65 °C with constant stirring for 1 h and then centrifuging the mixture to separate the oil. After degumming process, phosphoric acid was neutralized by CaO (De and Bhattacharyya, 1998). The second step is bleaching to remove colored particles and substances such as carotenoid and chlorophyll. The bleaching agents used are natural or acid-activated.

The third step is dewaxing, which is performed at 5 °C and filtration. This step is used to separate crystal wax from rice bran oil (Orthoefer, 2005). Deodorizing step is the de-acid step. It is done by using steam stripping under vacuum to remove free fatty acids (FFA), volatile compounds and unsaponifiable

matters. Usually deodorization is carried out at 230-250 °C at 200 Pa. The final step is called winterization to remove wax at 4-5°C from de-acid oil (Čmolík and Pokorný, 2000; Orthoefer, 2005).

Physical refining is more environmental friendly than the chemical refining process (Prasad, 2006). It is a good substitute for chemical refining when the rice bran oil contains high FFAs level (Prasad, 2006). The main difference between chemical refining process and physical process is the neutralizing step before deodorizing step, which is used in chemical refining process: the caustic soda process. After degumming, the degummed oil is neutralized alkaline solution to remove FFAs and excess phosphoric acid. The reaction of with alkaline solution with fatty acids leads to the formation of soap (Dumont and Narine, 2007). Therefore, most of minor constituents are concentrated in the soapstock in chemical process; but they are concentrated in the deodorizer distillate (DD) in physical refining process (Greyt and Kellens, 2005). Moreover, during the chemical refining, the major bioactive compounds, such as γ-oryzanols, are destroyed or removed, causing significant losses and reduced phytochemicals in the refined oil (Prasad, 2006).

1.2 Co-products during refining process

1.2.1 Deodorizer distillate

The deodorizer distillate from RBO refining process is composed of FFAs, monoacylglycerol (MAG), diacylglycerol (DAG) and valuable phytochemicals such as phytosterols, squalenes, tocotrienols and tocopherols. Utilization of FFAs has been investigated extensively on the methylation process to produce biodiesel. Other co-products such as MAG and DAG, phytosterols, squalenes and tocols could be used in pharmaceutical, food and feed industries (Orthoefer, 2005). The processes commonly used to separate FFAs from deodorizer distillate including: chemical method (saponification), enzymatic method (esterification) and physical method - particularly molecular distillation (MD) and supercritical CO_2 extraction (Dumont and Narine, 2007; Gunawan and Ju, 2009).

These methods can be used to concentrate and/or purify the phytochemicals from deodorizer distillate for further application.

The saponification is mainly used to separate FFAs from sterols and tocopherols to minimize tocopherol oxidation (Dumont and Narine, 2007). However, this method requires high amount of solvent that are not environmental friendly and results in low recovery yield. Esterification is based on the conversion of compounds into their methyl ester form to improve their separation. However, there are numerous parameters involved, such as enzyme concentration, process time and temperature that are not easily controlled (Dumont and Narine, 2007).

Molecular distillation (MD), or short-path distillation, could separate heat sensitive and high boiling point materials at low temperatures due to the low pressure during distillation (Moraes *et al*., 2006). Free fatty acids are stripped into evaporated fraction; whereas the high molecular weight (MW) substances remain in the unevaporated fraction (UMD). Therefore, γ-oryzanols and phytosterols, which have higher boiling points than do FFAs, could be concentrated in the unevaporated fraction after molecular distillation, designated as UMD fraction. Major factors affecting the composition of UMD are distillation temperature, flow rate and vacuum. The potential utilization of the UMD after molecular distillation of RBO includes the use of UMD as a source of rice phytochemicals. These phytochemicals can be used in foods and cosmetics. Moreover, MAG and DAG concentrated in the UMD can be used as surfactants in food industries (Dumont and Narine, 2007).

Other physical method such as supercritical CO_2 extraction, which uses CO_2 passing through a deodorizer distillate at a certain temperature and pressure. However, this process requires high capital and operating cost (Matins *et al*., 2006; Posada *et al*., 2007). Nevertheless, this method could be used to concentrate phytochemicals from deodorizer distillate of soybean, corn, sunflower and canola oils. The operating conditions of supercritical CO_2 extraction are carried out at temperature range 25-35 °C and pressure ranging from 10 to 40 MPa depending on the types of phytochemicals to be concentrated (Mendes *et al*., 2005).

1.2.2 Rice bran wax

Rice bran wax (RBW) is a co-product of RBO refinery obtained during dewaxing and winterizing steps. It is composed of long-chain carboxylic acids and long-chain alcohols. Waxes are also present as long-chain fatty acid esters with fatty alcohols, methanol, and ethanol. Fatty acid analysis showed that behenic acid (C22:0), lignoceric acid (C24:0), are the major fatty acids for a long alkyl ester group. Oleic acid (C18:1) and palmitic acid (C16:0) are considered as a medium alkyl ester (Orthoefer, 2005). The major alcohols found in long alkyl esters include tetratriacontanol (C34:0), dotriacontanol (C32:0), triacontanol (C30:0), octacosanol (C28:0) and tetracosanol (C24:0). Straight-chain alkanes, alkenes, and branched-chain alkenes (squalene) are detected in the hydrocarbon fraction. The squalene content in crude wax was around 120 mg/100 g (Orthoefer, 2005).

Hard and soft waxes can be recovered from crude RBO. The RBW has melting point ranges between 74 and 80 °C. The hard wax consists of 64.5% fatty alcohols, 33.5% fatty acids, and 2% hydrocarbons; while soft wax contains 51.8% fatty alcohols, 46.2% fatty acids, and 2% hydrocarbons (Orthoefer, 2005). The RBW is widely used as an ingredient in pharmaceutical, food, polymer, leather, polishing and cosmetic industries (Yoon and Rhee, 1982; Vali *et al*., 2005).

The utilization of RBW in food industry depends on suitable purifying methods (Vali *et al*., 2005). The main purpose of purifying crude rice bran oil (CRBO) is to eliminate resinous matters (RM), which are dark reddish-brown substance and unpleasant odor. In the past, chemical agents and methods used for bleaching CRBO were CrO_3 and 40% H_2SO_4 (1:1.5 w/w) at 95 °C for 2 h, treatment of wax with acid and bleaching with $NaClO_2$ followed by H_2O_2 etc. However, these methods were not commercially accepted at present because of corrosive carcinogenic chemicals and a long process time (Roy *et al*., 2009). Vali and coworker (2005) revealed that a two-step method could be used to prepare food-grade wax. The first step was using solvent, refluxing and cooling process to de-fat crude wax. However, the crude wax was dark brown and had melting point around 75-79 °C. The RM in

crude wax can be further removed by bleaching with sodium borohydride in isopropanol. This step gave a pale yellow, odorless wax with purity of more than 99% and a melting point range around 80-83 °C.

Some long-chain alcohol, namely octacosanol, is a high MW primary aliphatic alcohol (Wang *et al*., 2007) known to have bioactivities. Octacosanol had cholesterol-lowering properties by reducing LDL cholesterol and increasing HDL cholesterol. It is known to help improving exercise performance of coronary heart arteries and lowering the risk of developing atherosclerosis. Moreover, it can reduce platelet aggregation or clot formation, which lead to decreasing the risks of stroke and deep-vein thrombosis (Taylor *et al*., 2003; Hwan *et al*., 2005).

2. Fat structure and its functional properties in food products

Fats have been used in food formulation as they provide functional properties such as hardness, viscosity, plasticity and spreadability in fat-containing products such as chocolate, butter, shortening and baked products (Shukla, 2005). The main component in fat is triacylglycerol (TAG), which is responsible for fat crystallization required in the textural characteristic of fat products and baked products. Different arrangement of TAG molecule, both in liquid phase and crystalline phase, results in different fat crystal network (Metin and Hartel, 2005; Sato and Ueno, 2005).

The elastic properties such as mouthfeel and hardness from colloidal fat crystal network of *trans* and saturated fat are required in food products. However, consuming saturated fat and *trans* fat diets could lead to metabolic syndromes and cardiovascular diseases due to the increasing of LDL-cholesterol and TAG in blood. Attempts have been made of modified fat solid structure that could provide similar functional properties to those from saturated and *trans* fat crystalline structure of liquid oil. Mechanisms involved in stabilizing the three-dimensional network in fat products include:

2.1 Traditional fat crystal network of triacylglycerol (TAG)

Fat crystallization is composed of 2 steps: nucleation and crystal growth (Metin and Hartel, 2005). During fat crystallization to form solid structure, a natural fat is in supersaturated state and the TAGs having highest melting point in the close proximity could form a nucleus, which is the smallest molecular association with a crystal lattice ordering. During nucleation, molecules in the liquid state give up energy and associate into lattice structure with other similar molecules.

Subsequent crystal growth is the incorporation of other TAG molecules from the liquid phase into an existing crystal lattice with correct configuration at the correct site on a crystal surface. The growth of crystal continuously proceeds as long as there is a driving force for crystallization; e.g. increasing the saturation or cooling rate (Davey and Garside, 2000).

Different fat polymorphs could be formed during crystallization. The α polymorph is usually found, but it is unstable because TAG is packed in a loose hexagonal subcell conformation (Metin and Hartel, 2005). The hexagonal subcell structure is a two-dimensional lattice (Sato and Ueno, 2005). The α-form would transform within a short period of time into the β′ polymorphic form. The β′ polymorph could form directly during crystal growth or as result from the α-form transformation. The β polymorph is more stable than is the α-form , with the subcell structure as triclinic. The β form has the highest packing density. For β′ form, the TAGs orient in a denser othorhombic subcell structure. This structure is quite stable and could maintain small to moderate crystal size (Rye *et al*., 2005). The conditions required for the formation of the β structure is at very slow rate or at low degree of subcooling (Metin and Hartel, 2005; Sato and Ueno, 2005).

Each polymorphic form has different specific crystallization temperature as shown in Figure 1. When tripalmitin was melted at 80 °C and cooled to different crystallization temperatures, fat crystal would form different polymorphs. The α form could be induced at 39-44 °C, while β′ form was induced at 45-50 °C and β form was

induced at 51-60 °C. The α form needed less time to nucleate than the others. The induction time for the most stable β polymorph was the longest. Thus, food manufacturer can use varying cooling schemes to get desirable fat crystal polymorphs.

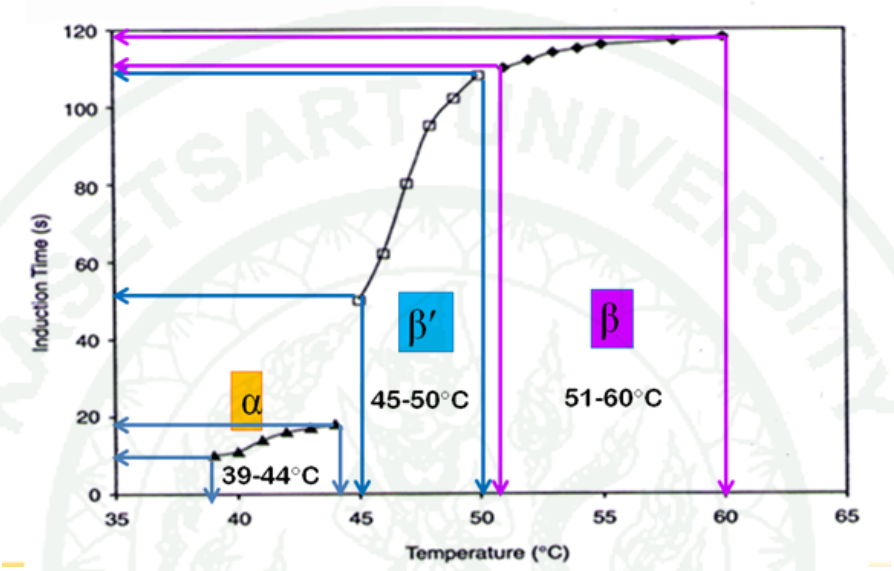

Figure 1 Induction time and crystallization temperature range for different polymorphic forms of tripalmitin.

Source: Metin and Hartel (2005)

Polymorphic transition is a reversible transition of a solid crystalline phase at a certain temperature to another phase of the same chemical composition with a different crystal structures as shown in Figure 1. When temperature was higher than the melting point of α form, the α polymorph would melt and change to β′ form under appropriate cooling scheme. When the β′ is melted at 51 °C, it could also transform into β form under appropriate condition. Thus, temperature control in processing and during storage is very important in controlling the polymorphic structures and their phase transitions. Apparently, these fat crystal polymorphs could have different melting temperatures although they have similar chemical characteristics.

The liquid oil - holding capacity of solid fat occurs due to the ability of crystalline fat that forms fat crystal network. Usually solidified fat (butter) with 12% solid fat content at 25 °C can hold the liquid oil (Rukke *et al*., 2013). After the TAGs form lamella structure, the lamella would stack to each other in the ordered fashion and form crystallite (Figure 2). The crystallites would assemble into clusters of crystallite. The clusters could associate into flocs and finally form macroscopic network. The solid fat existed in a three-dimensional fat crystal network is responsible for functional properties of fat products *via* the size of crystal, the type of crystal, the strength of the links between the crystal, the geometry of the network, and the network density (Tang and Marangoni, 2006a). All fat functionalities such as hardness, viscosity, plasticity, and spreadability are thus governed by how these crystals stack to each other into clusters and networks. Therefore, the composition of fatty acid in TAG and fat processing conditions (cooling rate, tempering and aging, as well as water content and/or surfactant) control fat product characteristics.

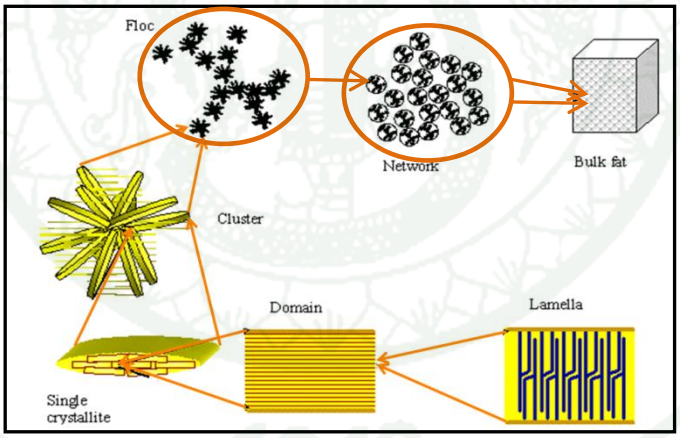

Figure 2 Structure in colloidal fat crystal network.

Source: Tang and Marangoni (2006b)

Apart from TAG fat crystal network, n-alkanes containing 29-33 carbons in food grade waxes could help structuring liquid oil (Vazquez *et al*., 2007) by aggregation of small crystalline particles into a three-dimensional network that entrap oil inside (Roger, 2009). Moreover, wax crystal network can form crystal similar to

that of TAG, but different in shape. TAG crystals are spherical shape; while wax crystals are needle-like shape. So the difference in crystal shape may affect the rigidity of the three-dimensional network as shown in Figures 3 and 4 (Omononov *et al*., 2010; Dassanayake *et al*., 2011).

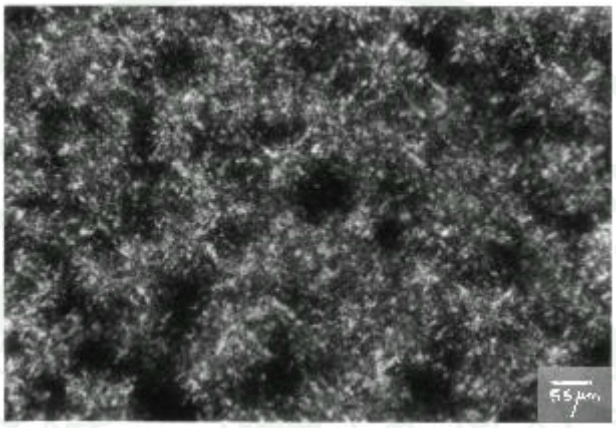

Figure 3 Optical micrograph of fat crystal network of high-melting milk fat fraction (90%) in oil sunflower oil.

Source: Martini *et al*. (2002)

The rice bran wax (RBW), candellila wax (CLW) and carnauba wax (CRW) can form crystals in different shape and size. RBW (1%) can form needle-like crystal with the size around 20 to 50 μm entrapping liquid oil at 20 °C (Figure 4a). On the other hand, crystals of 2% CLW and 4% CRW in olive oil at 20 °C showed spherulitic structure having diameter of less than 10 μm. The crystal structure of RBW provided good crystal matrices to inter-crystalline interface to form three-dimensional network. However, round shape of RBW crystal could present in liquid paraffin. This was because different molecular components in the wax and solvent had effects on the size and shape of crystal in different liquid oil (Dassanayake *et al*., 2009; 2011).

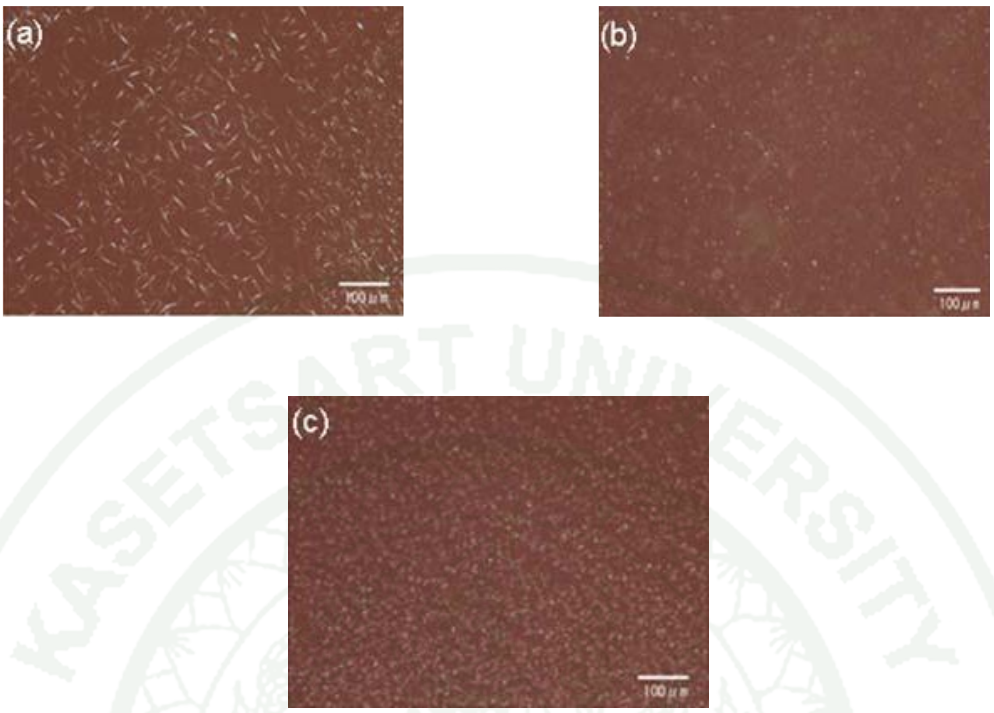

Figure 4 Optical micrograph of wax crystals in olive oil (1% w/w) at 20 °C (a) RBW in olive oil, (b) CLW in olive oil and (c) CRW in olive oil.

Source: Dassanayake *et al*. (2009)

In 2004, Mayamol and coworker studied the effect of composition of the blends and processing conditions (agitation rate and fat crystallization temperature) on crystallization of shortening using palm stearin and RBO. First, palm stearin was mixed with RBO at different ratio as 50:50, 60:40 and 65:35, respectively. The blends were stirred at 70 °C for 10 min to ensure complete melting, then pumped through the scraped surface heat exchanger at 20-27 °C. At this temperature, partial crystallization occurred and the viscosity of oil blends increased. Crystallization was carried out at 29 °C at agitation speed of 50, 200 or 250 rpm. The semisolid shortening was tempered at 28.7 °C, 29.8 °C or 30.5 °C and packed. The resulting shortenings were analyzed for fatty composition, solid fat content, slip melting point, polymorphic forms and fat crystal network. The result showed that palm stearin had high saturated fatty acid, particularly palmitic acid (C16:0); while RBO had high oleic

acid (C18:1) and linoleic acid (C18:2). When the ratio of RBO was increased from 35 to 50%, the oleic and linoleic fatty acids increased, slip meting point of blended shortening was therefore decreased from 39 °C to 37 °C. This was due to the increase in polyunsaturated fatty acid from RBO. Decreasing crystallization temperature from 30.5 °C to 28.7 °C led to the smaller and densely packed crystal. This is because low temperature can induce faster nucleation and thus small size fat crystal. When the agitation rate was slow, large crystal were formed. However, higher agitation rates resulted in the formation of small crystals. High agitation rate aided cooling, thus enhancing more heat and mass transfer in TAG during crystallization and network arrangement.

2.2 Non-traditional structuring network: the oleogels

Oleogels are bi-continuous colloidal system containing liquid organic phase such as edible oil and the gelling agent or gelators. The gelator in organic system is usually called oleogelators since they are solubilized or dispersed mainly in organic phase. The oleogelators have the characteristics of self-assembling or being a polymeric strand. Thus, they can form continuous gel network entrapping liquid oil in their structure (Figure 5) (Marangoni and Garti, 2011; Samuditha *et al*., 2011). The oleogels can be prepared by mixing oil and oleogelators, followed by heating until the gelator dissolves, and cooling to the temperature lower than the gelation and/or crystallization temperature of oleogelators (Gandolfo *et al*., 2004). Continuous gel network having numerous structures can be categorized depending on structure forming process of oleogels (Roger, 2009; Marangoni and Garti, 2011) as follows:

Figure 5 Polarized light image of self-assembled monoacylglycerol (light color) entrapping liquid cod liver oil (dark area), shear rate at 0 s^{-1}.

Source: Pieve *et al*. (2010)

2.2.1 Self-assembled crystalline surfactants

Monoacylglycerol (MAG), which is known as surfactant having low hydrophile-lipophile balance (HLB) around 1, can form spontaneous reverse bilayer in pure oil system (Roger, 2009) due to its amphiphilic structure of polar head and hydrophobic alkyl chain. Therefore, after cooling and aging, they can form β crystal network. For example, this self-assembled MAG structure can entrap cod liver oil in three-dimensional network (Figure 5) when used at 5%. The structure forming process, physical and microstructural properties of MAG network in edible oil depended on the concentration of self-assembled surfactants, temperature, aging process, cooling rate and shear rate (Ojijo *et al*., 2004; Chen and Terentjev, 2011).

Not only the reverse bilayer of surfactant in the oil phase, but also the rod-shaped tubules of inverse bilayer or hexagonal II structure of some surfactants such as sorbitan monostearate (Figure 6) can be used as self-assembled oleogelator (Roger, 2009). After solubilizing sorbitan monostearate (10% w/v) in hexadecane solvent at 60 °C, Murdan *et al*. (1999) reported that the mixture became turbid due to

the insolubility of surfactant upon cooling to room temperature (25 °C), which led to the formation of rod-shaped tubules appeared as opaque crystal structure (Figure 7).

Figure 6 Chemical structure of sorbitan monostearate.

Source: Anonymous (2014 a)

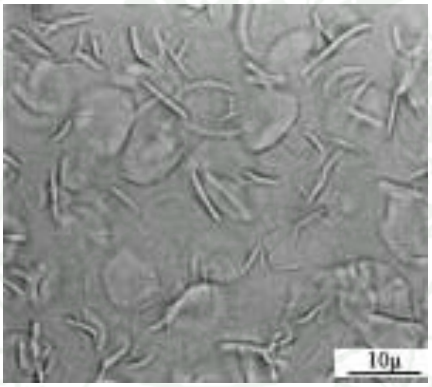

Figure 7 Organogel microstructure: tubular aggregates formed by self-assembled sorbitan monostearate molecules in hexadecane solvent.

Source: Murdan *et al*. (1999)

Although sorbitan tri-stearate (STS) and lecithin could not form oleogel in sunflower oil when each existed alone (Figure 8a), mixing lecithin to STS at the ratio of 50:50 resulted in gelation of sunflower oil. The morphology of STS varied compact spherical crystals to fine needle-like crystals (Figure 8, Pernetti *et al*., 2007). However, the gels are shear-sensitive and temperature-sensitive. The

sunflower oil gels collapse at 30 °C and could not hold liquid oil. Nonetheless, the gels were thermoreversible and could re-fabricate upon cooling at 5 °C into firm gels. The presence of lecithin enhanced inter-floc connection and resulted in elastic continuous network (Figure 8b) (Pernetti *et al*., 2007).

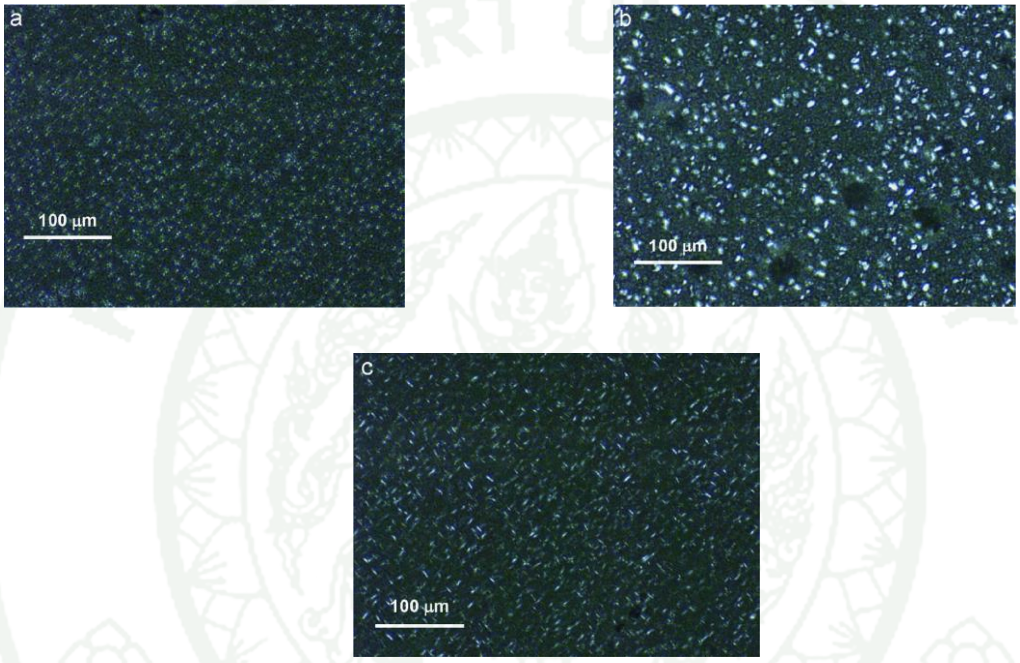

Figure 8 Micrographs of sunflower oil under crossed polarizers in the presence of (a) 6% STS (b) 6% lecithin (c) 6% STS+ 6% lecithin in oil. The samples were observed at 5°C.

Source: Pernetti *et al*. (2007)

2.2.2 Self-assembled fibril of phytosteryl moieties

Bot and Agterof (2006) revealed that the self-assembling nanotubules can be formed in the presence of both β-sitosterol and γ-oryzanol. The structures which promoted the oleogel formation in sunflower oil of phytosterols and ferulic ester of phytosterols (i.e. γ-oryzanol) was due to the presence of hydroxyl

group and the presence of four isoprenoid rings of sterol in structure (Figure 9). The presence of hydroxyl group is essential because it could limit the solubility of phytosterol in the oil phase. Subsequently they could self-assemble through phytosteryl moieties and stack together to form tubule wall. The sterol part plays an important role in the formation of the helical ribbon structure of self-assembled tubules (Figure 10). Alamprese and coworker (2013) investigated the effect of mixed β-sitosterol and γ-oryzanol at the total concentrations of 3.1, 3.5, 4.0, 4.5, 5.0, 5.5 and 5.9% when used at the ratio of 2:3 on rheological properties of sunflower oil oleogel comparing against those of butter. Increasing total concentration of mixed β-sitosterol and γ-oryzanol from 3.1 to 5.9% increased storage modulus (G′) of oleogel from 1×10^2 to 1×10^5 Pa, loss modulus (G″) from 1×10^2 to 1×10^5 Pa. Moreover, storage modulus of all treatments was higher than loss modulus, which indicated solid-like behavior. Sunflower oil oleogel fabricated using 4.5% oleogelator showed similar rheological properties with those of butter.

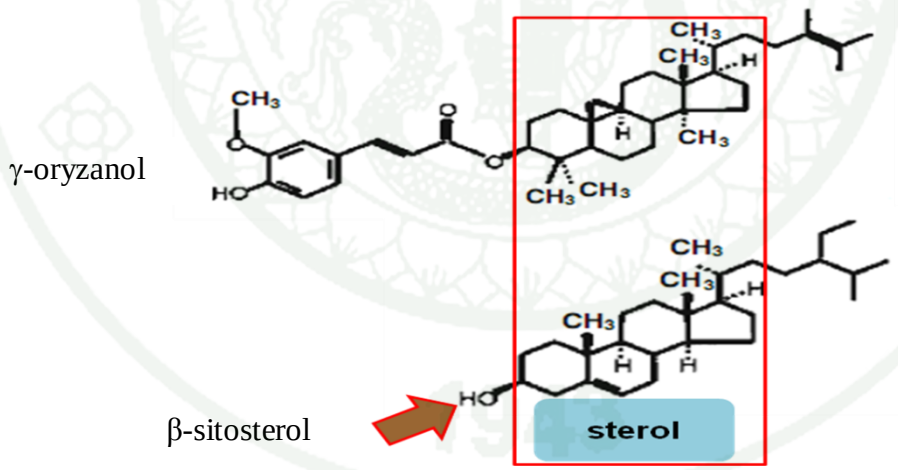

Figure 9 Structure of γ-oryzanol and β-sitosterol.

Source: Bot *et al*. (2008)

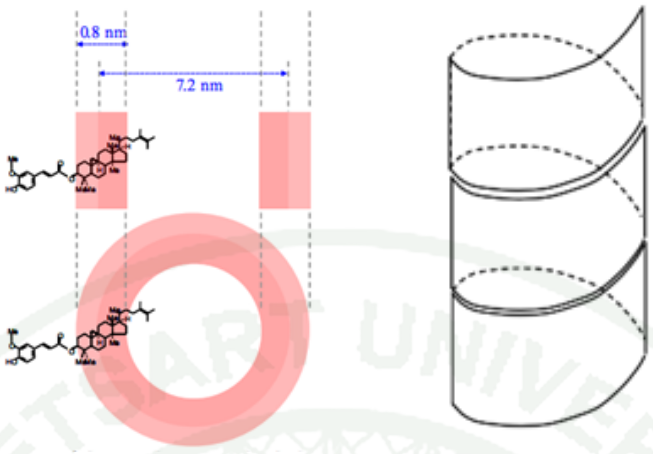

Figure 10 Proposed structure of the sterol + oryzanol tubules and on the right hand side, a schematic representation of a helical ribbon.

Source: Adel *et al*. (2010)

2.2.3 Polymeric strands

The structure of oleogel stabilized by polymer can be fabricated by solubilizing oil-soluble polymers in the organic phase or oil phase. The polymer absorbs organic/oil solvent, swells and interpenetrates or entangles to form three-dimensional network entrapping liquid oil in solidified structure of oleogel. The degree of swelling depends on temperature and molecular interactions between polymer and solvent (Li *et al*., 2012). Polymer network can be surrounded by solvent molecules, similarly to aqueous thermoreversible gels (Laredo *et al*., 2011). One of polymers which can be used in the formation of oleogel is ethyl cellulose (EC) (Co and Marangoni, 2012).

Recent work reported by Zetzl *et al*. (2012) indicated that the oleogel strength depended on polymer molecular weight and concentration of polymer, as well as fatty acid composition of vegetable oil. The high contents of polyunsaturated fatty acid and polymers having high molecular weight resulted in gels with higher elastic modulus. According to the work of Laredo *et al*. (2011), the

interactions responsible for the gelation of oil could be divided into: polymer-polymer, polymer-solvent and solvent-solvent interactions. Polymer-polymer interaction involves H-bondings between EC polymer strands. The H-bonds can occur between the OH groups of different strands or the OH groups of the same strand (most likely on the C6) and an ethoxy substituent of another strand (Laredo *et al*., 2011). Strong polymer-polymer interactions could result in strong oleogel.

The conformation of lipid chains is mainly responsible for solvent-solvent interaction *via* dipole/dipole or van der Waals interactions in oil. The TAGs having more double bonds can pack in a tighter fashion due to the kinks of fatty acid conformation. Therefore the polyunsaturated TAGs would be more restricted and denser in the gel compared to monounsaturated TAGs, resulting in stronger oleogel when polyunsaturated oil is used in oleogel fabrication.

Moreover, polymer-solvent interactions also play significant roles in determining the gel strength of oleogel. The oil composed of lower number of double bond requires larger molar volume, resulting in lower density (g/cm^3) compared to the oil having polyunsaturated fatty acid. This could lead to an increase in phase separation of EC chains from the oil solvent and the numbers of tie point in the network are reduced. Weaker gel is eventually obtained when saturated oil or monounsaturated oil is used (Laredo *et al*., 2011).

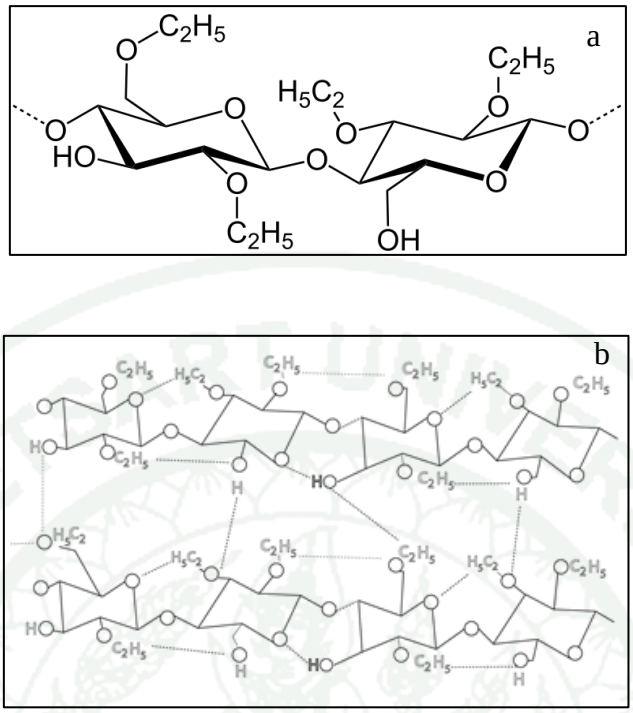

Figure 11 (a) Chemical structure of EC (b) hydrogen bonding between EC strands.

Source: (Anonymous, 2014b)

Canola oil oleogel, which contained mostly oleic acid (C18:1), had hardness around 1.5 N; while soybean oil oleogel and flaxseed oil oleogel showed hardness of 2.1 N and 6.1 N, respectively (Laredo *et al*., 2011). It is apparent that the flaxseed oil which contained mainly linolenic acid (C18:3) resulted in the strongest oleogels compared with the oils having linoleic acid (C18:2) as soybean oil and monounsaturated fatty acid (C18:1) like canola oil. Nonetheless, canola oil oleogel can replace beef fat in frankfurters and showed no significant difference in chewiness or hardness compared to the control product (Zetzl *et al*., 2012).

Utilization of oleogels in industries depends on the required physical, functional and nutritional properties of edible oil oleogels. In food industry, oleogels are considered as replacement for *trans* fat and saturated fat due to the low post-prandial serum TAG and serum fatty acid in blood after eating. Eating oleogels containing canola oil gelled with 2% w/w 12-hydroxy stearic acid (12-HSA) resulted

in lower post-prandial serum TAG and serum concentration of free fatty acid in blood compared to that after consumption of butter or margarine (Hughes *et al*., 2009).

2.2.4 Minimum concentrations of oleogelator to form network

The non-traditional network of oleogelator requires a much lower concentration of the network constituents compared to that of traditional network of fat crystal network of TAG. Structural and physical properties of oleogel could be different due to the molecular structure and concentration of oleogelators. The appropriate concentration of gelators to obtain solidified oil structure or gel was only around 3-4 %. At very low concentrations, the gelator could be completely soluble in the oil and could not form gel (Schaink *et al*., 2007). At high concentration of oleogelator, the structure-forming mechanisms would involve both self-assembled molecule of gelator and fat-crystal network.

The morphology of gelator in oleogel depends on the types, concentration and composition of oleogelators. When stearic acid and stearyl alcohol were used at different ratio to form sunflower oil oleogel, the plate-like and hexagonal shape of oleogelator consisting of stearic acid alone could be formed (Figure 12a). However, when stearic acid and stearyl alcohol was used at the ratio of 3:7, the small needle structure could be formed (Figure 12d), resulting in denser structure and harder texture due to more crystal-crystal contacts in gel network (Schaink *et al*., 2007)

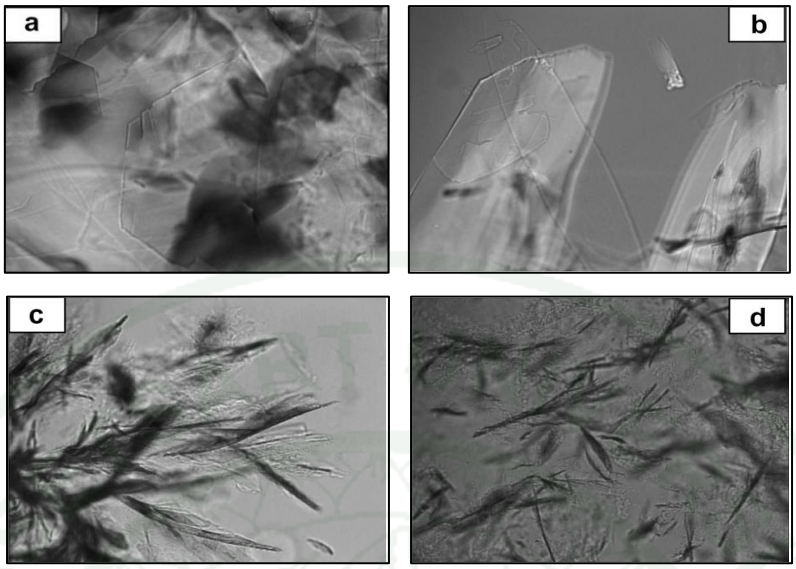

Figure 12 Microscopy images of the crystals in oil + structurant systems for different stearic acid: stearyl alcohol ratios: (a) 1:0; (b) 7:3; (c)1:1 and (d) 3:7.

Source: Schaink *et al*. (2007)

A minimum volume fraction (ϕ) of MAG at around 0.063 was necessary to form oleogel of olive oil under self-assembled surfactant mechanism. At this volume fraction of MAG in olive oil, the aggregated colloidal dispersions of MAG fat crystal network could occur. At lower volume fraction of MAG (i.e. $\phi <$ 0.013), the mixed oil and MAG showed entangled network characteristic rather than three-dimensional network of oleogel since G″ was higher than G′. At high volume fraction of MAG, the oleogel could be formed due to the lateral aggregation of MAG crystal network and cross-linked chains via London force, van der Waals interactions and hydrogen bonds (Ojijo *et al*., 2004).

The formation of nanotubule of γ-oryzanol and β-sitosterol entrapping sunflower oil depended on the total concentration and ratio of both substances. Oleogels could not be formed if γ-oryzanol or β-sitosterol was used individually. An 8% mixture of γ-oryzanol and β-sitosterol, transparent oleogels

could be formed. Raising the total concentration to 16% mixture resulted in a turbid oleogel. Increasing the β-sitosterol concentration in the mix could also increase the turbidity of oleogel, indicating inter-tubule aggregation. The oleogels prepared at high ratio of γ-oryzanol were transparent due to the least bundle aggregation. The ferulic acid moiety in γ-oryzanol structure helped keep the nanotubules apart as a spacer (Bot *et al*., 2008).

2.3 Factors affecting functionalities of fat in fat processing

2.3.1 Lipid composition

Neutral fats are composed of a wide range of TAGs. These TAGs contain fatty acids of differing chain length or molecular weight, degree of unsaturation, and positional arrangement on glycerol backbone. Fatty acids can be classified into saturated fatty acid and unsaturated fatty acid. Saturated fatty acids in vegetable oils are a long-chain carboxylic acid usually between 12 and 24 carbon atoms and contain no double bonds. As the molecular weight increases, the melting point increases. This can be observed in the series of lauric acid (C12:0), palmitic acid (C16:0), stearic acid (C18:0).

Unsaturated fat fatty acid has one or more double bonds in the fatty acid chain. Their melting points increase when the number of double bond decrease (Metin and Hartel, 2005). The ratio of saturated to unsaturated fatty acids (S/U ratio) in RBO is highly related to the palmitic acid content. *Japonica* lines were characterized by a low palmitic acid content and S/U ratio, whereas *Indica* lines showed high palmitic acid content and a high S/U ratio. The variation found suggested it is possible to select RBO with different fatty acid profiles (Goffman *et al*., 2003) in alter functionalities of RBO such as melting point.

Table 1 Fatty acid composition of vegetable oil.

Saturated fatty acid (%)	Rice bran oil(1)	Rice bran oil(2)	Sun flower oil	Olive oil	Coconut oil	Palm oil
Caprylic (C8:0)	-	-	-		6.21	-
Capric (C10:0)	-	-	-		6.15	-
Lauric (C12:0)	-	-	-		51.02	-
Myristic acid (C14:0)	0.3	0.3	-		18.94	1.23
Palmitic acid (C16:0)	20.8	21.6	6.52	14.69	8.62	41.78
Stearic acid (C18:0)	1.8	4.7	1.98	2.64	1.94	3.39
Arachidic acid (C20:0)	0.7	1.0	-	0.47	-	-
Total of saturated fatty acid	**23.6**	**27.6**	**8.5**	**17.8**	**86.67**	**46.4**
Unsaturated fatty acid (%)						
Palmitoleic acid (C16:1)	-	0.3	-	1.66		-
Oleic acid (C18:1, *cis*-9)	41.5	42.6	45.39	66.14	5.84	41.90
Linoleic acid (C18:2, *cis*)	34.4	28.0	46.02	12.83	1.28	11.03
γ-Linolenic acid (C18:3n6)	0.3	0.8	0.12	1.02	-	-
Total of unsaturated fatty acid	**76.2**	**71.7**	**91.53**	**81.65**	**7.12**	**52.93**
Melting point (°C)	-39		-17	-9	25	35

Note: Rice bran oil 1 = chemically refined rice bran oil, Rice bran oil 2 = physically refined rice bran oil.

Source: Zigger (2005); Chowdhury *et al*. (2007); Krishna *et al*. (2009), Zarrouk *et al*. (2009); Saidin and Ramli (2010)

2.3.2 Minor lipid components

The minor components such as MAG, DAG, FFAs, phospholipids and unsaponifiable matters can promote or inhibit fat crystallization and subsequent functionalities of fats. They may limit mass transfer rates of TAG crystallization for the incorporation of TAG molecules onto the correct site on lattice and adsorption on the surface of the growing crystal or cluster. The limited mass transfer could inhibit further incorporation of the crystallizing TAG (Metin and Hartel, 2005).

However in some cases, the minor components could increase the crystallization rate. If a macro-crystallizing substance and additive have a similar structure or form similarly structured complexes to the lattice of crystallizing substance (liquid oil), then new growth sites on the crystal lattice can be formed by adsorption. These active sites may be energetically more favorable for incorporating other substances, resulting in increased crystallization rate (Metin and Hartel, 2005). The addition of phospholipids in the stearin was reported to increase melting point and co-crystallization with TAG. Nevertheless, the presence phospholipids in palm oil had no effect on fat crystallization (Smith *et al*., 2001).

The emulsifiers can play important roles as impurities and perform a catalytic action resulting in an acceleration of heterogeneous nucleation (Fredrick *et al*., 2008). Adding 1% MAG to palm oil could reduce induction time for nucleation. Added MAG could serve as nucleating seed and then facilitated aggregation of the TAG molecules. However, the presence of MAG did not affect final solid fat content after isothermal crystallization (Basso *et al*., 2010). Moreover, saturated MAG could increase the melting point and accelerated crystal growth slightly in the hydrogenated soybean and palm kernel oil; while the presence of unsaturated MAG decreased the melting point (Fredrick *et al*., 2008).

2.3.3 Processing conditions during tempering and aging in the applications of targeted

Tempering is the process to ensure the formation of crystallized fat with a thermodynamically stable polymorphic structure (Lannes and Ignácio, 2013). Generally, a 1-2% solid content can act as a seed when the melt is cooled to a temperature close to the melting temperature of fat. The tempering process consists of melting, cooling with no crystallization, forming of crystals with different polymorphic structures, and melting out of unstable polymorphs.

Tempering process is temperature and time technique for controlling pre-crystallization employed to induce the most stable solid fat and stable polymorphic fat in finished fat product (Lannes and Ignácio, 2013), used particularly in chocolate industries. Time-temperature protocols and shearing are employed to induce nucleation of stable polymorphs (V form) with the formation of three-dimensional network structure and melting of unstable polymorphs. The process consists of shearing chocolate mass at a controlled temperature at 45 °C to melt all fat crystal. Next, the chocolate mass was cooled to 27 °C for induce fat crystallization in IV and V form at this temperature the chocolate was agitated to create many small crystal (seeding) after that the chocolate was heat to 31 °C for eliminated IV form (unstable form) of fat crystal and still have only V form (stable form) (Afoakwa *et al*., 2008). Over-tempering occurred when relatively lower temperatures were exchanged between the multi-stage heat exchangers of the tempering equipment. Such process could affect hardness, stickiness with reduced gloss and darkening of chocolate surfaces. On the other hand, under-tempering (insufficient tempering, higher temperature and quick cooling), where liquid fat was transformed quickly into solid form, could result in the formation of very few stable fat crystal nuclei and chocolate bloom (Afoakwa *et al*., 2008).

Aging, however, is a process that could induce segregation of fat having varying chain length and degree of saturation (Sato, 1999). Therefore, during aging, the presence of mono, di - acylglycerol (MDG) could increase in crystallinity

with closer packing of hydrocarbon chains in the MAG bilayers and reorganization and became to the three-dimensional network (Ojijo *et al*., 2004; Chen and Terentjev, 2011).

Aging process has influences on three-dimensional network and reorganization of surfactant at low temperature, particularly in ice-cream industries (Chen and Terentjev, 2011). Proportional aging time and temperature could increase intensity of crystalline of MAG bilayers (Ojijo *et al*., 2004). The MAG in hydrophobic solutions can form an elastic gel network (Ojijo *et al*., 2004; Chen and Terentjev, 2011) as shown in Figure 13. The spontaneous reverse bilayer of MAG in oil is formed by the hydrophilic part of glycerol backbone, which can rearrange in middle of bilayer. The lateral area of reverse bilayer is the hydropholic part of aliphatic chain, dipping into the oil. Upon decreasing of temperature to below the gelation temperature shown in Figure 13, the inverse bilayer subsequently grows and organizes into inverse lamellar phase and sub-α crystal, entrapping the oil within its structure. Over time during aging process, the sub-α crystals transform into β-crystal, leading to the formation of a continuous three-dimensional network of surfactants in oil phase by aggregation as shown in Figure 13. The oil in the system is then immobilized by aggregating network with capillary force.

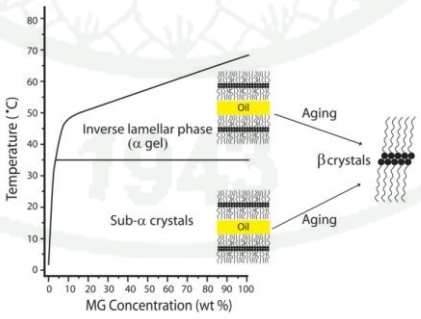

Figure 13 Phases of MAG-hazelnut oil mixtures showing inverse lamellar, sub-α crystal and β-crystalline.

Source: Chen and Terentjev (2011)

In 2000, Herrera and Hartel also reported the effect of processing conditions on physical properties of a milk fat model system. They blended high-melting point fraction with low melting point fraction of milk fat at the ratio 50:50. The processing conditions included crystallization at 25, 27.5 or 30 °C, agitation at 50 or 200 rpm, and cooling rate of 0.2 or 5.5 °C/min. The crystalline structure of solid fat in liquid oil was observed by the confocal laser scanning microscopy (CLSM). The result on CLSM images of milk fat (Figure 14) showed the black sphere as air bubble, white area was liquid oil and gray particle was crystal phase of fat. When milk fat was blended and crystallized slowly at 0.2 °C/min, the fat crystals were larger in size, compared to milk fat crystallized at 5.5 °C/min. Figure 15 indicated that after storage at 10 °C decreasing the temperature from 30 °C to 25 °C prior crystallization not only reduced the size of crystal, which is shown as gray area, but also resulted in closely packed crystal network. It is thus apparent that aging of fat crystal network could further modify the geometry and network density of traditional fat crystal network.

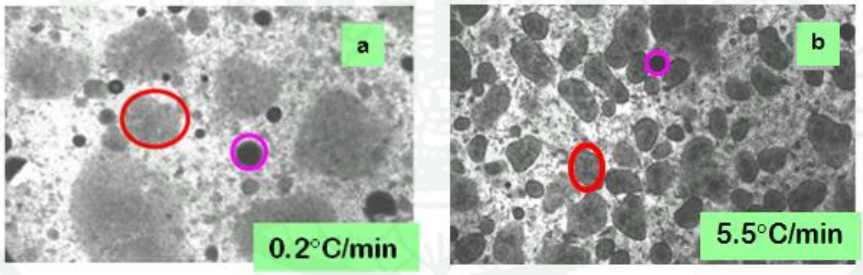

Figure 14 CLSM images of a 50–50% blend of high- melting fraction with low melting fraction of milk fat crystallized at cooling rate of (a) 0.2 °C/min (b) 5.5 °C/min. Images were taken at 3-μm increments from the surface 6 μm.

Source: Herrera and Hartel (2000)

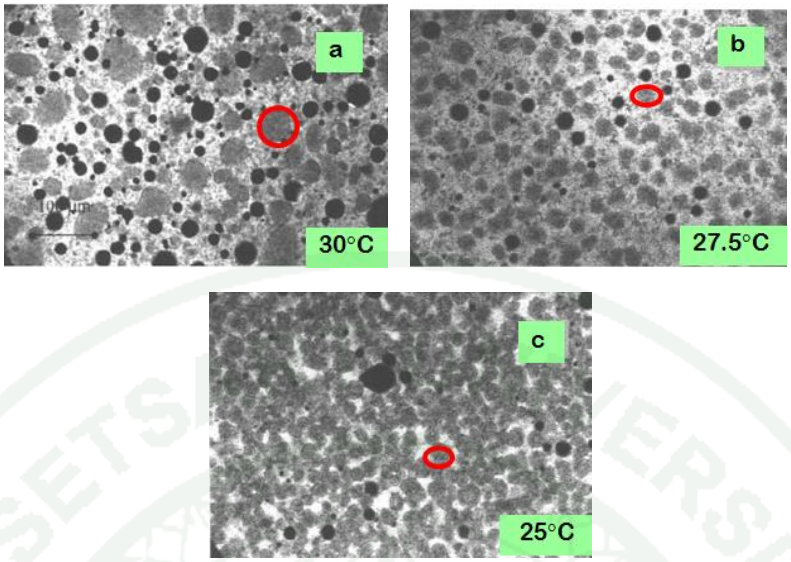

Figure 15 CLSM images of a 50–50% blend of high-melting fraction with low-melting fraction of milk fat crystallized at a cooling rate of 5.5 °C/min and an agitation rate of 200 rpm at a crystallization temperature of (a) 30 °C; (b) 27.5 °C; and (c) 25 °C. Samples were stored 24 h at 10 °C.

Source: Herrera and Hartel (2000)

Decreasing crystallization temperature from 30.5 °C to 28.7 °C led to the smaller and densely packed crystal of palm stearin and RBO (Figure 16) (Mayamol *et al*., 2004). This was because low temperature could induce faster nucleation and small size fat crystal. When the agitation rate was low as 50 rpm, large crystal of palm stearin and RBO was formed. At higher agitation rate of 150 rpm, the small crystals were formed (Figure 17). High agitation rate aided cooling, thus enhancing more heat and mass transfers in TAG during the arrangement of TAG molecules in palm stearin and RBO (Mayamol *et al*., 2004).

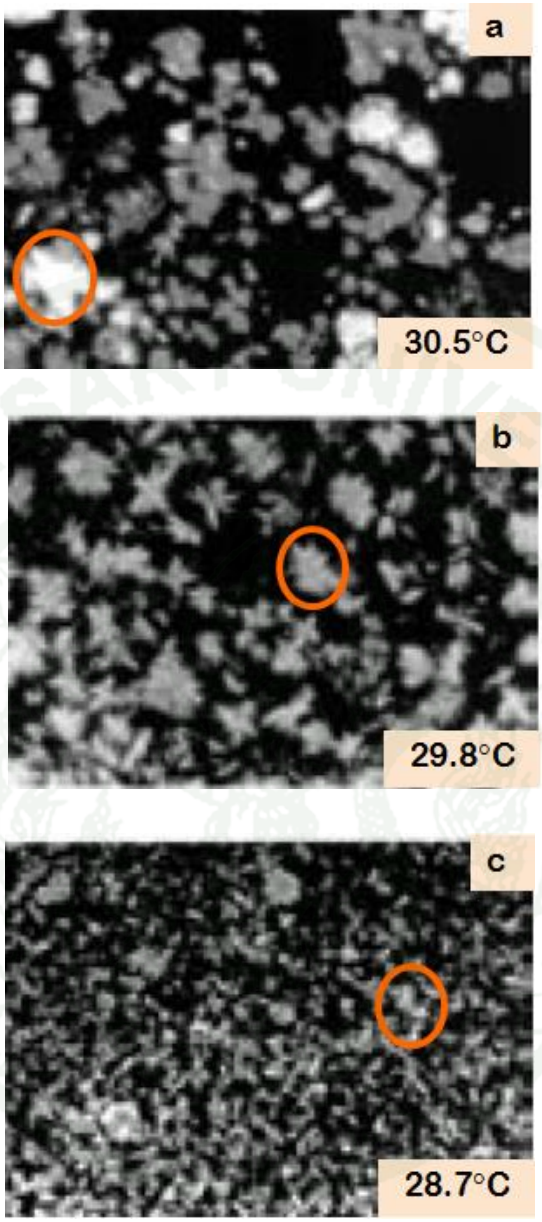

Figure 16 Light micrograph under polarized light of 50:50 PS/RBO blended shortenings crystallized at (a) 30.5 °C, (b) 29.8 °C, and (c) 28.7 °C.

Source: Mayamol *et al*. (2004)

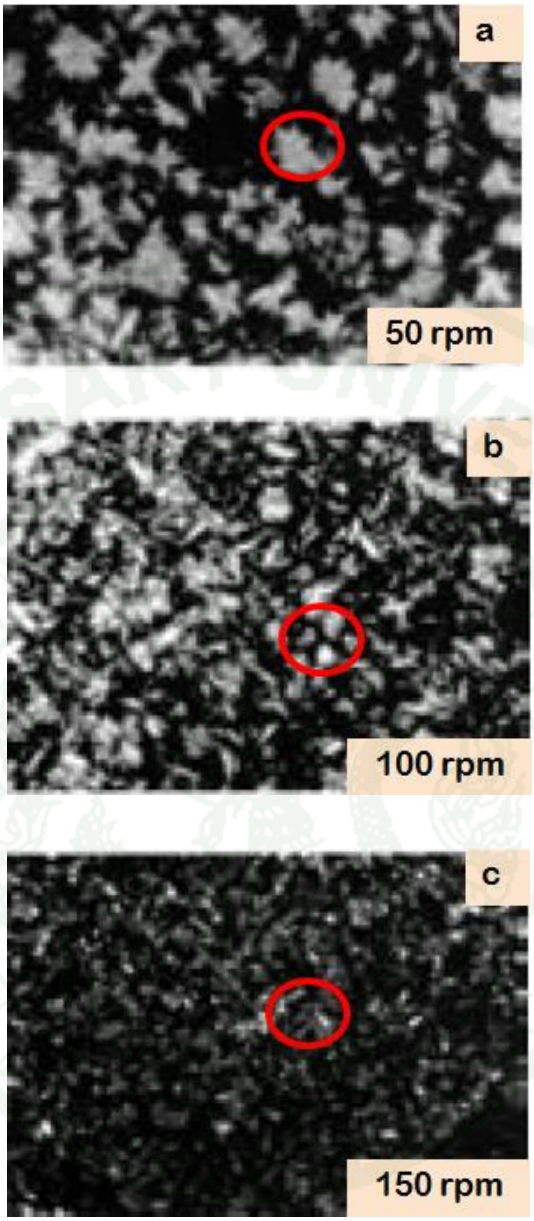

Figure 17 Light micrograph under polarized light of shortenings composed of 50:50 PS/RBO blend crystallized at 29.8 °C, and agitation rates of (a) 50 rpm, (b) 100 rpm and (c) 150 rpm.

Source: Mayamol *et al*. (2004)

MATERIALS AND METHODS

Materials

1. Raw Materials

1.1 Rice bran oil from physical refining process was kindly supported by Surin Bran Oil Company, Surin, Thailand.

1.2 Rice bran wax from winterizing step of physical refining process was kindly supported by Surin Bran Oil Company, Surin, Thailand.

1.3 Deodorizer distillate from physical refining process was used as raw material for a pilot-scale molecular distillation unit was kindly supported by Surin Bran Oil Company, Surin, Thailand.

1.4 Anhydrous milk fat was kindly provided by Vicchi Enterprise Company, Bangkok, Thailand.

1.5 Mixed herb (Krauterrost-bratwurst) from Gewurzmuller Company (70525, Korntal-Muchingen, Germany).

1.6 Paprika extract (Paprikaoleoresin) 100.00 cu (Meat Cracks Technologie, 49439, Muhlen, Germany).

1.7 Pork loin steaks with 10 mm thickness (MEGA Company, Stuttgart, Germany).

1.8 Commercial mono- and diacylglycerol (MDG) (HLB=1) was kindly supported by Berli Jucker Company, Bangkok, Thailand. It contained 0.04% capric acid, 0.46% lauric acid, 1.87% myristic acid, 62.39% palmitic acid, 30.64% stearic acid and 0.21% arachidic acid from fatty acid analysis.

1.9 Sucrose palmitate (SP) (HLB=1) was kindly provided by Mitsubishi-Kagaku Foods Corporation, Minato-ku, Tokyo, Japan. It was composed of 0.03% lauric acid, 0.55% myristic acid, 82.02% palmitic acid, 12.93% stearic acid and 0.06% arachidic acid from fatty acid analysis. The ester composition of SP was 99% di-, tri- and polyester and 1% monoester according to manufacturer's datasheet.

2.0 Ethyl cellulose (EC) with 48% ethoxyl content, viscosity 100 mPa·s of 5% in toluene/ethanol 80:20 at 25°C (Sigma Aldrich Chemistry, Steinheim, Germany)

Fatty acid profiles of physically refined rice bran oil (RBO), crude rice bran wax, anhydrous milk fat (AMF), commercial MDG and SP were determined for fatty acid profiles by a gas chromatography (ACFS, 2003)

2. Equipments

2.1 Differential scanning calorimeter (DSC) (Pyris 1; PerkinElmer, Norwalk, CT, USA)

2.2 High performance thin layer chromatography (HPTLC) unit (Camag, Berlin, Germany) composed of

2.2.1 HPTLC glass plate: Camag, Germany

2.2.2 Linomat IV(Sample application bandies): Camag, Germany

2.2.3 Sprayer : Camag, Germany

2.2.4 TLC plate heater III: Camag, Germany

2.2.5 Densitometer: TLC scanner 3, Camag, Germany

2.2.6 Glass chamber: Camag, Germany

2.2.7 Analyzed software program (CATS)

2.3 UV-Vis spectrophotometer (Spectronic GENESYS 10; Thermo Scientific, Waltham, MA, USA)

2.4 Brookfield viscometer equipped with a UL adapter (DV-III programmable rheometer; Brookfield Engineering, Middleborough, MA, USA)

2.5 Anton Parr Modular Compact Rheometer (MCR300, Anton Paar, Stuttgart,Germany) equipped with a coaxial cylinder base.

2.6 Anton Parr Modulus Compact Rheometer (MCR300, Anton Paar, Stuttgart,Germany) equipped with glass plate and plate geometry (43 mm diameter)

2.7 Scraped-surface freezer (KATOMO, China)

2.8 Soctex apparatus (Soxtec system HT1043 Extraction Unit, Tecator, Hoganas,Sweden)

3. Chemicals

3.1 Hexane (C_6H_{14} :Analytical grade, MERCK, Merck KGaA, Darmstadt, Hesse, Germany)

3.2 Diethyl ether ((C_4H_{10})O: Analytical grade and HPLC grade, MERCK, Merck KGaA, Darmstadt, Hesse, Germany)

3.3 Methyl acetate ($C_3H_6O_2$: HPLC grade, Carlo Erba Co., Ltd, Zi Valdonne, Peypin, France)

3.4 Isopropanol (C_3H_8O: Analytical grade, Asia Pacific Specialty Chemical Ltd., Seven Hill, New South Wales, Australia)

3.5 Chloroform ($CHCL_3$: HPLC grade, MERCK, Merck KGaA, Darmstadt, Hesse, Germany)

3.6 Methanol anhydrous; (CH_3OH: HPLC grade, Macron chemicals, Petaling Jaya, Selangor, Malaysia)

3.7 Potassium chloride (KCl Analytical reagent, UNIVAR, Ajax Finechem Pty Ltd, Seven Hill, New South wales, Australia)

3.8 Sodium chloride (NaCl: Analytical reagent, UNIVAR, Ajax Finechem Pty Ltd, Seven Hill, New South wales, Australia)

3.9 Cupric acetate ($Cu(CH_3COO)_2$: UNIVAR, Ajax Finechem Pty Ltd, Seven Hill, New South wales Australia)

3.10 Phosphoric acid (H_3PO_4: CH_3COOH ; Baker Analyzed®, Mallinckrodt Baker, Phillipsburg, New Jersey, USA)

3.11 Glacial acetic acid (CH_3COOH : Baker Analyzed®, Mallinckrodt Baker, Phillipsburg, New Jersey, USA)

3.12 Acetic acid ($C_2H_4O_2$: Analytical grade,Brightchem SDN BHD, Rawang Selangor)

3.13 Standard oleic acid, monoolein, diolein and triolein of HPLC grade: (Sigma-Aldrich Chemical Co., Sigma, St.Louis, Missouri, USA)

3.14 Standard octacosanol ($C_{28}H_{58}O$) and heptacosanol ($C_{27}H_{56}O$: Sigma-Aldrich Chemical Co., Sigma, St.Louis, Missouri, USA)

Methods

1. Influences of mono-and di-acylclycerols on thermophysical properties of rice bran oil and rice bran oil-milk fat blends before and after aging and storage

1.1 Characteristics of mono-and di-acylglycerols concentrated from deodorizer distillate of rice bran oil refinery

Deodorizer distillate (DD), a co-product from the de-acid step of the physical refining process of RBO, was used as the raw material for molecular distillation (MD) to evaporate FFAs. The unevaporated fractions, designated as UMDs, were obtained after processing at different operating temperatures of 120, 140 and 160°C at 0.1 Pa and 10.4 kg/h flow rate. The UMDs were characterized as detailed below.

1.1.1 Thermal properties

Ten mg samples of UMDs obtained at different operating temperatures were weighed into individual stainless steel pan and analyzed by differential scanning calorimetry (DSC) (Pyris 1; PerkinElmer, Norwalk, CT, USA). The DSC program was set for the following cycle: heating from 25 °C to 90 °C and holding at 90 °C for 3 min, cooling from 90 °C to (-)60 °C at 10 °C/min and holding at (-)60 °C for 3 min, and heating from (-)60 °C to 90 °C at 10 °C/min. The onset temperature (*To*) and end temperature of melting (*Te*) were determined (Ortiz-Gonzalez *et al*., 2007).

1.1.2 Composition of the unevaporated fractions after molecular distillation (UMDs)

1.1.2.1 Ratio of mono-and di-acylglycerol

Saponifiable matter in the UMDs obtained after MD process at different temperatures was determined by high-performance thin-layer chromatography (HPTLC) (Camag, Berlin, Germany). First, a silica plate was pre-developed in hexane and diethyl ether using a ratio of 1:1 (v/v). The plate was activated at 110 °C to remove impurities. Next, 5, 10 and 15 μL of standards and the UMD samples were spotted near the bottom of the plate using a glass micro-syringe. The plate was first developed at a distance of 4.5 cm from the origin. The solvent system consisted of a mixture of methyl acetate: isopropanol: chloroform: methanol: 0.25% (w/v) KCl in a ratio of 25: 25: 25: 10: 9 by volume. The plate was dried over NaOH in a desiccator for 30 min. Second development of the plate was performed at a distance of 9.5 cm in a mixture of hexane: diethyl ether: glacial acetic acid in a ratio of 80: 20: 2 (v/v). Separate lipid classes were detected by spraying with 3% (w/v) cupric acetate in 8% (w/v) phosphoric acid, followed by charring at 160 °C for 20 min to visualize the bands (Olsen and Henderson, 1989).

1.1.2.2 Determination of γ-oryzanol content

The γ-oryzanol content in UMD samples was evaluated by spectrophotometric technique (Khatoon and Gopalakrishna, 2004). Briefly, 10 mg of sample was weighed into a 10 mL volumetric flask. Hexane was used to dissolve the sample and adjust the volume. The γ-oryzanol content was determined by measuring the absorbance at 314 nm using a UV-Vis spectrophotometer (Spectronic GENESYS 10; Thermo Scientific, Waltham, MA, USA). The γ-oryzanol content was then calculated as follows: Eq.(1)

$$\gamma - \text{oryzanol content (mg/100g)} = \frac{\text{Absorbance at 314 nm in hexane solution} * 10000}{\text{g of sample} * 358.9} \quad (1)$$

1.2 Thermal characteristics of rice bran oil (RBO) supplemented with the unevaporated fraction (UMD) and commercial mono-and di-acylglycerol (MDG)

One g samples of RBO, RBO supplemented with 1% UMD obtained after distillation at 140 °C, RBO supplemented with 1% commercial MDG, and RBO supplemented with 1% UMD and 1% commercial MDG were heated at 70 °C. Fifteen mg samples were weighed into stainless steel pans and analyzed by DSC. The DSC program was set for the following cycle: heating from 25 °C to 60 °C and holding at 60 °C for 3 min, cooling from 60 °C to (-)60 °C at 10 °C/min and holding at (-)60 °C for 3 min, and heating from (-)60 °C to 60 °C at 10 °C/min. The onset temperature (*To*) and end temperature of melting (*Te*) were determined. Solid fat content (SFC) was calculated by dividing the partial area under the melting curve by the total area from (-)60 to 60 °C and multiplying by 100 (Ortiz-Gonzalez *et al*., 2007).

1.3 Apparent viscosity of rice bran oil (RBO) and RBO mixed with anhydrous milk fat (RBO-AMF) and presence/absence of the unevaporated fraction (UMD) and commercial mono-and di-acylglycerol (MDG)

RBO and RBO-AMF in the absence or presence of 1% UMD obtained after distillation at 140 °C, or 1% commercial MDG were melted at 70 °C and cooled down to 25 °C. The apparent viscosity of each sample was measured using a Brookfield viscometer equipped with a UL adapter (DV-III programmable rheometer; Brookfield Engineering, Middleborough, MA, USA) at 60 rpm and 25-28 °C.

1.4 Effect of aging regime on liquid oil holding capacity by solid fat of RBO and RBO-AMF with added surfactants

The volume of solid fat phase separated from liquid oil was determined. RBO and RBO-AMF in the absence or presence of 1% UMD obtained after distillation at 140 °C, or 1% commercial MDG were characterized for the volume of solid fat phase after aging at 5 °C and storing at 30 °C. First, 1.5 L of samples with designated surfactants added were heated at 70 °C and then cooled to (-)22 °C in a scraped-surface freezer (KATOMO, China) at a cooling rate of 5.5 °C/min to crystallize fat. Ten mL of each sample was put into a plastic 15 mL centrifuge tube with a marked volume. The samples were aged at 5 °C for 12 h or 24 h; then stored at 30 °C for 12 h or 24 h and the liquid oil was discarded. The opaque solid fat phase in the centrifuge tube was measured and calculated as % volume of solid fat phase.

1.5 Composition of physically refined RBO and AMF

Fatty acids composition in RBO and AMF were determined by gas chromatographic technique using method TMC-05: Mixed standard fatty acid C_4-C_{22} (ACFS. 2003).

2. Influences of high melting point surfactant and rice bran wax on thermophysical properties of solidified rice bran oil before and after aging storage

Sample preparation

The RBO blended with different types and concentrations of RBW and surfactants were prepared using RBO as a control treatment. The treatments include (i) RBO added with 1% MDG or 1% SP; (ii) RBO added with 5% crude wax to provide 0.65% RBW, together with 1% MDG or 1% SP; and (iii) RBO added with 10 % crude wax to provide 1.3% RBW, together with 1% MDG or 1% SP. Each

blend was heated at 90 °C to solubilize RBW and surfactant in RBO until the RBO blends were clear.

2.1 Characteristics of crude wax

2.1.1 Determination of rice bran wax (RBW) content and types of policosanol in crude wax

Crude wax obtained from winterizing step during physical refining process was determined for rice bran wax (RBW) content by washing crude wax with hexane and isopropanol in a Soctex apparatus (Soxtec system HT1043 Extraction Unit, Tecator, Hoganas, Sweden) to wash out non-polar fractions. Briefly, 70 g of crude wax was extracted by 50 mL of hexane at 65 °C for 30 min, chilled for at 5°C for 2 h, and filtered to remove solvent and residual TAGs using filter paper. The undissolved fraction after solvent extracting with hexane and chilling was washed with 95 mL hot hexane and 50 mL isopropanol in a Soctex at 80 °C for 30 min, chilled at 5 °C for 2 h and filtered to remove solvent to obtain white crystal designated as rice bran wax (RBW). The residual solvent in RBW was evaporated in a hot air oven at 70 °C and RBW was accurately weighed. The concentration of RBW in crude wax was calculated as shown in Eq.(2):

$$RBW\ (\%) = \frac{Weight\ (g)\ of\ RBW\ after\ solvent\ extraction}{Weight\ (g)\ of\ crude\ wax\ before\ extraction} \times 100 \qquad (2)$$

Selected policosanols in crude wax was determined by a high-performance thin-layer chromatography (HPTLC). First, octacosanol standard and heptacosanol standard, as well as crude wax samples were dissolved in chloroform. A silica plate was pre-developed in hexane and diethyl ether using a ratio of 1:1 (v/v). The plate was activated at 110 °C to remove impurities. Next, 5, 10 and 15 μL of standards and RBW samples were spotted near the bottom of the plate using a glass

micro-syringe. The plate was first developed at a distance of 9.5 cm from the origin. The solvent system consisted of a mixture of hexane: diethyl ether: acetic acid 85:15:2 (v/v). Separate lipid classes were detected by spraying with 3% (w/v) cupric acetate in 8% (w/v) phosphoric acid, followed by charring at 150 °C for 30 min to visualize the bands using method described by Hwang *et al*. (2005).

2.1.2 Determination of thermal properties of crude wax

Ten mg samples of crude wax were weighed into individual stainless steel pans and analyzed by differential scanning calorimetry (DSC) (Pyris 1; PerkinElmer, Norwalk, CT, USA). The DSC program was set for the following cycle: heating from 25 °C to 90 °C and holding at 90 °C for 3 min, cooling from 90 °C to (-)60 °C at 10 °C/min and holding at (-)60°C for 3 min, and heating from (-)60 °C to 90 °C at 10 °C/min. The onset temperature (*To*) and end temperature of melting (*Te*) were determined.

2.2 Effect of surfactants on thermal properties of RBO containing crude wax

Thermal characteristics of RBO blends containing different concentrations of RBW (0-1.3% w/w), surfactants (0-1% w/w) were determined. The RBO added with crude wax and surfactants were heated at 90 °C until clear liquid was obtained. Fifteen mg of oil blends were weighed into stainless pan and analysed by DSC (Pyris1). The DSC program was set following cycle: heating from 25 to 90 °C and holding at 90 °C for 3 min, cooling from 90 °C to (-)60 °C at 10 °C / min and holding at (-)60 °C for 3 min and heating from (-)60 °C to 90 °C at 10 °C / min. Melting enthalpy and temperature data of melting such as *To, Tp, Te,* range of melting temperature and enthalpy were determined. Solid fat content was calculated from thermograms by dividing the partial area under the melting curve with total area and multiplied by 100 (Ortiz-Gonzalez *et al*., 2007).

The influences of RBW and surfactants on thermal properties of RBO blends were summarised by cluster analysis (SPSS Software version 12, SPSS Inc,Chicago, lllinois, USA.). This technique is often used to identify the objects in the same group that are more similar to each other than those in other groups. The order of dissimilarity was shown as a distance index displayed as dendrogram (Mooi, and Sarstedt, 2011). For this study, cluster analysis used to produce data from dendograms explained the effects of RBW, MDG and SP on thermal properties of RBO blends based on their statistical similarity.

2.3 Effect of crude wax and surfactants on viscoelastic properties of rice bran oil during structure-forming process (cooling loop) and fat crystal network melting (heating loop)

Thermo-mechanical characteristics of RBO blend containing different concentration of RBW (0-1.3 % w/w) from crude wax and surfactants (0-1 % w/w) were determined using an Anton Paar Modular Compact Rheometer (MCR300) equipped with a coaxial cylinder measuring geometry (CC 17, Couette cell). The RBO added with crude wax and surfactants were heated at 90°C until clear liquid was obtained.

Twenty mL of RBO blends were transferred into a cylinder base and rheological data were analysed using a program set as following cycle: heating from 25 to 70 °C and holding at 70 °C for 3 min, cooling from 70 °C to (-)15 °C at 2 °C/min and holding at (-)15 °C for 3 min, and heating from (-)15 °C to 70 °C at 2 °C/min. Heating and cooling rates were set at 2 °C/min. The measurements were performed at a strain of 0.001, which was in the linear regime and a frequency of 1 Hz. Changing of viscoelastic transition of sample from viscous (G″) to elastic (G′) and elastic (G′) to viscous (G″) were recorded together with transition temperature and time.

2.4 Effect of RBW and surfactants on stability of solidified RBO after aging at 5°C

Thermo-stability of RBO blends containing different concentration of RBW (0-1.3% w/w) and surfactants (0-1% w/w) were determined. Ten mL of RBO added with crude wax and surfactants in a 14 mL bottle was heated at 90 °C until clear liquid was obtained, cooled in a freezer at (-)22 °C for 1 h to induce nucleation of fat crystal, and aged at 5 °C for 24 h. The bottles of sample were inverted and let stand at 22 °C. Thermo-stability of RBO oleogel was recorded as the time required before samples flew completely.

3. Influence of ethyl cellulose (EC) and rice bran wax (RBW) concentration on rheological properties of rice bran oil oleogel

Preparation of RBO oleogel containing different oleogelator

The RBO-EC, RBO-RBW and RBO-EC-RBW samples were prepared by base on of 100%RBO exclude RBO in crude wax. The RBO blends containing ethyl cellulose (EC) at 2.50%, 3.75% and 5.00% were prepared by gradually mixed EC in RBO and heated the blends to 180 °C within 30 min. RBO-EC blends were stirred continually with magnetic stirrer to ensure that the RBO-EC were clear liquid. RBO mixed with crude wax and ethyl cellulose (EC) were prepared to obtain final concentration of RBW of 0.65%, 1.30% and 1.95% RBW. The RBO-RBW blends were heated up to 90 °C until RBW absolutely melted, then the EC was gradually dispersed in a hot oil blends to obtain final concentration of 2.50%, 3.75% and 5.00% EC in RBO-RBW-EC mixtures. The mixtures were further heated to 180 °C within 30 min and stirred continuously with magnetic bar until no more solids were seen in liquid oil blends. After that, the samples were cooled at room temperature (25 °C) for 24 h.

3.1 Effect of ethyl cellulose (EC) and rice bran wax (RBW) concentration on rheological properties of rice bran oil oleogels containing different types of oleogelator

A controlled stress rheometer (Anton Parr, Germany) equipped with glass plate-and-plate geometry (43 mm diameter) with a gap of 1.2 mm was used to determine rheological properties of RBO-RBW, RBO-EC and RBO-RBW-EC oleogels. Frequency sweep tests at 0.5% strain, which was within the linear viscoelastic range of all samples, were performed from 0.1-100 Hz at 25 °C. The oscillatory rheological parameters used to compare the viscoelastic properties were storage modulus (G′) and loss modulus (G″).

4. Use of rice bran oil oleogel containing rice bran wax and ethyl cellulose (RBO-RBW-EC) in preventing salt sedimentation

4.1 Influence of EC and RBW concentrations on (resistance to) salt sedimentation

RBO containing different concentration of RBW and EC were prepared. After clear liquid oil blends were obtained, 5 g of oil blends was poured into a glass centrifuge tube, and cooled at room temperature (25 °C). Salt (NaCl) was dispersed in the oil blends to obtain the final concentration of 15% salt manually using a spatula. The samples were stored at 90 °C for overnight.

For salt sedimentation test, samples were centrifuged at 500 rpm at 25 °C for 10 min to separate salt to the bottom of the tubes. After that, the supernatant RBO was removed from the tubes to get salt sediment. The sedimented salt was washed using petroleum ether to remove residual oil phase, dried in a hot air oven at 90 °C (1h) and weighed. The % salt sedimentation was calculated as shown in Eq.3:

$$\% \text{ Ws} = \frac{(W_{tube+salt} - W_{tube}) \times 100}{W_{salt}} \qquad (3)$$

where Ws is the weight of sedimented salt, $W_{tube+salt}$ is the weight of centrifuge tube and sedimented salt in the centrifuge tube after washing the oil out with petroleum ether and drying at 90 °C (1h), W_{tube} is Weight of initial centrifuge tube, and W_{salt} is the weight of initial salt added at the beginning.

4.2 Effect of liquid RBO, RBO-RBW oleogel, and RBO-RBW-EC oleogel on the qualities of marinating pork steak before and after grilling

Marinade formulation

Liquid RBO and RBO oleogels containing different concentrations of RBW and EC were mixed with 19% salt, 10% dried spice and 2% paprika extract and aged overnight at room temperature (25 °C) before marinating with pork steak.

Marination of pork steak

Marinated pork steaks were prepared by manually mixing the marinades. The pork steaks before marinade were kept at 2-4 °C. Pork steak marinated with 2.1% salt and 1.1% dried spice was used as a control sample designated as "dried spice" treatment. The RBO oleogel marinades were prepared in the presence of 1.3% RBW (designated as RBO-RBW oleogel), or of 3.75%EC (designated as RBO-EC), or 1.3% RBW and 3.75%EC (designated as RBO-RBW-EC). They were mixed with 10% salt and spice before marinating.

Marinated pork steak samples were chilled at 2 °C for 24 h and then the samples were analyzed for marinade retention. Moreover, samples after marinating and aging at 2 °C for 48h were grilled at 260 °C for 5 min on each side until internal

temperature of steak at 75 °C was reached. The sample were analyzed for cooking loss and cooking yield.

4.2.1 Determination of marinade retention in raw marinated pork steak

The weight of raw marinated pork steak before and after suspending on a sieve tray for 24 h at 2-4°C was determined. The difference in the weight was calculated and reported as % marinade retention as shown in Eq. 4:

$$\% \text{ marinade retention} = [(w1 - w2)/w1]*100 \quad (4)$$

where w1 is the weight of marinade used and w2 is the weight of marinade flow through the sieve collected on a tray.

4.2.2 Determination of weight loss in grilled marinated pork steak

The weight loss after cooking the marinated steak with different types of RBO and RBO oleogels were determined after grilling at 260°C and calculated as shown in Eq. 5:

$$\% \text{ weight loss} = [(w3 - w4)/w3]*100 \quad (5)$$

where w3 is the weight of marinated steak before grilling and w4 is the weight of grilled steak.

4.2.3 Determination of sensorial attributes of raw marinated steak and grilled marinated steak

Raw marinated pork steak and grilled marinated pork steak were evaluated by 20 untrained panelists resided in Stuttgart. Samples were labeled with a random three-digit number and using 9-point hedonic scale for evaluation. For raw marinated pork steak, the appearance, odor, overall liking and % likelihood of buying

were asked. For grilled marinated pork steak, the panelists were asked to evaluate their acceptance for appearance, odor, taste, juiciness and overall liking.

5. Statistical analysis

The data were analyzed by analysis of variance (ANOVA) at a significance level of $P<0.05$. Significant differences between the treatments were analyzed by Duncan's multiple range test (DMRT). All statistical analyses were performed using SPSS software version 12 (SPSS, Chicago, lllinois, USA). Moreover, the effect of RBW and surfactants addition on thermal properties was explained by cluster analysis, which was displayed as dendrogram showing the order of dissimilarity between groups.

RESULTS AND DISCUSSION

Results

1. Influences of mono- and diacylglycerols on thermophysical properties of rice bran oil and rice bran oil-milk fat blends before and after aging and storage

1.1 Characteristics of mono- and diacylglycerols concentrated from deodorizer distillate of rice bran oil refinery

Figure 18 illustrates the thermograms of UMDs obtained after molecular distillation (MD) process at different temperatures, i.e. 120, 140 and 160 °C, at 0.1 Pa and a flow rate of 10.4 kg/h. The UMDs obtained at distillation temperatures of 140 and 160 °C started melting at (-) 46 °C. However, the UMD obtained at a distillation temperature of 120 °C started melting at (-) 29 °C. All UMDs completely melted at 38 °C. Similar thermograms of UMDs obtained after distillation at 140 and 160 °C suggested that both UMDs had similar constituents, but they were different from those of the UMD obtained after MD process at 120 °C. Unlike the UMDs obtained from distillation at high temperature, the UMD obtained after distillation at 120 °C showed an endothermic peak between around (-) 29 and (-) 9 °C.

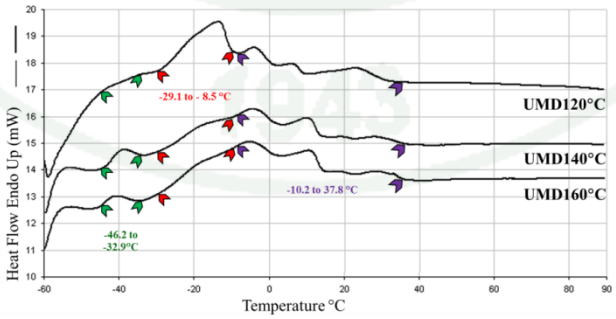

Figure 18 Effect of distillation temperature during molecular distillation on melting profiles of the unevaporated fraction (UMD) of deodorizer distillate from physically refining process of RBO.

The endothermic peak was most likely residual FFAs present in the UMD; this was confirmed by HPTLC chromatograms as a band of oleic acid, which was found only in the UMD obtained after distillation at 120 °C (Figure 19). The constituents from UMDs obtained at different distillation temperature contained TAGs the most, followed by DAGs or MAGs depending on distillation temperature. The HPTLC chromatograms showed only triolein, diolein and monoolein as compared to the standards.

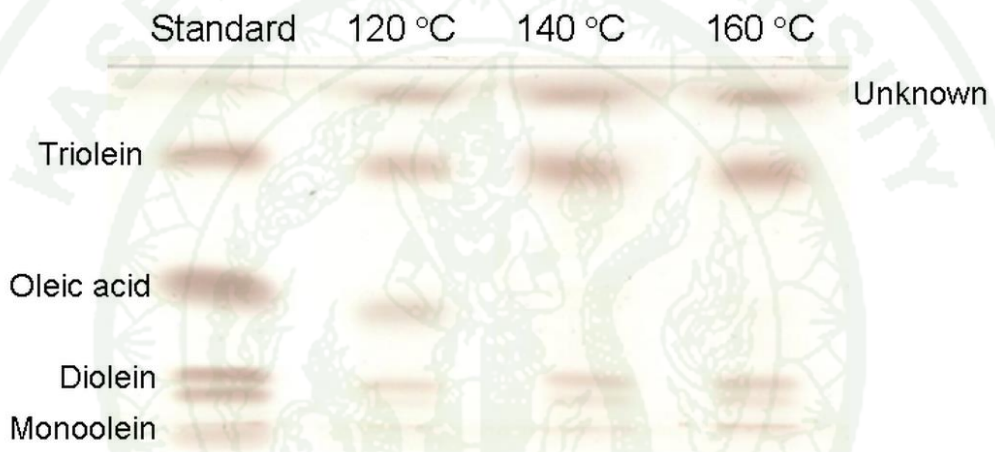

Figure 19 Effect of distillation temperature during molecular distillation on the profile of non-polar compounds of the unevaporated fractions (UMD), determined by high-performance thin-layer chromatography.

Densitometric analysis revealed differences in the ratios of non-polar fractions of FFA: MAG: DAG: TAG in UMDs obtained after distillation at different temperatures (P<0.05; Table 2). The increase in the distillation temperature from 120 °C to 140 °C markedly reduced FFA content. TAG still remained at a level of more than 50% in all UMDs, regardless of distillation temperature. The increase in temperature from 140 °C to 160 °C during MD process, however, did not significantly change the γ-oryzanol content.

The UMD obtained after distillation at 140 °C (UMD_{140}) was used in further investigations as the source of mono- and diacylglycerols from rice bran source on physical characteristics of RBO blends, since the UMD_{140} contained no FFA, had high γ-oryzanol content, and the MAG: DAG ratio was 0.1: 0.2 (Table 2).

Table 2 Effect of distillation temperature during molecular distillation on the mass ratios of non-polar fractions and γ-oryzanol content in the unevaporated fraction (UMD).

Characteristics	Distillation temperature during molecular distillation		
	120 °C	140 °C	160 °C
Melting temperature range (°C)			
First range	Not detected	(-)46.2 - (-)32.9	(-)46.2 - (-)32.9
Second range	(-)29.1 - (-)8.5	Not detected	Not detected
Third range	(-)10.2 - 37.8	(-)10.2 - 37.8	(-)10.2 - 37.8
Mass ratios of saponifiable fractions			
Free fatty acid	$0.20^{a} \pm 0.04$	$0.00^{b} \pm 0.00$	$0.00^{b} \pm 0.00$
Monoacylglycerol	$0.30^{a} \pm 0.05$	$0.10^{b} \pm 0.00$	$0.30^{a} \pm 0.01$
Diacylglycerol	$0.00^{c} \pm 0.01$	$0.20^{a} \pm 0.01$	$0.10^{b} \pm 0.02$
Triacylglycerol	$0.50^{c} \pm 0.00$	$0.70^{a} \pm 0.01$	$0.60^{b} \pm 0.01$
Rice phytochemicals			
γ-oryzanol (mg/100g)	$840.00^{b} \pm 0.02$	$1030.00^{a} \pm 0.01$	$1030.00^{a} \pm 0.03$

Mean values in the same row followed by different superscripts are significantly different ($P < 0.05$).

1.2 Thermal characteristics of rice bran oil (RBO) supplemented with the unevaporated fraction (UMD) and commercial mono- and diacylglycerol (MDG)

The commercial MDG contained 62.39% palmitic acid, 30.64% stearic acid, 1.87% myristic acid, 0.46% lauric acid, 0.21% arachidic acid and 0.04% capric

acid. It is apparent that the commercial MDG had high content of saturated fatty acid; while the majority of the MAG and DAG in UMD was monounsaturated fatty acid of oleyl esters. Thermograms of RBO containing UMD and/or commercial MDG are shown in Figure 20. The addition of UMD and/or commercial MDG did not significantly change the melting characteristics of RBO although they were different in terms of chemical composition and melting point. The melting point range of UMD was between (-) 46.2 to 37.8 °C (Table 2); while the melting point range of commercial MDG was between 45-65 °C (results not shown). The melting temperature of RBO, in the absence or presence of surfactants, lay within a range of (-) 30 to 5 °C. This was due to the low concentration of the surfactant of 1-2%, which was lower that the concentration used to induce nucleation and crystallization of the surfactants (Ojijo *et al.*, 2004). Such low concentration was selected due to food additive regulations for the use of surfactants in fat products of not exceeding 1% (Moonen and Bas, 2004).

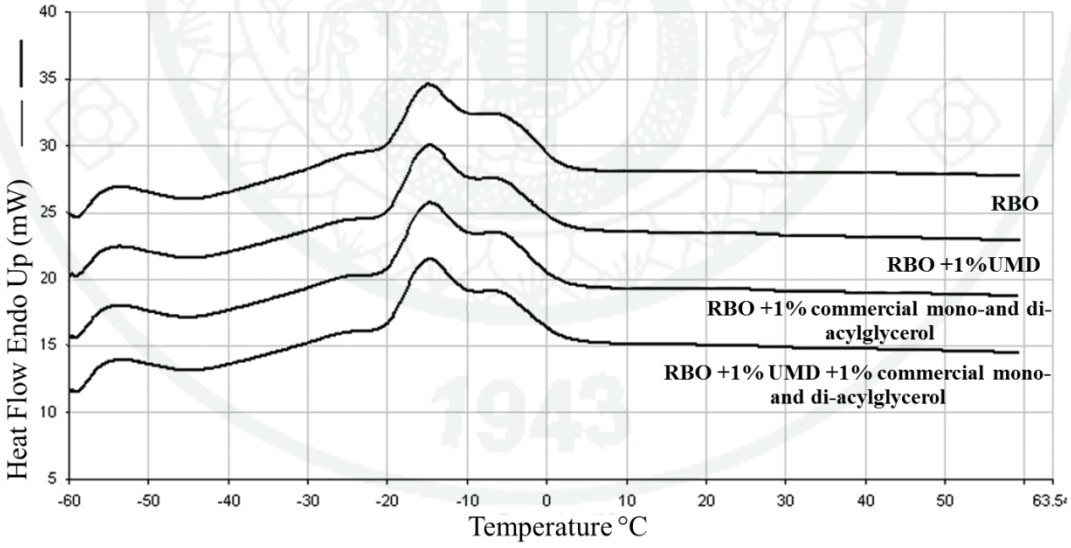

Figure 20 Effect of surfactant addition on the melting profiles of rice bran oil (RBO). The surfactants used were the unevaporated fraction after molecular distillation at 140 °C (UMD) and commercial mono- and diacylglycerol (MDG).

From practical standpoints, physically refined RBO was prone to clouding when stored at low temperatures (15 and 25 °C) as in the refrigerator or in temperate zone, observed as the solid fat content (SFC) at low temperature (Table 3). Although the melting profiles of RBO supplemented with UMD and commercial MDG were not significantly different, addition of UMD and MDG slightly increased SFC of RBO at 15 °C (P<0.05). The presence of MDG slightly increased the SFCs of RBO at 25 °C (P<0.05), indicating that commercial surfactant could induce nucleation of solid fat crystal RBO shown as clouding defect in liquid oil. However, such crystallization of solid fat was too low to form fat crystal network between 15-35 °C.

Table 3 Effect of surfactant addition on the onset of melting (*To*), end of melting temperarture (*Te*) and solid fat content (SFC) of rice bran oil (RBO). Surfactants used were the unevaporated fraction after molecular distillation at 140 °C (UMD) and commercial mono- and diacylglycerol (MDG)

Treatments	RBO	RBO +1% UMD	RBO +1% commercial MDG	RBO + 1% UMD + 1% commercial MDG
To (°C)	(-)30.6^{a} ± 1.0	(-)28.5^{a} ± 1.2	(-)28.6^{a} ± 1.1	(-)27.7^{a} ± 1.6
Te (°C)	4.9^{a} ± 0.7	4.9^{a} ± 0.3	5.4^{a} ± 0.6	5.0^{a} ± 0.4
SFC at 15°C (%)	0.68^{c} ± 0.0	0.77^{b} ± 0.1	0.84^{ab} ± 0.0	0.88^{a} ± 0.1
SFC at 25°C (%)	0.39^{b} ± 0.0	0.48^{ab} ± 0.1	0.58^{a} ± 0.0	0.56^{a} ± 0.1
SFC at 35°C (%)	0.12^{a} ± 0.0	0.11^{a} ± 0.0	0.13^{a} ± 0.0	0.13^{a} ± 0.0

Mean values (± standard deviation) in the same row followed by different superscripts are significantly different (P<0.05).

1.3 Apparent viscosity of rice bran oil (RBO) and RBO mixed with anhydrous milk fat (RBO-AMF) and presence/absence of the unevaporated fraction (UMD) and commercial mono-and di-acylglycerol (MDG)

The addition of UMD did not affect the apparent viscosity of RBO and mixed RBO-AMF at the ratio of 75:25. However, the addition of commercial MDG increased the apparent viscosity of RBO and RBO-AMF (P<0.05; Table 4). This suggested that the solid fat particles induced by commercial MDG, despite little amount, could induce nucleation that resisted liquid flow of RBO observed as a slight increase in viscosity of RBO-MDG blend. Although the presence of UMD caused a minute amount of SFC to be retained at 25°C (Table 3), it did not affect the viscosity of RBO at SFC similar to that of MDG (Table 4). The influences of both surfactants on solid fat particle, aging, and storage of RBO at above melting temperature of 5°C were then investigated further.

Table 4 Effect of surfactant addition on apparent viscosity of rice bran oil (RBO) and rice bran oil-anhydrous milk fat (RBO-AMF) blended at a ratio of RBO to AMF of 75:25. Surfactants used were the unevaporated fraction after molecular distillation (UMD) obtained at 140°C and commercial mono- and diacylglycerol (MDG). Viscosity was measured at 25°C.

Treatments	Apparent viscosity (mPa·s)
RBO	$79.2^{b} \pm 3.5$
RBO + 1% UMD	$75.9^{b} \pm 1.7$
RBO + 1% commercial MDG	$88.6^{a} \pm 3.2$
RBO-AMF	$75.9^{b} \pm 9.4$
RBO-AMF + 1% UMD	$73.6^{b} \pm 2.3$
RBO-AMF + 1% commercial MDG	$85.6^{a} \pm 2.8$

Mean values (± standard deviation) followed by different superscripts are significantly different (P<0.05).

1.4 Effect of aging regime on liquid oil holding capacity by solid fat of RBO and RBO-AMF with added surfactants

The influence of UMD and commercial MDG on the ability of fat crystal network of oil phase and/or self-assembled surfactant network to hold liquid oil at a normal room temperature range in Thailand (25-30 °C) was further investigated. The storage stability investigation was carried out after different aging time at the temperature close to melting temperature of RBO (Table 5).

During the preparation of oil blends prior to aging, the RBO and RBO-AMF were liquefied and cooled to crystallize fat in a scraped-surface freezer at (-) 22 °C. Then, the solidified oil blends were aged at 5°C for 12 h or 24 h and stored at 30°C for another 12 or 24 h (Table 5). After aging, the RBO aged at 5°C for 12 h and 24 h, both in the absence or presence of UMD, melted thoroughly (Table 5), since the temperature was the end temperature (*Te*) of crystallized RBO (Table 3). Prolonging aging time at 5°C from 12 h to 24 h did not help structure-forming process of UMD to entrap liquid RBO. This is likely due to the similarity of oleyl ester of MAG and DAG in the UMD, which were close to that of major fatty acid of RBO (Table 6). Thus, the MAG and DAG in UMD could not help forming surfactant network during aging to hold liquid RBO during storage at 30°C.

Table 5 Effect of aging and surfactant addition on % volume of solid fat phase in rice bran oil (RBO) and rice bran oil–anhydrous milk fat (RBO-AMF) blended at a ratio of RBO to AMF of 75:25. Surfactants used were the unevaporated fraction after molecular distillation at 140°C (UMD) and commercial mono- and diacylglycerol (MDG).

Types of oil blend	% Volume of solid fat phase					
	Aged at 5°C, 12 h			Aged at 5°C, 24 h		
	Before storage at 30 °C	Storage at 30°C for 12 h	Storage at 30°C for 24 h	Before storage at 30 °C	Storage at 30°C for 12 h	Storage at 30°C for 24 h
RBO	$0.0^{b} \pm 0.0$	$0.0^{c} \pm 0.0$	$0.0^{c} \pm 0.0$	$0.0^{b} \pm 0.0$	$0.0^{c} \pm 0.0$	$0.0^{c} \pm 0.0$
RBO + 1% UMD	$0.0^{b} \pm 0.0$	$0.0^{c} \pm 0.0$	$0.0^{c} \pm 0.0$	$0.0^{b} \pm 0.0$	$0.0^{c} \pm 0.0$	$0.0^{c} \pm 0.0$
RBO +1% commercial MDG	$100.0^{a} \pm 0.0$	$17.6^{b} \pm 2.8$	$17.6^{b} \pm 2.8$	$100.0^{a} \pm 0.0$	$46.4^{b} \pm 3.9$	$34.5^{b} \pm 2.9$
RBO-AMF	$100.0^{a} \pm 0.0$	$0.0^{c} \pm 0.0$	$0.0^{c} \pm 0.0$	$100.0^{a} \pm 0.0$	$0.0^{c} \pm 0.0$	$0.0^{c} \pm 0.0$
RBO-AMF +1% UMD	$100.0^{a} \pm 0.0$	$0.0^{c} \pm 0.0$	$0.0^{b} \pm 0.0$	$100.0^{a} \pm 0.0$	$0.0^{c} \pm 0.0$	$0.0^{c} \pm 0.0$
RBO-AMF +1% commercial MDG	$100.0^{a} \pm 0.0$	$89.4^{a} \pm 11.1$	$92.9^{a} \pm 5.4$	$100.0^{a} \pm 0.0$	$93.8^{a} \pm 6.9$	$92.5^{a} \pm 7.1$

Mean values (± standard deviation) in the same column followed by different superscripts are significantly different(P<0.05).

Table 6 Fatty acid composition of physically refined rice bran oil (RBO), anhydrous milk fat (AMF) and rice bran oil blended with anhydrous milk fat (RBO-AMF) at a mass ratio of RBO to AMF of 0.75:0.25.

Fatty acid	g/100 g RBO	g/100 g AMF	g/100g RBO-AMF blend (calculated)
Caprylic acid (C8:0)	-	1.36	0.34
Capric acid (C10:0)	-	5.20	1.30
Lauric acid (C12:0)	-	7.24	1.81
Myristic acid (C14:0)	0.51	17.58	4.78
Palmitic acid (C16:0)	24.21	33.22	20.46
Stearic acid (C18:0)	1.70	9.09	3.55
Arachidic acid (C20:0)	0.40	-	0.30
Total of saturated fatty acid	26.82	73.69	32.54
Palmitoleic acid (C16:1)	0.21	1.47	0.53
Oleic acid (C18:1, cis-9)	40.87	20.33	35.74
Linoleic acid (C18:2, cis)	29.07	0.85	22.02
γ-Linolenic acid (C18:3n6)	0.45	0.55	0.48
Eicosenoic acid(C20:1)	0.50	0.97	0.62
Total of unsaturated fatty acid	71.1	24.17	59.39

However, when the commercial MDG (which contained above 90 % of saturated fatty acid was used as structurant holding liquid oil, it was found that the RBO-commercial MDG and RBO-AMF-commercial MDG blends remained solidified at 5 °C prior to storage. This was due to both fat crystal networks generated by MDG and/or AMF. After storage at 30 °C for 12 h, all samples melted although to the different degree. Solidified RBO-commercial MDG blend aged at 5 °C for 12 h could retain the volume of solid fat phase of 17% after storing at 30 °C, although the RBO contained mostly unsaturated fatty acid (Table 6). A longer aging time at 5 °C of 24 h resulted in a more stable network holding liquid RBO than an aging time of 12 h. This was due to the presence of commercial MDG, which initiate fat crystal formation or seeding in RBO during aging at 5 °C, as well as the formation of self-assembled surfactant network holding liquid RBO. Such network could stabilize solidified RBO to some extent at 30 ° C up to 24 h although the MDG was present at a low concentration of 1%. Prolonging aging time at 5 °C from 12h to 24h even enhanced the stability of solidified RBO at 30 °C to the higher extent. Since commercial MDG was present at only 1%, it is likely that the self-assembled commercial MDG was responsible for solid gel structure of RBO, a so-called oleogel, as mentioned in Section 2.2.1.

When AMF was blended with RBO to alter the saturated fatty acid ratio and create varying molecular composition of fat to enhance segregation of fat crystal, it was found that the solid fat phase was stabilized and the volume of solid phase was retained at 100% in solidified RBO-AMF prior to storage at 30 °C. However, when the aged RBO-AMF blends, both in the absence or presence of UMD, were stored at 30 °C, they melted thoroughly despite the increased proportion of saturated fatty acids from AMF. This corroborated that the acyl group of surfactants played an important roles in initiating nucleation and fat crystal network during aging rather than the acyl groups in bulk oil phase, otherwise the fat crystal network of RBO-AMF would have been retained after storage at 30 °C. The melting point of AMF was within the range of 31-34 °C (according to manufacturer's datasheet). At 30 °C, AMF alone could retain SFC around 45% (Tuntragul and Hongsprabas, 2010).

The results revealed that although UMD increased SFC (Table 4), it could not stabilize the solid fat phase, particularly when RBO was subjected to storage at 30 °C. In the presence of UMD, RBO-AMF remained in a liquid state although it contained a high content (38.54%) of saturated fatty acids. On the other hand, with the addition of commercial MDG, RBO-AMF was able to retain the volume of solid fat phase, observed as 92.5-93.8% volume of solid fat phase at 30 °C, although up to 75% liquid RBO was present in the oil blends.

The results of this study suggested that although the surfactants, at a level of 1–2% of RBO, did not significantly affect the DSC melting profiles of RBO, they could affect other thermophysical properties of both RBO and RBO-AMF after the oils had been aged in their presence. The addition of commercial MDG to RBO-AMF could stabilize the solid fat network that held the liquid oil. This is due to the ability of commercial MDG to induce nucleation of solid fat crystals, as well as the formation of self-assembled surfactant during aging at 5 °C, and stabilize the solidied structure of RBO-AMF blends. For the case of RBO, the self-assembled MDG may, in part, be responsible for liquid oil holding after aging. This was due to the molecular rearrangement during aging as described by Chen and Terentjev (2011). Such influence of commercial MDG could be used in the fabrication of *trans*-free solidified vegetable oil at 30 °C as the replacer for hydrogenated edible fat.

Rice UMD, however, was not able to stabilize the aged RBO-AMF blends. This was probably due to the presence of DAG in the UMD, whose structure was most likely esterified by unsaturated fatty acids like oleic acid. Such molecular structure does not favor fat crystallization and therefore could prevent fat crystal network formation even in oil blends containing saturated fat from AMF.

It is apparent that fat crystal network of surfactants having different molecular acyl structures from those of bulk oil phase could help structuring solidified fat provided that the mixture was aged for 12-24 h at the temperature close to melting temperature of bulk oil phase. The commercial MDG, which had palmityl esterified mainly, could phase separate from the bulk oil phase of RBO, which contained oleic

acid as major fatty acid. Phase separation of commercial MDG thus led to the formation of self-assembled crystalline surfactant, that functioned as oleogelator holding liquid RBO after aging (Ojijo *et al*., 2004; Chen and Terentjev, 2011).

2. Influences of commercial MDG and rice bran wax (RBW) on thermophysical properties of solidified RBO before and after aging and storage

2.1 Characteristics of crude wax

Crude wax from winterizing step in physical refining process of RBO contain 87.09% TAGs and 12.91% rice bran wax (RBW) by weight in the form of crystal after crude wax was washed with hexane and isopropanol to remove TAGs and non-polar compounds. HPTLC revealed that the RBW contained long chain alcohol not extractable by hexane and isopropanol. Heptacosanol was found in crude wax after washing with hexane and isopropanol (Figure 21). However, the fatty acid profiles of crude wax were different from those in refined RBO. Crude wax contained higher ratio of palmitic acid than the refined RBO (Tables 6, 7). Crude wax from winterizing step showed two melting temperature ranges (Figure 22). The first peak was between (-)24.8 to 5.1 °C, which was close to the melting temperature range of RBO. This was due to the presence of residual TAGs of 87.09% in the crude wax. The second peak between 18.5 to 43.7 °C was most likely the melting temperature of high molecular weight compounds, particularly long chain alcohol (Table 8). Crude wax obtained from winterizing step was then used in the following experiments without removal of residual TAGs.

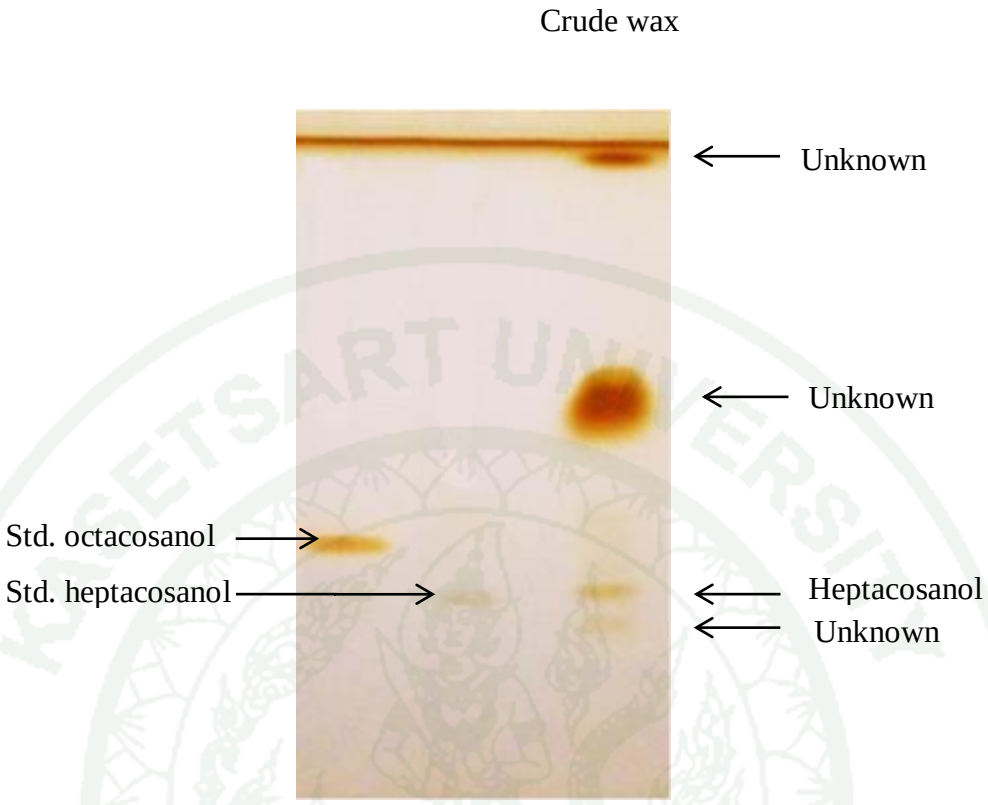

Figure 21 HPTLC plate indicating the presence of heptacosanol in crude wax from winterizing step in physical refining process of RBO.

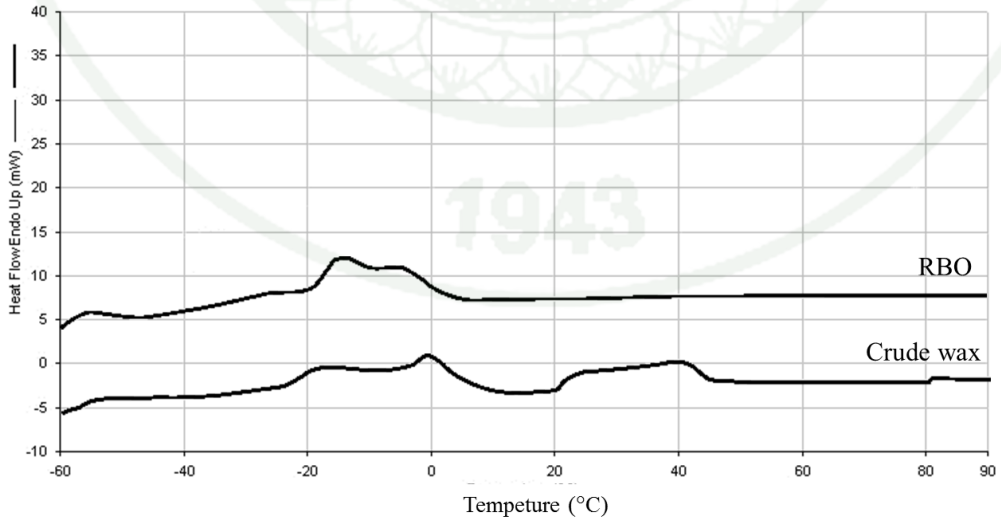

Figure 22 Thermogram of RBO and crude wax analyzed by DSC.

Table 7 Composition of fatty acid in crude wax.

Fatty acid g/100 g	Crude wax
Myristic acid (C14:0)	0.65
Palmitic acid (C16:0)	36.38
Stearic acid (C18:0)	2.78
Total of saturated fatty acid	39.81
Palmitoleic acid (C16:1)	-
Oleic acid (C18:1, cis-9)	33.55
Linoleic acid (C18:2, cis)	22.24
Total of unsaturated fatty acid	55.79

Table 8 Melting temperature of crude wax from physical refining process.

Sample	T_{onset}	T_{peak}	T_{end}
Peak 1	(-)24.78±0.88	(-)1.05± 0.09	5.14 ± 0.19
Peak 2	18.48±0.10	39.01±0.10	43.70±0.33

The presence of higher content of palmitic acid compared to normal range found in RBO, as well as the existence of long-chain alcohol and a high melting point compounds suggested potential use of crude wax to alter composition of bulk RBO phase in solidified RBO. Sucrose palmitate (SP) and commercial MDG, which had high contents of saturated fatty acids over 90% most of which was palmitic acid, were used as structurant or oleogelator by initiating nucleation and crystal growth of bulk RBO, as well as the formation of self-assembled surfactant network to hold bulk liquid oil at temperature higher than melting temperature of RBO and reported in Section 2.2.

2.2 Effect of RBW and commercial surfactants on thermal properties of RBO blends

The RBO had melting temperature range from (-)30 to 5 °C (Table 3). Addition of 1.3%RBW prepared from 10% crude wax with presence of surfactant increasing melting temperature of RBO (first endothermic peak; Table 9). The presence 1.3% RBW and addition surfactant increased *To*, *Tp*, range of temperature and *Te* of RBO. Furthermore, the presence of 1% MDG did not significantly change *To*, *Tp*, range of temperature, *Te* and ΔH of RBO-RBW (Table 9). However, the presence of SP decreased *Te* of RBO-RBW (Table 9). Moreover, Addition of 1.3% RBW could result in the 2nd endothermic peak within the range of 11.2 to 26.9 °C (Table 9, Figure 23). Addition of 1% MDG further increased the *To*, *Te* and *Tp* but resulted in a narrower melting temperature range, lower melting enthalpy despite of the increased solid fat content at 20°C. The commercial MDG could enhance nucleation of some fraction in RBO at higher temperature of RBO melting temperature range since the melting temperature of commercial MDG itself was 45-65°C, which was higher than the 2nd peak represented melting point range of RBO-RBW-MDG blends. Results indicated that could indicated the compounds responsible for the second endothermic peak were involved in structure which holding RBO when temperature was higher than melting temperature of RBO.

Table 9 Effect of crude wax and surfactant addition on thermal properties of physically refined rice bran oil.
RBW defined as the insoluble fraction of crude wax after solubilisation of crude wax in hexane and isopropanol.

	1st Endothermic peak					2nd Endothermic peak					
Treatments	To (°C)	Tp (°C)	Te (°C)	Range of temperature (°C)	ΔH (J/g)	To (°C)	Tp (°C)	Te (°C)	Range of temperature (°C)	ΔH (J/g)	SFC at 20 °C
RBO + 1.3%RBW	-22.97^{a} ± 0.52	-15.11^{a} ± 0.00	9.74^{a} ± 0.22	32.71^{a} ± 0.30	4.46^{a} ± 0.04	11.2^{c} ±0.01	15.2^{c} ±0.01	26.9^{ab} ±0.55	15.7^{a} ±0.56	2.4^{a} ±0.23	10.01^{d} ±0.06
RBO + 1.3%RBW + 1%MDG	-22.37^{a} ± 0.73	-14.61^{a} ± 0.70	8.90^{a} ± 0.27	31.26^{a} ± 0.45	6.20^{a} ± 0.76	14.3^{a} ±0.09	19.0^{a} ±0.25	27.4^{a} ±0.14	13.0^{b} ±0.23	1.7^{bc} ±0.06	10.63^{c} ±0.16
RBO + 1.3%RBW + 1%SP	-24.11^{a} ± 0.16	-15.61^{a} ± 0.00	7.70^{b} ± 0.47	31.81^{a} ± 0.31	5.41^{a} ± 0.66	9.8^{d} ±0.05	14.3^{c} ±0.35	25.0^{c} ±0.10	15.1^{a} ±0.04	1.9^{b} ±0.04	11.61^{a} ±0.00
RBO + 1.3%RBW + 1%MDG +1%SP	-24.23^{a} ± 0.63	-15.53^{a} ± 0.35	7.14^{b} ± 0.31	31.37^{a} ± 0.32	5.67^{a} ± 0.16	12.3^{b} ±0.31	16.8^{b} ±0.82	26.2^{b} ±0.25	13.8^{b} ±0.06	1.5^{c} ±0.08	11.05^{b} ±0.02

Means ± sd in the same column followed by different superscripts are significantly different ($P < 0.05$).

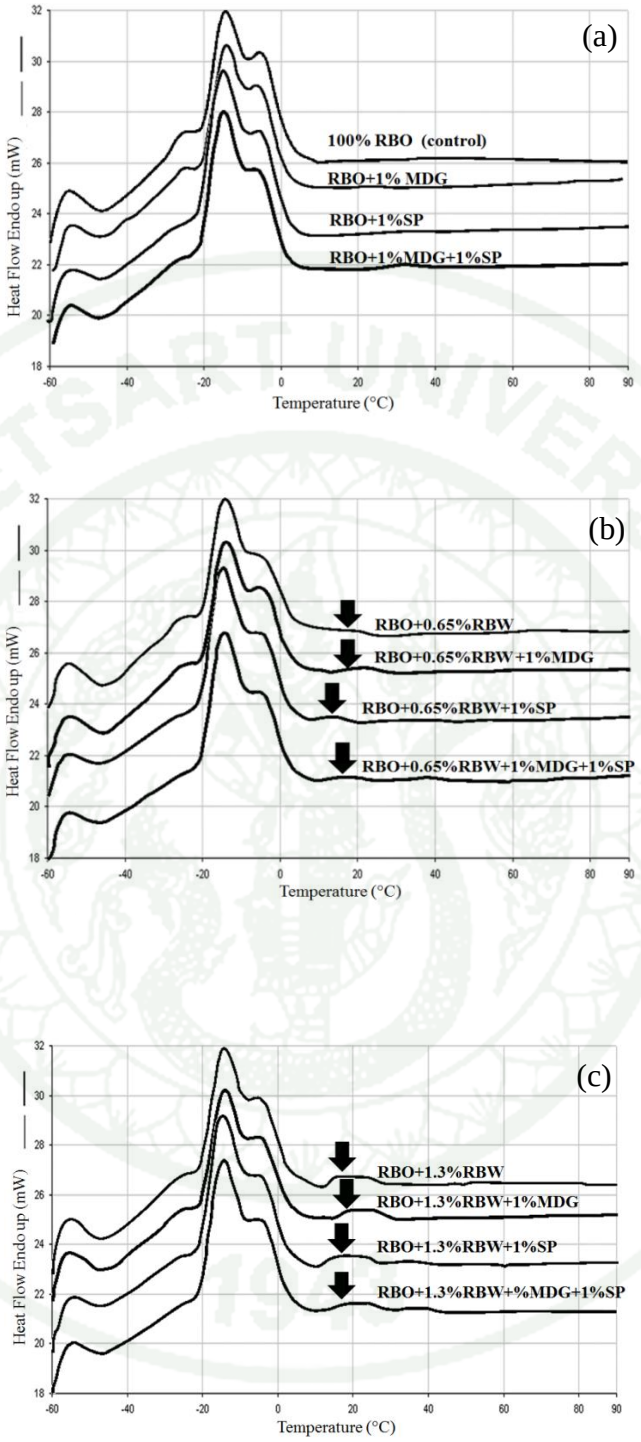

Figure 23 Effect of surfactants and RBW concentration on thermal properties of rice bran oil containing (a) RBO with and without 1%MDG and 1%SP (b) RBO mixed 0.65% RBW with and without 1%MDG and 1%SP (c) RBO mixed1.3% RBW with and without 1%MDG and 1%SP.

The ability of commercial MDG in forming elastic self-assembled surfactant network entrapping liquid oil during initial aggregation upon cooling (Chen and Terentjev, 2011), together with crystallization of RBW and some fraction of RBO could, in part, explain the alterations in melting characteristics of RBO blended with crude wax (Dassanayake *et al.*, 2009). The difference in molecular structure of commercial MDG compared to bulk RBO, as well as the presence of RBW, helped raise the SFC at 20°C, but lowered melting enthalpy of the mixed RBO-RBW-MDG. The presence of palmityl ester in commercial MDG likely promoted nucleation of fat crystal (Smith *et al*, 2011). However, the metastable ordering structure of MDG could lead to the decrease in melting enthalpy of fat crystal aggregates or flocs (Chen and Terentjev, 2011).

The presence of SP, however, lowered melting temperature and enthalpy of RBO-RBW blend in second endothermic peak (Table 9). The SP could retard nucleation and inhibit crystal growth because of the size of hydrophilic head of SP, as well as dissimilarity in chemical structure of hydrophobic tail with the major fatty acid in TAG (Yuki *et al.*, 1990; Cerdeira *et al.*, 2005). Nonetheless, the SFC of RBO-RBW-SP blend was higher than that of RBO-RBW blend. Sucrose esterified with mainly palmitic acid used in the present study was 99% di-, tri- and polyester as shown in manufacturer's datasheet. Different molecular structures between MDG *vs.* SP may induce different mechanisms in structure-forming process of three-dimensional network entrapping liquid RBO.

Due to the complexity of composition in blends, the temperature data in the 1st endothermic peaks were summarized by Cluster analysis to understand the influences of RBW, MDG and SP on melting characteristic of 1st endothermic peak, which reflected mainly the arrangement of bulk RBO itself. The maximum distance acquired from Cluster analysis was 25 (Figure 24). At distance 12.5, the data was grouped into 4 Clusters. Cluster I involved thermal properties of mixed RBO containing SP. Their thermal properties of oil blends were low regardless of MDG and/or RBW. Cluster II included RBO-RBW blends containing 0.65 and 1.3% RBW. Cluster analysis suggested that both samples had similar thermal properties despite

different concentrations of RBW. Cluster III, however, included RBO mixed with MDG with and without RBW. The oil blends in Cluster III had solid structure at high temperature confirmed by rheological properties shown in Section 2.3. The fourth cluster are the RBO and RBO+1%MDG blend, which had lower thermal properties compared to those in Cluster II and III but higher than those in Cluster I, which contained SP.

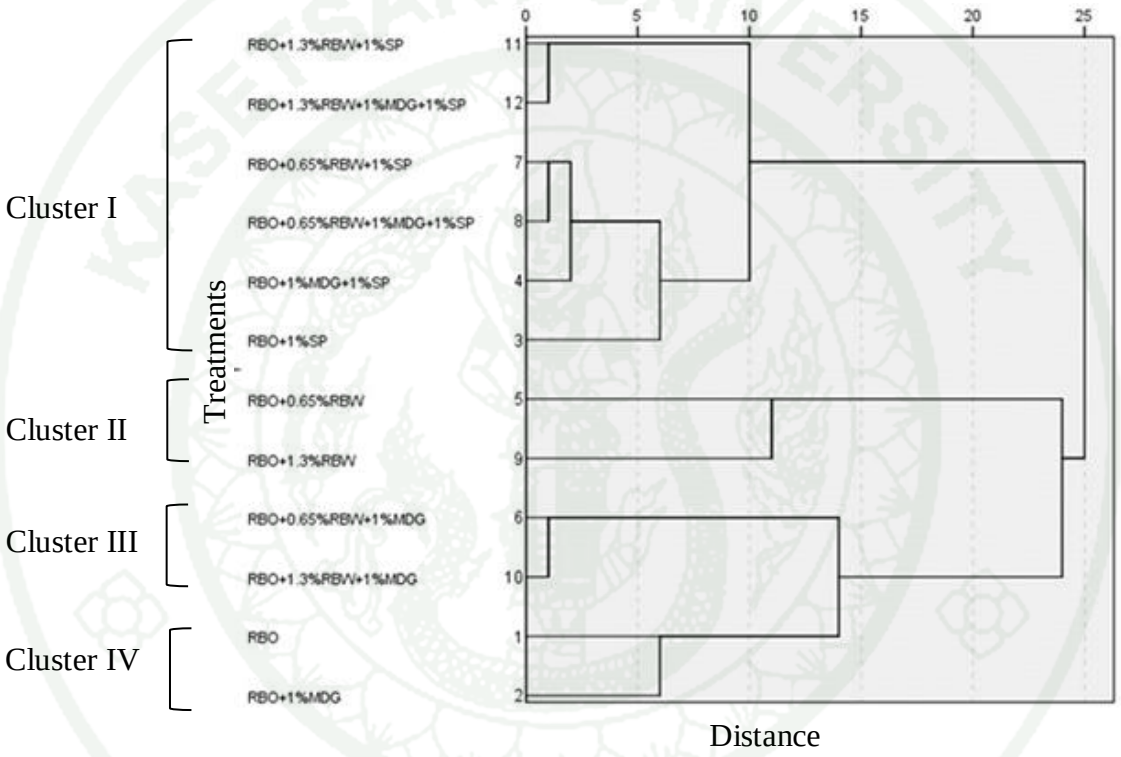

Figure 24 Dendogram using average linkage (between groups) in cluster analysis to describe similarity in same group.

2.3 Effect of crude wax and commercial surfactants on viscoelastic properties of RBO during structure-forming process and network melting

The effect of RBW and both surfactants during cooling process on storage modulus (G′) of RBO blends was shown in Figure 25. During structure-forming process (cooling from 70 to (-) 15 °C), the presence of surfactant MDG in RBO blends resulted in increased G′ compared to RBO alone (Figure 25a). Addition of

MDG to RBO-RBW (RBO-RBW-MDG) increased G′, indicating that MDG could help forming oleogel at low temperature *via* self-assembled MDG (Smith *et al*., 2011). On the contrary, the presence of SP in RBO-RBW resulted in a decreased G′ in RBO-RBW-SP blend. This indicated that SP retarded crystallization of oil blends and the formation of three-dimensional network of SP entrapping liquid oil in RBO oleogel (Cerdeira *et al*., 2005). In the presence of RBW in RBO, the increase the G′ of RBO-RBW was observed (Figure 25b). The presence of surfactants in RBO-RBW at the concentration of 0.65% RBW increased G′ in RBO-RBW-MDG, but decreased G′ in RBO-RBW-SP (Figure 25c). Moreover, the addition of 1% MDG in RBO-RBW at 1.30% RBW showed the highest modulus of RBO-RBW-MDG blends (Figure 25d). This suggested that the high concentration of RBW and the presence of MDG could synergistically induce the solidified structure of RBO.

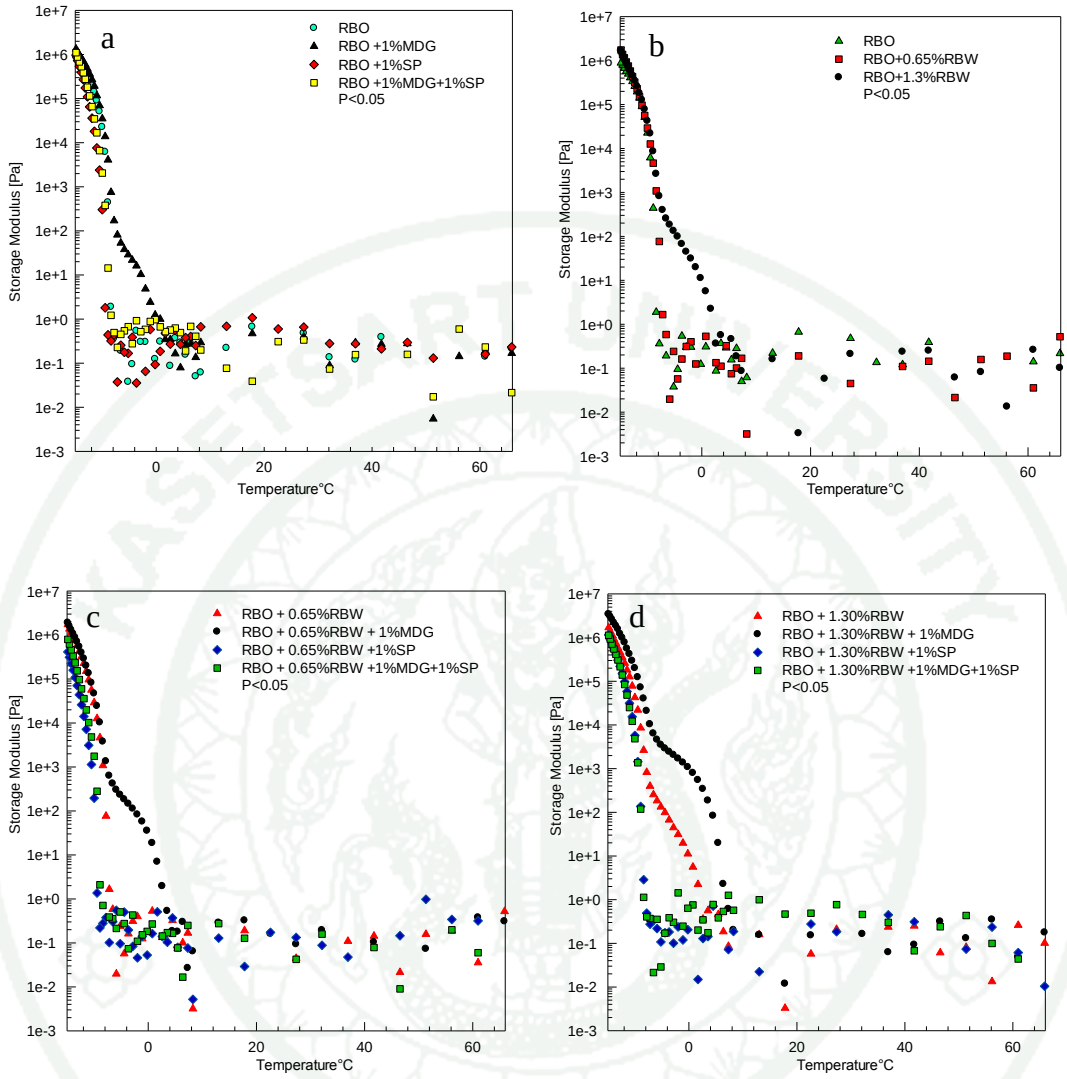

Figure 25 Effect of crude wax and surfactant concentration on storage modulus (G′) of solidified RBO during cooling from 70 to (-)15°C; (a) RBO and RBO mixed with 0.65 and 1.3%RBW; (b) RBO and RBO mixed with 1%MDG and 1%SP; (c) RBO mixed with 0.65%RBW with and without 1%MDG and 1%SP and (d) RBO mixed with 1.30%RBW with and without 1%MDG and 1%SP ($P < 0.05$).

During melting process (heating) the presence MDG in RBO increased G′ of RBO-MDG blend. However, the addition of SP in RBO resulted in lower G′ of RBO-SP blend compared to RBO alone (Figure 26a). Increasing of RBW concentration from 0.65 to 1.30% increase G′ of RBO-RBW because of the high presence of saturated fatty acid and high molecular weight policosanol. This facilitated RBW to form fat crystal network that could persist to higher temperature in RBO-RBW blend. Addition of MDG to RBO-RBW blend increased G′ of RBO-RBW-MDG. On the contrary, the presence of SP in RBO-RBW resulted in decreased G′ of RBO-RBW-SP. This result confirmed that the MDG could help forming three-dimensional network of RBO blends better than SP.

Table 10 shows the effect of surfactants on the viscoelastic transition temperature and transition time from viscous to elastic (cooling process) or elastic to viscous behaviours (heating process). MDG and RBW increased the transition temperature of RBO-RBW-MDG from solid to liquid. Time required to change viscoelastic solid to viscoelastic liquid was prolonged in the presence of MDG and RBW. This resulted in the widening in plastic range of RBO blends. On the other hand, SP decreased the transition temperature and shortened the time viscoelastic solid became viscoelastic liquid.

Fat spread and butter had spreadable temperature around 4.5-10°C and 22°C, respectively. Butter, which had fat crystal network holding liquid oil usually has G′ at 22°C around 4.5×10^{4} Pa. At 40°C, the fat crystal network melted and butter became liquid-like material (Vithanage *et al*., 2009). Apparently solidified RBO fabricated in the presence of 1.3%RBW and 1%MDG During melting process (heating) the presence MDG in RBO increased G′ of RBO but presence SP in RBO resulted in lower G′ compared to RBO alone (Figure 26a). Increasing of RBW concentration from 0.65 to 1.30% increase G′ of RBO because of RBW compose of high saturated fatty acid then RBW can form fat crystal network that could persist to higher temperature in RBO-RBW. Addition of MDG to RBO-RBW blend increased G′ of RBO-RBW-MDG. On the contrary, the presence of SP in RBO-RBW resulted

in decreased G′ of RBO. This result confirmed that the MDG could help forming three-dimensional network better than SP.

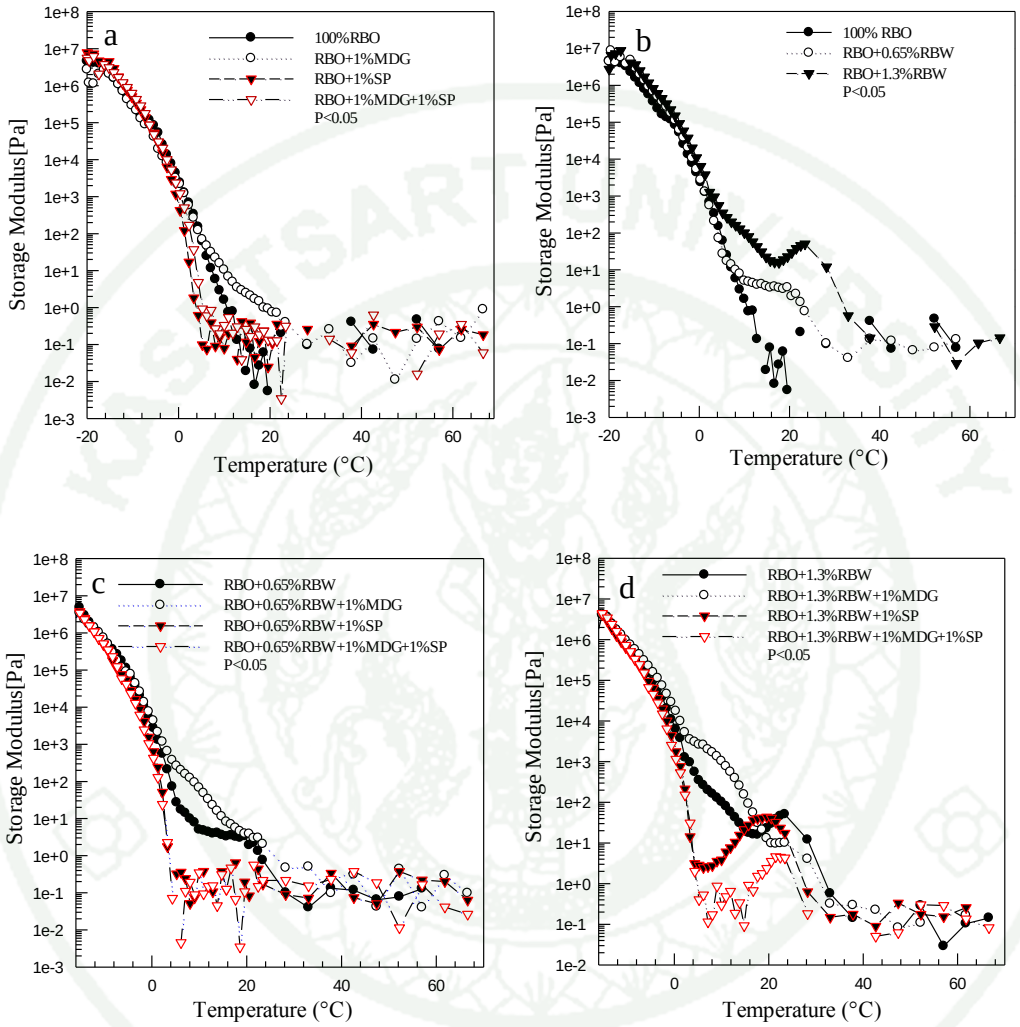

Figure 26 Effect of crude RBO concentration and surfactants on storage modulus (G′) of solidified RBO when heating (a) RBO and RBO mixed with 0.65 and 1.3%RBW (b) RBO and RBO mixed with 1%MDG and 1%SP (c) RBO mixed with 0.65%RBW with and without 1%MDg and 1%SP (d) RBO mixed with 1.30%RBW with and without 1%MDg and 1%SP.

Table 10 Effect of RBW and surfactants on transition temperature and time required for transition from liquid to solid and solid to liquid behaviours.

Composition of RBO mixtures	Cooling loop Liquid →Solid		Heating loop Solid→Liquid	
	T(°C)	Time(s)	T(°C)	Time(s)
RBO	(-)9.0^{fg}±0.2	2782.5^{bc}±16.3	6.6^{d}±0.2	4744.0^{d}±5.7
RBO + 1% MDG	(-)2.6^{c}±0.1	2510.5^{e}±6.4	11.0^{c}±2.2	4876.0^{c}±65.1
RBO + 1% SP	(-)9.8^{h}±0.3	2831.5^{ab}±3.5	2.4^{e}±0.3	4634.0^{e}±9.9
RBO + 1% MDG + 1% SP	(-)8.8^{fg}±0.2	2812.0^{ab}±22.6	3.7^{e}±0.4	4656.0^{e}±12.7
RBO + 0.65%RBW	(-)7.6^{e}±0.1	2710.0^{c}±2.8	6.6^{d}±2.5	4743.5^{d}±78.5
RBO + 0.65%RBW + 1%MDG	1.2^{b}±0.3	2348.0^{f}±8.5	16.9^{b}±2.1	5051.5^{b}±62.9
RBO + 0.65%RBW + 1%SP	(-)9.4^{gh}±0.2	2864.5^{a}±47.4	2.6^{e}±0.3	4624.0^{e}±7.1
RBO + 0.65%RBW + 1%MDG +1%SP	(-)9.2^{fgh}±0.2	2802.5^{ab}±0.7	2.4^{e}±1.0	4619.0^{e}±28.3
RBO + 1.3%RBW	(-)3.7^{d}±0.8	2596.5^{d}±92.6	29.9^{a}±0.01	5442.0^{a}±0.7
RBO + 1.3%RBW+ 1%MDG	5.6^{a}±0.2	2251.5^{g}±3.5	29.7^{a}±0.4	5435.0^{a}±12.7
RBO + 1.3%RBW+ 1%SP	(-)8.6^{f}±0.01	2779.0^{bc}±9.9	11.2^{c}±0.1	4881.0^{c}±1.4
RBO + 1.3%RBW+ 1%MDG + 1%SP	(-)8.7^{fg}±0.2	2782.5^{bc}±3.5	3.5^{e}±0.04	4650.0^{e}±1.4

Means ± sd in the same column followed by different superscripts are significantly different (P<0.05).

2.4 Effect of RBW and surfactants on stability of solidified RBO after aging at 5°C

Table 11 and Figure 27 show the ability of solidified RBO-RBW-surfactant blends after freezing at (-)22°C to induce fat crystallization and aged at 5°C for 24 h to induce self-assembled surfactant network holding liquid oil at 22°C for a period of time. Increasing RBW concentration and addition of MDG increased oil-holding capacity of RBO-RBW-MDG oleogel at 22°C, indicated by the time required for oleogel to flow after storage at 22°C of more than 1,440 min (24h). On the other hand, the presence of SP shortened the time required for RBO-RBW-SP to flow, thus reducing the oil-holding capacity of RBO-RBW-SP oleogel. It is likely that the fat crystal network and self-assembled MDG and RBW are responsible for the stability of RBO oleogel at 22 °C.

(a) After freezing at -22°C for 1h

(b) After aging at 5°C for 1day

(c) After storage at 22°C for more than 24 h

Figure 27 Effect of 1.3%RBW + 1%MDG on storage time of solidified RBO

Table 11 Effect of aging at 5 °C on liquid oil holding capacity at 22 °C of solidified RBO

Composition of RBO mixtures	Stability of RBO oleogel (measured as time required at 22°C for oleogel to flow)
RBO	$3 \pm 0.51 min^{h}$
RBO +1% MDG	$10 \pm 0.73\ min^{g}$
RBO + 1% SP	Melted instantaneously
RBO +1% MDG + 1% SP	$4 \pm 0.59 min^{h}$
RBO + 0.65% RBW	$13 \pm 0.68 min^{f}$
RBO + 0.65% RBW + 1% MDG	$22 \pm 0.64 min^{e}$
RBO + 0.65% RBW + 1% SP	$8 \pm 0.83 min^{h}$
RBO + 0.65% RBW + 1% MDG+ 1% SP	$10 \pm 0.46 min^{g}$
RBO + 1.3% RBW	$60 \pm 0.97 min^{b}$
RBO + 1.3% RBW + 1% MDG	Require more than 1,440 min^{a}
RBO + 1.3% RBW + 1% SP	$26 \pm 1.04 min^{d}$
RBO + 1.3% RBW + 1% MDG +1% SP	$28 \pm 0.75 min^{c}$

Means ± sd in the same column followed by different superscripts are significantly different ($P < 0.05$), (n = 3/1trials)

The result reported in this section indicated that thermal properties and rheological properties of RBO-RBW-surfactant oleogel were controlled by chemical structure of surfactant and RBW concentration. The hydrophilic part of mono- and dipalmityl glycerol in commercial MDG revealed that mono- and dipalmityl glycerol had one or two OH groups of glycerol part, respectively. On the other hand, sucrose palmitate (SP), which had eight OH groups of sucrose (Moonen and Bas, 2004), may provide different geometery of surfactant SP from that of MDG although both had HLB around 1. The presence high content of OH group in SP could result in the

higher polarity of the polar head compared to MDG. Upon cooling, each MDG molecule could come close and formed inverse lamellar phase and sub-α crystals (Chen and Terentjev, 2011) better than did SP. Moreover, increasing crude wax (and subsequent RBW concentration) could help formation of fat crystal network in both liquid oil phase and self-assembled surfactants. As a result, MDG and RBW could fabricate the network entrapping liquid RBO at temperature higher than the melting temperature of RBO. This structure could withstand at 22 °C for more than 24 h.

3. Effect of ethyl cellulose (EC) and rice bran wax (RBW) concentrations on rheological properties of RBO oleogel

In the absence of RBW, the RBO remained liquid flow behavior shown as higher loss modulus (G″) than storage modulus (G′) (Figure 28a). The increase of RBW at the level of 0.65-3.25% increased both G′and G″ of the mixture (Figures 28b-f). Increasing RBW concentration also resulted in an increase in crossover point at higher angular frequency. This indicated that raising RBW helped forming stronger or more elastic structure of RBO oleogel. Nevertheless, the three-dimensional network of RBW induced oleogel (RBO-RBW oleogel) was quite weak, observed as the crossover point occurred at G′ within the range of 0.1-2.2 Pa. The RBO-RBW showed liquid-like behavior because the G″ was much higher than the G′ (Grillet *et al*., 2012).

When EC was used as oleogelator at the range of 2.5-5%, both G′ and G″ of RBO-EC oleogel were drastically increased (Figure 29). The structure of RBO-EC oleogel was quite strong, observed as the crossover point occurred around G′ of 33 Pa at the frequency of 50 s^{-1} when EC was used at the level of 2.5% (Figure 29a). Increasing EC concentration up to 3.75% resulted in solid structure that gelled instantaneously when the mixed RBO-EC was cooled down to 25°C after solubilizing at 180°C during the preparing of oil blends. The G′ of RBO-EC oleogel could be as high as 100-400 Pa with no crossover point when EC was used at high concentration of 3.75-5% (Figures 29c-e).

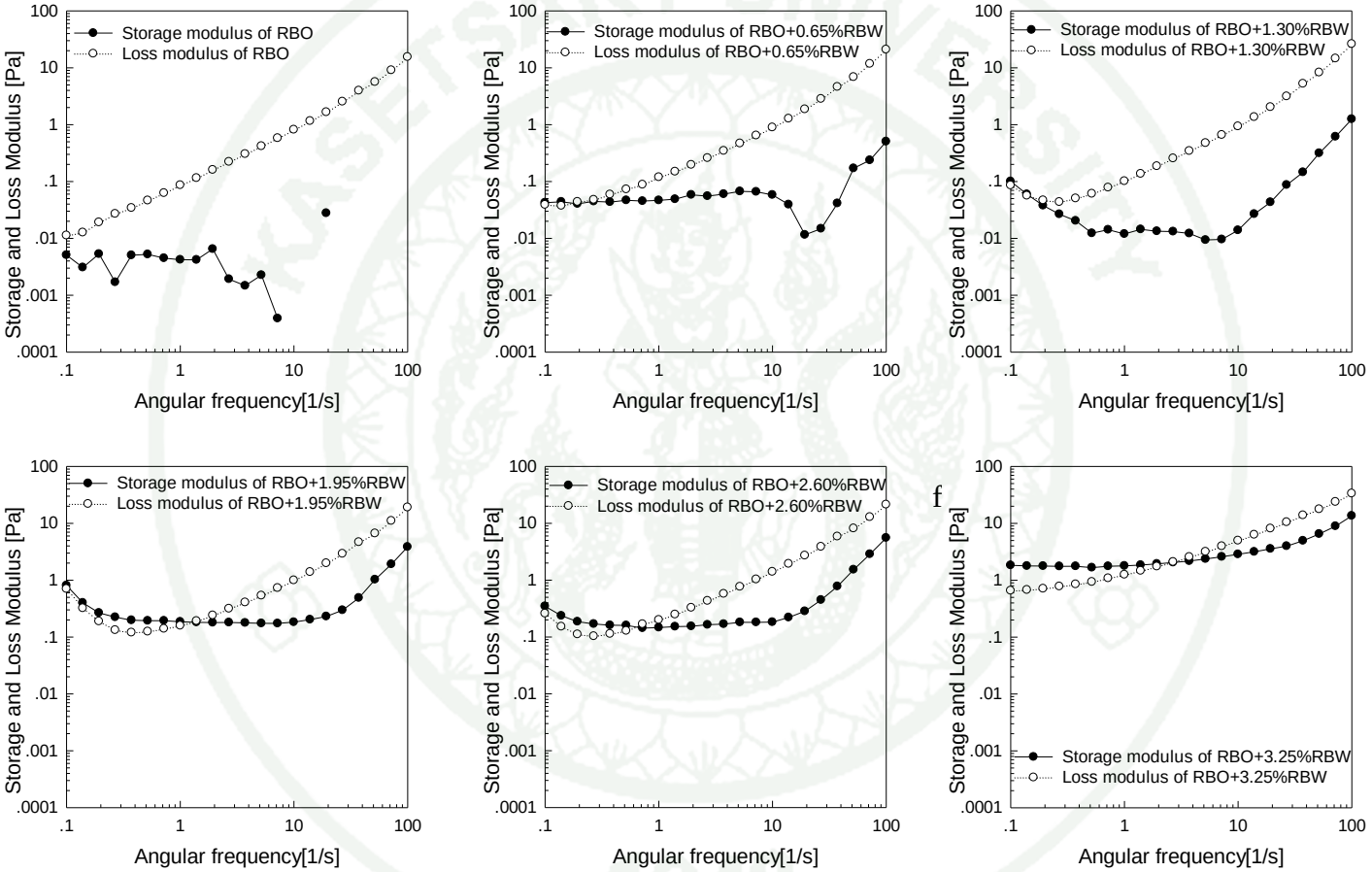

Figure 28 Effect of RBW concentration on storage modulus (G′) and loss modulus (G″) of RBO (a) 0%RBW, (b) 0.65%RBW (c) 1.30%RBW, (d) 1.95%RBW, (e) 2.60%RBW and (f) 3.25%RBW.

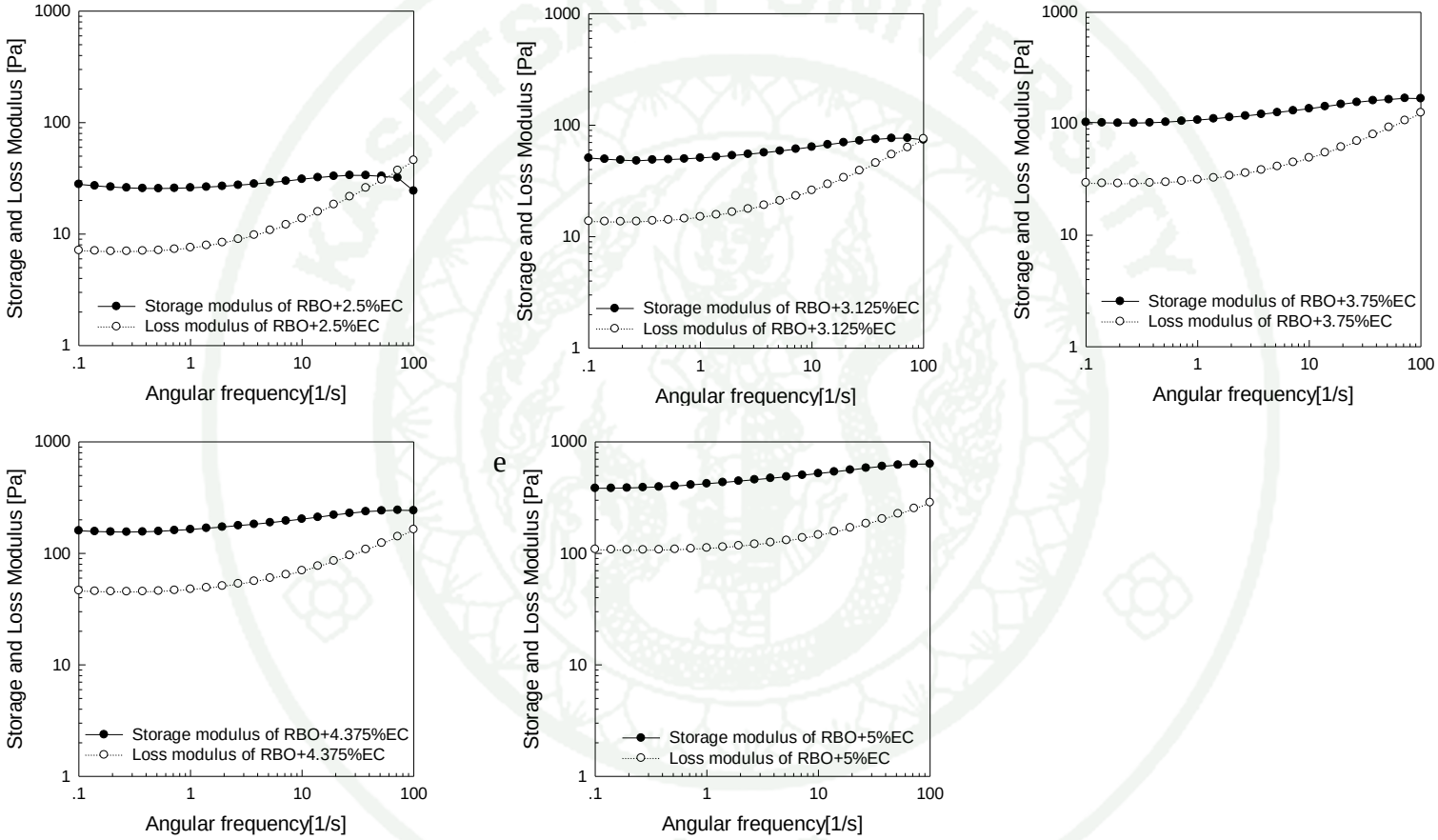

Figure 29 Effect of EC concentration on storage modulus (G′) and loss modulus(G″) of RBO (a) 2.5%EC (b) 3.125%EC (c) 3.75%EC (d) 4.375%EC (e) 5%EC.

Due to the differences in mechanisms involved in oleogel formation induced by RBW and EC, RBO oleogel fabricated by both oleogelators at different concentration was further investigated. Figure 30 illustrates that the solid behavior of RBO-EC oleogel could be reduced in the presence of RBW. Further increase in RBW concentration lowered the G′ or solid behavior of RBO-EC-RBW oleogel.

The presence of RBW could interfere with the oil holding capacity of EC network in RBO-RBW-EC. The conformation of long-chain alcohol RBW was composed of saturated alkyl chain. RBW addition could reduce flexibility of oil in solvent-solvent interaction as described in Section 4. Moreover, the presence RBW could increase the phase separation of EC chains, and then the number of tie point in the network was reduced due to the reduction in solvent-polymer interactions. This resulted in a weaker gel. Another possible reason could be due to the long chain alcohol in RBW, which could compete for the H-bonds with OH group of EC strands (Laredo *et al*., 2011). Overall, the presence RBW destabilized gel network, weakened the structure of oleogel, and decreased oil holding capacity of RBO-RBW-EC.

The EC formed polymer network could entrap liquid oil after storage at 2°C for 24 h. RBW could, however, form needle or platelet shape crystals and increased viscosity of viscous phase of oleogel (Dassanayake *et al*., 2009). Such particulate structure of RBW could likely disrupt the interpenetrating strands in RBO-RBW-EC gel network.

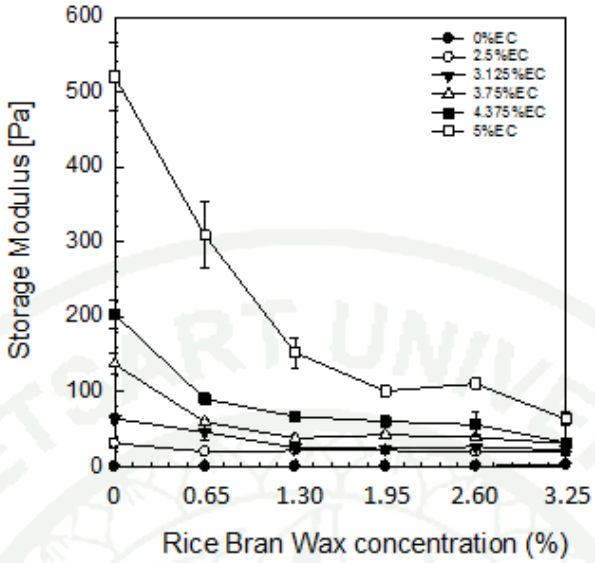

Figure 30 Storage modulus of RBO added with different concentration of rice bran wax (RBW) and ethyl cellulose (EC) measured at 10 s^{-1} angular frequency. Bars represent standard deviation.

Figure 31 illustrates that when RBW was used as oleogelator of RBO oleogel, the turbidity of the mixture increased, particularly when RBW was added up to 2.60%. In addition, the solid structure was weak and could not withstand storage temperature at 25°C. All RBO-RBW mixture exhibited flow after the tubes were inverted (Figure 31a). The use of EC, however, enhanced the formation of RBO-EC oleogels when the concentration of EC was up to 4.375% (Figure 31b). The RBO-EC oleogel exhibited no flow at 25°C for more than 24 h. This is in agreement with the frequency sweep results (Figures 29 and 30) that the gel was quite strong as the G′ was 200 Pa when 4.375%EC was used as oleogelator.

Higher concentration of EC (i.e. 5%) and presence RBW content was not exceed 1.3% could be fabricated and quite stable at 25°C for more than 24 h. The appearance of RBO-RBW-EC oleogel was in accordance with results shown in Figure 30 that both oleogelators creating network having G′ of 150-300 Pa and could offer their use as thermostable oleogel network.

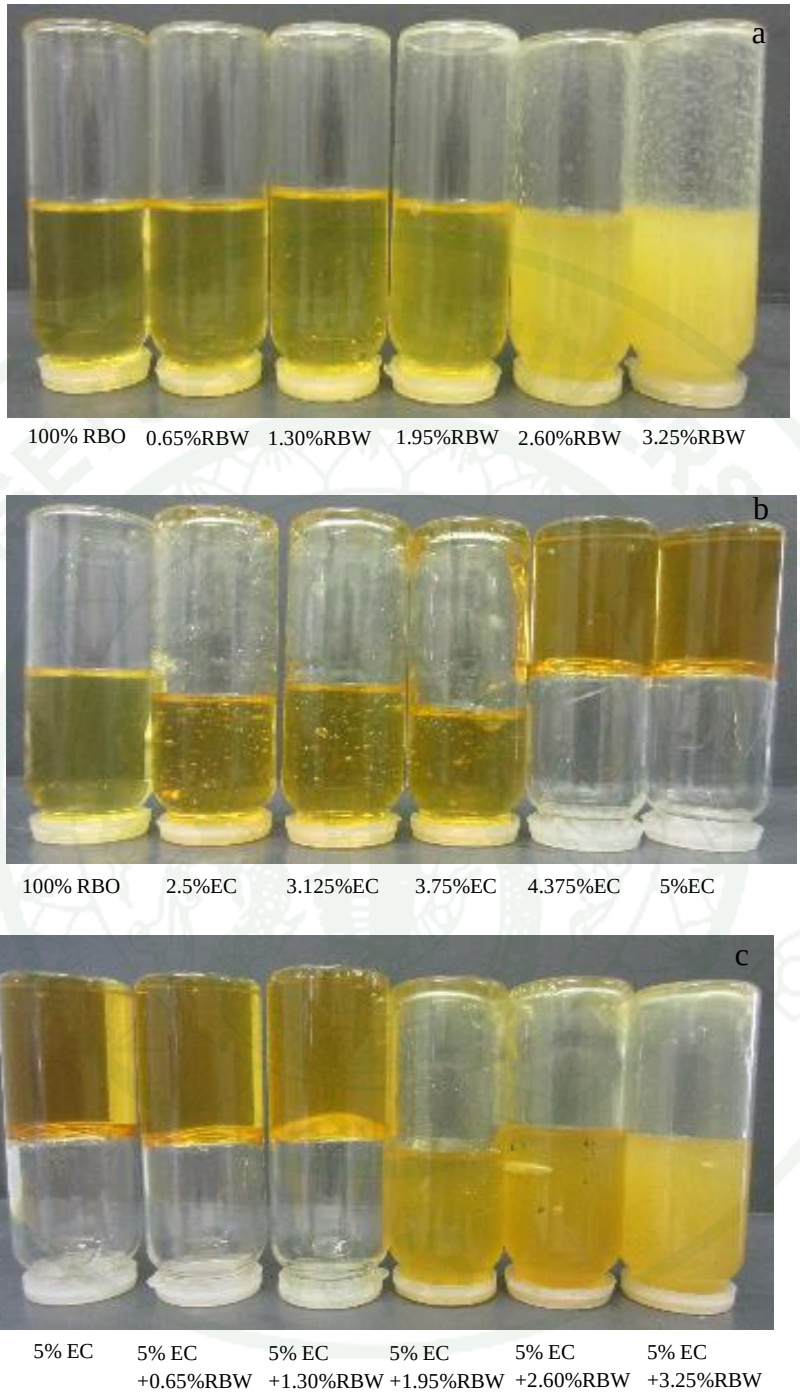

Figure 31 Effect of RBW and EC concentration on appearance of oleogel (a) RBO RBW blends (b) RBO-EC blends and (c) RBO-EC-RBW blends.

4. Use of rice bran oil oleogel containing rice bran wax and ethyl cellulose (RBO-RBW-EC) in preventing salt sedimentation in oil marinade for pork steak

Industrial marinades in meat industry are essential in improving meat yields by increasing water retention, as well as to add flavor and taste compounds. Although general marinades are composed of water, salt and phosphate for both vacuum-tumbling and injecting application systems, sometimes oil marinades with particulates of spice and herbs are used in marinated steak industries.

Using oil marinades requires dispersion of dried ingredients such as salts and spices in the oil phase. Sedimentation of salt is considered a defect of marinades. Result in Table 12 shows that using RBO-EC oleogel at high EC content above 3.75% resulted in no sedimentation of salt. Such RBO-EC oleogel structure was quite stable and did not melt at 90°C as shown in Table 13. However, the high elastic modulus or solid behavior of RBO oleogel at high EC concentration could make difficulties during tumbling of raw meat with marinades prior to grilling.

Using lower concentration of 2.5%EC resulted in almost 100% of salts sedimentation despite RBW was added up to 1.95% (Figure 32). Nevertheless, using 3.75% EC could disperse salt within RBO-RBW-EC network structure at 90°C in the presence of 0.65-1.30%RBW. Such weak network could help retain coated marinade on the surface of steak during heating up to 90°C before meat is fully cooked.

Table 12 Effect of oleogelators on salt sedimentation in rice bran oil oleogel after storage at 90°C for 12 h.

Types of oleogel	% Salt sedimentation of salt after storage at 90°C
RBO + 2.5%EC	96.2 ± 2.1
RBO + 2.5%EC + 0.65%RBW	96.3 ± 1.1
RBO + 2.5%EC + 1.30%RBW	98.2 ± 1.2
RBO + 2.5%EC + 1.95%RBW	99.10± 0.4
RBO + 3.75%EC	No sedimentation
RBO + 3.75%EC + 0.65%RBW	No sedimentation
RBO + 3.75%%EC + 1.30%RBW	No sedimentation
RBO + 3.75%EC + 1.95%RBW	78.1 ± 1.6
RBO + 5%EC	No sedimentation
RBO + 5%EC + 0.65%RBW	No sedimentation
RBO + 5%EC + 1.30%RBW	No sedimentation
RBO + 5%EC + 1.95%RBW	No sedimentation

Figure 32 Effect of oleogelators on salt sedimentation in rice bran oil oleogel after storage at 90°C for 12 h.

Results on marinade retention of raw marinated pork steak and weight loss of grilled marinated pork steak (Table 13) indicated that using 1.30% RBW and 3.75% EC in RBO-RBW-EC oleogel resulted in a lower weight loss and higher retention salts and spices compared with those using liquid RBO in marinating ($P<0.05$).

Table 13 Marinade retention of raw marinated pork steak and weight loss of marinated pork steak after grilling at 260°C.

Treatments	%Marinade retention in raw steak	%Weight loss in grilled steak
Liquid oil		
RBO+spice+salt	$46.25^{b} \pm 3.74$	$32.58^{a} \pm 0.73$
Oleogel		
RBO+1.3%RBW+spice+salt	$63.46^{a} \pm 0.56$	$28.44^{b} \pm 1.96$
RBO+3.75% EC+spice+salt	$64.12^{a} \pm 1.47$	$28.23^{b} \pm 1.47$
RBO+3.75%EC + 1.3%RBW+spice+salt	$63.89^{a} \pm 1.03$	$27.44^{b} \pm 0.33$

Mean within column followed by different letters are significantly different ($P<0.05$).

Sensorial attributes of raw marinated steak and grilled marinated pork steak were evaluated by 20 panelists using 9-point hedonic scaling (Tables 14, 15, respectively). The liking score of steak marinated with RBO-EC and RBO-RBW-EC oleogel in appearance was higher than those marinated with RBO-RBW oleogel and the RBO marinade in the form of oil and dried spices ($P<0.05$). The oleogel marinade was able to spread and cling onto the surface of steak (Figure 33).

On the other hand, steak marinated with liquid oil had lower score due to the flow of RBO. Moreover, RBO-RBW oleogel was more opaque due to crystallization of RBW at low temperature, dried spice in the marinade exhibited greenish color of herb. This resulted in the lowest liking score in appearance characteristics. For odor characteristic, pork steak marinated with RBO and dried spice had the lowest liking

score ($P<0.05$) due to strong smell of herbs. The overall liking and likelihood of buying scores indicated that steak marinated with RBO-EC oleogel had the highest liking score and likelihood of buying.

Sensorial evaluations of grilled steak, however, revealed that the odor and juiciness characteristics of all samples were not significantly different ($P\geq0.05$). In contrast with raw marinated steak, the grilled steak marinated with RBO-RBW oleogel had highest liking score.

The differences in appearance of pork steak marinated with different formula are shown in Figure 31. Although the panelists indicated that they likely bought raw steak marinated with RBO-EC oleogel the most, they liked the grilled steak marinated with RBO-RBW oleogel the most and that marinated with dried spice the least. This was because the presence of 3.75%EC resulted in the appearance of thin film coated on the surface of grilled pork steak since the carbohydrate polymers did not melt upon grilling.

It is apparent that although the EC could help forming the thermostable RBO-EC oleogels at temperature below 90°C, further heating of pork steak to 260°C during grilling could result in the flow of the bulk oil initially entrapped within the EC network, leaving the thin film of EC coated on the surface of grilled steak, which resulted in an unappealing appearance of grilled pork steak.

Table 14 Result of 9-point hedonic scale score and %likelihood of buying of marinade raw pork steak. All of treatment mixed with 19% salt and 10%dried spice and 2% paprika extract.

Treatments	Appearance	Odor	Overall Liking	%Likelihood of buying
Dried spice	$3.50^{c} \pm 1.64$	$6.00^{b} \pm 1.56$	$4.40^{d} \pm 1.63$	15%
RBO+spice+salt	$5.55^{b} \pm 1.54$	$6.85^{a} \pm 1.35$	$5.95^{c} \pm 1.39$	50%
RBO+1.3% RBW +spice+salt	$5.80^{b} \pm 1.77$	$6.95^{a} \pm 1.10$	$6.30^{bc} \pm 1.26$	70%
RBO+3.75% EC +spice+salt	$7.60^{a} \pm 0.99$	$7.15^{a} \pm 1.04$	$7.45^{a} \pm 1.00$	95%
RBO+3.75%EC+ 1.3%RBW+spice+salt	$6.95^{a} \pm 1.43$	$6.85^{a} \pm 1.14$	$7.00^{ab} \pm 1.12$	85%

Mean within column followed by different letters are significantly different ($P<0.05$), n=20 panelist.

Table 15 Effects of different oil marinades on sensory attributes of grilled pork steak

Treatments	Appearance	Odor	Taste	Juiciness	Overall Liking
Dried spice	4.90[b]	5.60[a]	5.65[c]	6.30[a]	5.45[d]
	± 1.77	±1.60	± 1.69	± 1.22	± 1.47
RBO+spice +salt	7.10[a]	6.50[a]	6.95[ab]	6.80[a]	6.98[ab]
	± 1.36	±1.50	± 1.54	±0.99	±1.38
RBO+1.3% RBW	6.85[a]	6.65[a]	7. 30[a]	6.60[a]	7.18[a]
+spice+salt	± 1.53	±0.81	± 0.86	±1.39	± 0.94
RBO+3.75% EC	5.15[b]	6.40[a]	6.40[bc]	6.70[a]	6.00[cd]
+spice+salt	± 1.63	±1.27	± 0.88	±1.26	±1.26
RBO+3.75%EC+	5.60[b]	6.65[a]	6.80[ab]	5.90[a]	6.35[bc]
1.3% RBW+spice+salt	± 1.47	±1.18	± 0.95	±1.55	±1.09

Means within column followed by different letters are significantly different ($P<0.05$), n=20 panelist.

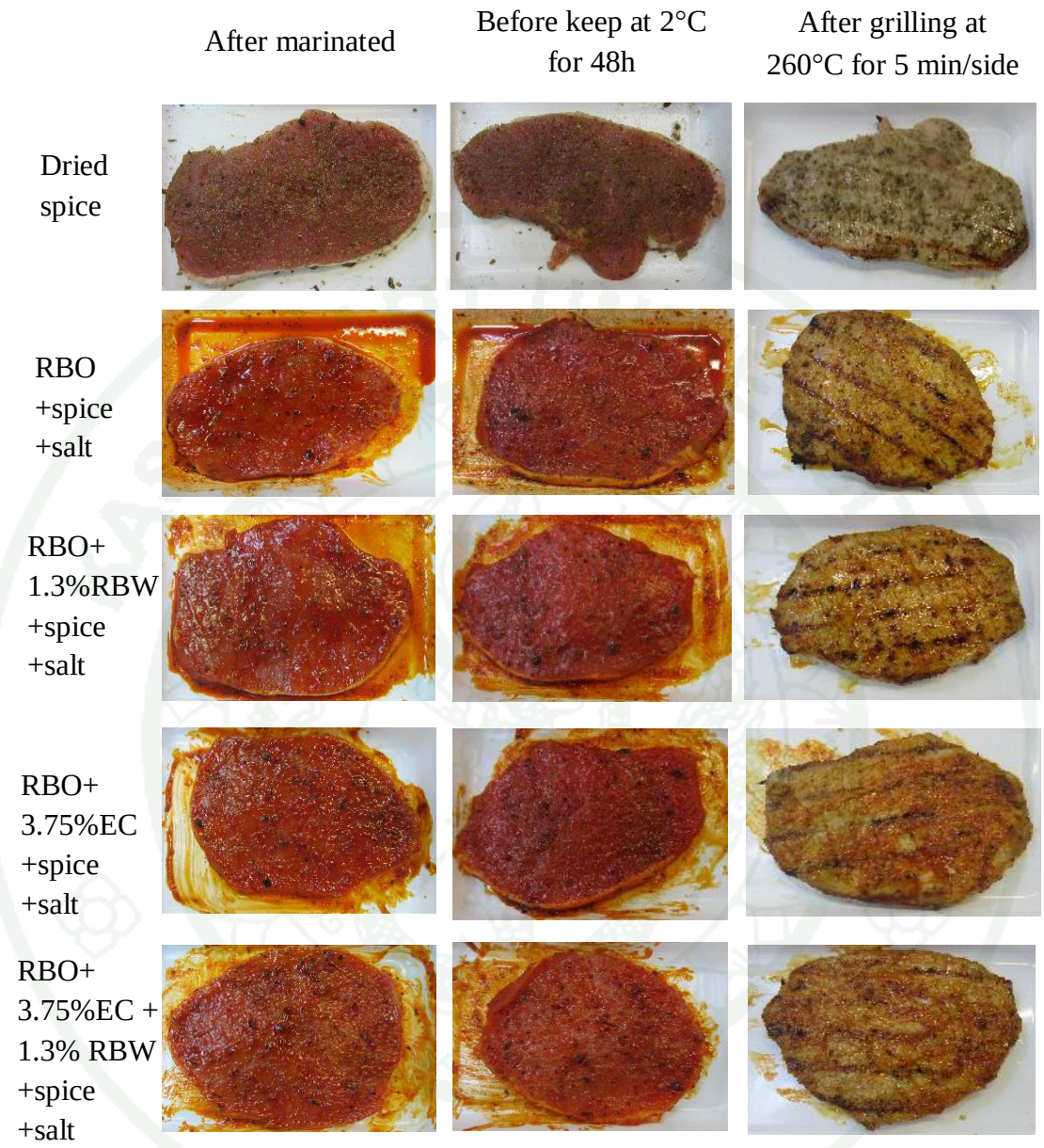

Figure 33 Appearance of raw and grilled pork steak.

Discussion

This study further elucidated the roles of surfactants and rice bran wax (RBW) in structure-forming process of solidified RBO which contained high contents of γ-oryzanol and phytosterols (Sawadikiat and Hongsprabhas, 2014). Different structurant such as AMF, which could provide fat crystal network and RBW, which contained long-chain alcohols such as heptacosanol and high ratio of palmitic acid in the TAGs, together with the self-assembled commercial MDG, played significant roles in the formation of RBO-RBW-MDG oleogels that withstand 22 °C for more than 24 h. The storage modulus of RBO-RBW oleogel could be further enhanced when EC was added to form RBO-RBW-EC oleogel, which found its use as oil marinade that can withstand 90 °C and helped prevent salt and spice sedimentation. Such strong oleogel had potential use in marinade industry for meat products.

Using different oleogelators or their mixture in RBO blends resulted in the interplay among three structure-forming mechanisms; namely self-assembled of surfactant, fat crystal network of TAGs and polymeric strand of carbohydrates. Each mechanism resulted in different thermo-physical properties of solidified RBO blends. The success of oleogel fabrication by self-assembled surfactant depended on the difference in the conformation of fatty acid of liquid oil and hydrophobic part of surfactants. When molecular conformations of TAGs in liquid oil and hydrophobic part of surfactant were different, such structure could induce phase separation of surfactants, followed by surfactant network entrapping liquid oil within solidified structure. Nonetheless, this structure could be modified to hold liquid RBO at temperature higher than the melting temperature of RBO by adding RBW.

Using self-assembled MDG incorporated into fat crystal network of TAG and RBW, as well as aging process to rearrange the alignment of acyl chains at the temperature close to melting temperature of RBO for 12 to 24 h, could help enhancing structure-forming process of solidified RBO or RBO oleogel at 22°C.

The carbohydrate EC could be used to further increase the strength and oil holding capacity of RBO oleogel at high temperature (90 °C). However, the strong structure of RBO-EC oleogel may not be suitable in all food products although it can help disperse salts and spices homogenously without sedimentation. The rheological properties of RBO-EC could be further modified by adding RBW to decrease the strength of EC network. It was most likely that the RBW could interact with EC by H-bondings, resulting in less interactions between EC and bulk liquid RBO.

CONCLUSION AND RECOMMENDATION

This study demonstrated, for the first time, the interplay among high melting temperature fat (AMF and RBW), high melting temperature surfactant (commercial MDG which had more than 90 % saturated fatty acid), and carbohydrate polymer that can solubilize in oil, on the fabrication of solidified RBO or RBO oleogel that can retain solid structure within the temperature range of 22 to 90 °C. Moreover, the presence high melting temperature fat and saturated MDG could synergistically induced nucleation of fat crystal and aggregation of fat crystal network, which could fabricate strong RBO oleogel. In the contrast, the presence RBW decreased polymer network strength due to the composition of RBW and conformation of saturated fatty acid. Not only the composition of the blends, but also proper condition of aging temperature and time, that allowed the acyl chains in the oil phase and surfactant to rearrange and form network over a period of 12 to 24 h to entrap bulk liquid RBO oil. Moreover, physically refined RBO oleogel showed potential use as candidate for oleogel fabrication.

However, these new findings were observed in the lab scale. Thus, these factors should be studied at pilot scale and when the proper oleogel (with suitable thermophysical properties) is used in other food products to replace saturated and *trans* fat such as in baked products. In addition, the microstructural of network and crystal alignment in three-dimensional network of RBO gel should be further investigated. The influences of EC molecular weight on the characteristics of RBO-EC or RBO-RBW-EC oleogels should be explored further, particularly in the applications in meat marinade due to the formation of a thin film after grilling. Such insights may help better understanding in the mechanisms of oleogel formation and their use in food products.

LITERATURE CITED

ACFS. 2003. TMC-05: Mixed standard fatty acid C_4-C_{22}. pp. 2-39. *In* ***Thai Compendium of Methods for Food Analysis***, *1st ed*, Department of Medical Sciences (DMSc), Bangkok.

Adel, R.D., P.C.M. Heussen and A. Bot. 2010. Effect of water on self-assembled tubules in β-sitosterol + γ-oryzanol-based organogels. **J. Phys.: Conf. Ser**. 247: 1-12.

Afoakwa, E.O., A. Paterson, M. Fowler and J. Vieira. 2008. Effect of tempering and fat crystallization behavior on microstructure, mechanical properties and appearance in dark chocolate systems. **J. Food Eng**. 89: 128-136.

Alamprese, C., L. Ferrari, M. Rossi, M. Lucisano and M. Mariotti. 2013. Rheological properties of β-sitosterol and γ-oryzanol organogels. *In* **Inside Food Symposium.** 9-12 April 2013. Leuven Belgium.

Anonymous. 2014 a. **Chemical structure of sorbitan monostearate**. Available Souce: http://en.wikipedia.org/wiki/Sorbitan_monostearate, April 13, 2014.

_____. 2014 b. **Chemical structure of ethyl cellulose**. Available Source: http://www.dow.com/dowwolff /en/industrial_solutions /polymer/ethylcellulose/. April 14 2014.

Bosso, R.C., A.P.B. Ribetro, M.H. Masuchi, L.A. Gioielli, L.A.G. Goncalves, A.O.das Santos, L.P. Cardoso and R. Grimaldi. 2010. Tripalmitin and monoacylglycerols as modifiers in the crystallization of palm oil. **Food Chem.** 122:1185-1192.

Bot, A. and W.G.M. Agterof. 2006. Structuring of Edible oils by Mixtures of γ-Oryzanol with β-sitosterol or related phytosterols. **J. Am. Oil Chem. Soc.** 83: 513-521.

_____., R.D. Adel and E.C. Roijers. 2008. Fibrils of γ-oryzanol + β-sitosterol in edible oil organogels. **J. Am. Oil Chem. Soc.** 85: 1127-1134.

Bruno, L., S. Kasapis, V. Chaudhary, K.T. Chow, P.W.S. Heng and L.P.Leong. 2011. Temperature and time effects on the structural properties of a non-aqueous ethyl cellulose topical drug delivery system. **Carbohyd. Polym.** 86: 644-651.

Cerdeira, M., V. Pastore, L.V. Vera, S. Martini, R.J. Candal and M.L. Herrera. 2005. Nucleation behavior of blended high-melting fractions of milk fat as affected by emulsifiers. **Eur. J. Lipid Sci. Technol.** 107: 877-885.

Chen, C.H. and E.M. Terentjev. 2011. Colloid-monoglyceride composites in hydrophobic solution. **Colloids Surf. A Physicochem. Eng. Asp.** 384: 536-542.

Chowdhury, K., L.A. Banu, S. Khan and A. Latif. 2007. Studies on the fatty acid composition of edible oil. **Bangladesh J. Sci. Ind. Res.** 42: 311-316.

Čmolík, J. and J. Pokorný. 2000. Physical refining of edible oils. **Eur. J. Lipid Sci. Technol.** 102: 472-486.

Co, E. and Marangoni, A.G. 2012. Organogels: an alternative edible oil-structuring method. **J. Am. Oil Chem. Soc.** 89: 749-780.

Dassanayake, L.S.K., D.R. Kodali, S. Ueno and K. Sato. 2009. Physical properties of rice bran wax in bulk and oleogels. **J. Am. Oil Chem. Soc.** 86: 1163-1173.

Dassanayake, L.S.K., D.R. Kodali, S. Ueno and K. Sato. 2011. Physical properties of organogels made of rice bran wax and vegetable oils. pp. 149-172. *In* Marangoni.A.G. and N. Garti., eds. **Edible oleogels structure and health implication.** AOCS Press, Illinois.

De, B.K. and D.K. Bhattacharyya. 1998. Physical refining of rice bran oil in relation to gumming and dewaxing. **J. Am. Oil Chem. Soc.** 75: 1683-1686.

Davey, R.J. and J. Garside. 2000. **From molecules to crystallizers: an introduction to crystallization.** 1st edition, Oxford University Press.

Dumont, M.J. and S.S. Narine. 2007. Soapstock and deodorizer distillates from North American vegetable oils: Review on their characterization, extraction and utilization. **Sep. Purif. Technol.** 40: 957-974.

Fredrick, E., I. Foubert, J.V.D. Sype and K. Dewettinck. 2008. Influence of monoglycerides on the crystallization behavior of palm oil. **Cryst. Growth Des.** 8: 1833-1839.

Gandolfo, F.G., A. Bot and E. Flöter. 2004. Structuring of edible oils by long-chain FA, fatty alcohols, and their mixtures. **J. Am. Oil Chem. Soc.** 80(1): 1-6.

Goffman, F.D., S. Pinson and C. Bergman. 2003. Genetic diversity for lipid content and fatty acid profile in rice bran. **J. Am. Oil Chem. Soc.** 80(5) 485-490.

Greyt, W.D. and M. Kellens. 2005. Deodorization, pp. 341-383. *In* F. Shahidi, ed. **Bailey's Industrial Oil & Fat Products.** 6th. John Wiley & Sons, Inc., Hoboken, New Jersey.

Grillet, A.M., N.B. Wyatt and L. M. Gloe .2012**. Polymer gel rheology and adhesion, rheology**, Dr. Juan De Vicente (Ed.), ISBN: 978-953-51-0187-1, InTech, DOI: 10.5772/36975. Available from: http://www.intechopen.com/books/rheology/rheology-and-adhesion-of-polymer-gels

Gunawan, S. and Y.H. Ju. 2009. Vegetable oil deodorizer distillate: characterization, utilization and analysis. **Sep. Purif. Technol.** 38(3): 207-241.

Herrera, M.L. and R.W. Hartel. 2000. Effect of processing conditions on physical properties of a milk fat model system: microstructure. **J. Am. Oil Chem. Soc.** 77:1197-1205.

Hughes, N.E., A.G. Marangoni, A.J. Wright, M.A. Rogers and J.W.E. Rush. 2009. Potential food applications of edible oil organogels. **Trends Food Sci. Tech.** 20: 470-480.

Hwang, K.T., J.E. Kim and C.L. Weller. 2005. Policosanol contents and compositions in wax-like materials extracted from selected cereals of Korean origin. **Cereal Chem.** 82(3): 242-245.

Khatoon, S and A. G. Gopala Krishna. 2004. Fat-soluble nutraceuticals and fatty acid composition of selected Indian rice varieties. **J. Am. Oil Chem. Soc.** 81(10): 939-943

Krishna, A.G.G., K.H. Hemakumar and S. Khatoon. 2006. Study on the composition of rice bran oil and its higher free fatty acids value. **J. Am. Oil Chem. Soc.** 83: 117-120.

Lannes, S.C.S. and R.M. Ignácio. 2013. **Structuring fat foods**. Aviable Source: http://cdn.intechopen.com/pdfs-wm/41623.pdf , April 14, 2014.

Laredo, T., S.Barbut. and A.G. Marangoni. 2011. Molecular interactions of polymer oleogelation. **Soft Matter.** 7: 2734-2743

Li,J., Y.Hu., J.J.Vlassak. and Z.Suo. 2012. Experimental determination of equations of state for ideal elastomeric gels. **Soft Matter.** 8: 812-8128.

Marangoni.A.G. and N. Garti. 2011. An overview of the past, present and future of oleogels, pp. 1-17. *In* Marangoni.A.G. and N. Garti., eds. **Edible Oleogels Structure and Health Implication.** AOCS Press, Illinois.

Martini, S., M.L. Herrera, and R.W. Hartel. 2002. Effect of processing conditions on microstructure of milk fat fraction/sunflower oil blends. **J. Am. Oil Chem. Soc.** 79: 1063-1068.

Martins, P.F., V.M. Ito, C.B. Batistella and M.R.W. Maciel. 2006. Free fatty acid separation from vegetable oil deodorizer distillate using molecular distillation process. **Sep. Purif. Technol.** 48: 78-84.

Mayamol, P.N., T. Samuel, C. Balachandran, A. Sundaresan, and C. Arumughan. 2004. Zero-trans shortening using palm stearin and rice bran oil. **J. Am. Oil Chem. Soc.** 81:407-413.

Mendes, M.F., F.L.P. Pessoa, G.V. Coelho and A.M.C. Uller. 2005. Recovery of the high aggregated compounds present in the deodorizer distillate of the vegetable oils using supercritical fluids. **J. Supercrit. Fluids.** 34: 157-162.

Metin, S. and R.W. Hartel. 2005. Crystallization of fats and oils. 45-76. *In* F. Shahidi., ed. **Bailey's Industrial Oil&Fat Products**. John Wiley & Sons, Inc., Hoboken, New Jersey.

Mooi, E. and M. Sarstedt. 2011. **Cluster analysis.** Available Source: file:///C:/Users/pin/Downloads/9783642125409-c1%20(1).pdf, March 10, 2014.

Moonen, H and H. Bas. 2004. Mono- and diglycerides. pp. 40-58. *In* R.J. Whitehurst, ed. **Emulsifiers in food technology.** 1st. Blackwell Publishing, Ltd., Ames, Iowa, USA.

Moraes, E.B.D., P.F. Martins, C.B. Batistella, M.E.T. Alvarez, R.M. Filho and M.R.W. Maciel. 2006. Molecular distillation. **Appl. Biochem. Biotechnol.** Vol.129-132: 1066-1076.

Murdan, S., G. Gregoriadis and A.T. Florence. 1999. Novel sorbitan monostearate organogels. **J. Pharm. Sci.** 88: 608-614.

Ojijo, N.K., I. Neeman, S. Eger and E. Shimoni. 2004. Effects of monoglyceride content, cooling rate and shear on the rheological properties of olive oil/monoglyceride gel networks. **J. Sci. Food Agr.** 84: 1585-1593.

Olsen, R.E. and R.J. Henderson. 1989. The rapid analysis of neutral and polar marine lipids using double-development HPTLC and scanning densitometry. **J. Exp. Mar. Biol. Ecol.** 129: 189-197.

Omonov, T.S., L. Bouzidi and S.S. Narine. 2010. Quantification of oil binding capacity of structuring fats: A novel method and its application. **Chem. Phys. Lipids.** 163: 728-740.

Ortiz-Gonzalez, G., R. Jimenez-Flores, D.R. Bremmer, J.H. Clark, E.J. Depeters, S.J. Schmidt and J.K. Drackley. 2007. Functional properties of butter oil made from bovine milk with experimentally altered fat composition. **J. Dairy Sci.** 90: 5018-5031.

Orthofer, F.T. 2005. Rice bran oil, pp. 465-489. *In* F. Shahidi, ed. **Bailey's Industrial Oil & Fat Products.** John Wiley & Sons, Inc., Hoboken, New Jersey.

Patel, M. and S.N. Naik. 2004. Gamma-oryzanol from rice bran oil. **J. Sci. Ind. Res.** 63: 569-578.

Pernetti, M., K.V. Melssen, D. Kalnin and E. Flöter. 2007. Structuring edible oil with lecithin and sorbitan tri-stearate. **Food Hydrocolloid.** 21: 855-861.

Pieve, S.D., S. Calligaris, E. Co, M.C. Nicoli and A.G. Marangoni. 2010. Shear nanostructuring of monoglyceride organogels. **Food Biophys.** 5: 211-217.

Posada, L.R., J. Shi, Y. Kakuda and S.J. Xue. 2007. Extraction of tocotrienols from palm fatty acid distillates using molecular distillation. **Sep. Purif. Technol.** 57: 220-229.

Prasad, R.B.N. 2006. Refining of rice bran oil. **Lipid Technology.** 18(12): 275-279.

Rye,G.G., J.W.Litwinenko and A.G. Marangoni. 2005. Fat crystal networks, pp. 121-160. *In* S.Fereidoon (ed.) **Bailey's Industrial Oil&Fat Products**. John Wiley & Sons, Inc., Hoboken New Jersey.

Rogers, M.A. 2009. Novel structuring strategies for unsaturated fats – Meeting the zero-trans, zero-saturated fat challenge: A review. **Food Res. Int.** 42: 747-753.

Roy, S.K., T.N.B. Kaimal, R.B.N. Prasad, B.L.A.P. Devi and B.V.S.K. Rao. 2009. **A process for the upgradation and bleaching of crude rice bran wax.** India 228674.

Rukke, E.O., C.S. Bringas, R.K. Abrahamsen, E. Skuterud and R.B. Schüller. 2013. Thermal influence on rheological characteristics of butter and margarine during distribution, storage and use. **Ann. T. Nord. Rheol. Soc.** 21: 179-186.

Saidin, S.M. and N. Ramli. 2010. Melting behavior of binary of palm mid fraction and rice bran oil. **Sains Malays.** 39: 785-790.

Samuditha, L., K.Dassanayake, D.R. Kodali and S. Ueno. 2011. Formation of oleogels based on edible material. **Curr. Opin. Colloid Interface Sci.** 16: 432-439.

Sato, K. and S. Ueno, 2005. Polymorphism in fats and oils, pp. 77-85. *In* F. Shahidi., ed. **Bailey's Industrial Oil and Fats Products.** John Wiley & Sons, Inc., Hoboken, New Jersey.

_____. 1999. Solidification and phase transformation behavior of food fats-a review. **Fett/Lipid.** 101: 467-474.

Sawalha, H., P. Venema, A. Bot, E. Floter and E. van der Linder. 2011. The influence of concentration and temperature on the formation of γ-oryzanol + β-sitosterol tubules in edible oil organogels. **Food Biophys.** 6:20-25.

Sawasdikiat, P. and P.Hongsprabhas. 2014. Phytosterols and γ-oryzanol in rice bran oils and distillates from physical refining process. **Int. J. Food Sci. Tech**. Published online: 3 MAR 2014.

_____ , S.Chaiseri and P. Hongsprabhas. 2014. Phytochemicals in refined vegetable Oils commercially available in Thailand, pp. 74-81. *In* Proceedings of the Kasetsart university annual conference: Agricultural science: Leading Thailand to world class standard.

Schaink, H.M., K.F.V. Malssen, S.M. Alves, D. Kalnin and E. van der Linden. 2007. Crystal network for edible oil organogels; Possibilities and limitations of the fatty acid and fatty alcohol systems. **Food Res. Int.** 40: 1185-1193.

Shukla, V.K.S. 2005. Margarine and Baking Fats , pp. 665-684. *In* C.C. Akoh and O.M.Lai, eds. **Healthful Lipids**. AOCS Press, USA.

Smith, K.W. 2001. Crystallization of Palm Oil and Its Fractions, pp.357-380. *In* N. Garti and K. Sato, eds. **Crystallization Processes in Fats and Lipid Systems.** Marcel Dekker, Inc., New York.

_____., K. Bhaggan, G. Talbot and K.F. van Malssen. 2011. Crystallization of fats: Influence of minor components and additives. **J. Am. Oil Chem. Soc.** 88: 1085-1101.

Tang, D. and A.G. Marangoni. 2006a. Microstructure and fractal analysis of fat crystal networks. **J. Am. Oil Chem. Soc.** 83:377–388.

_____ and _____ . 2006b. Quantitative study on the microstructure of colloidal fat crystal networks and fractal dimensions. **Adv. Colloid Interface Sci.** 128–130: 257–265.

Taylor, J.C., L.Rapport and G.B. Lockwood. 2003. Octacosanol in human health. **Nutrition.** 19: 192-195.

Trani, M.T.T., K.M. Phillips, L.E. Lemar and J.M. Holden. 2006. New and existing oils and fats used in products with reduced trans-fatty acid content. **J. Am. Diet. Assoc.** 106: 867-880.

Tuntragul, S., S. Surapat and P. Hongsprabhas. 2010. Influences of rice bran oil and rice flours on physicochemical properties of mozzarella cheese analogue. **Kasetsart J. (Nat. Sci.).** 44: 924-934.

Van Hoed, V., G. Depaemelaere, J.V. Ayala, P.Santiwattana, R. Verhe and W.De Greyt. 2006. Influence of chemical refining on the major and minor components of rice bran oil. **J. Am. Oil Chem. Soc.** 83: 315-321.

Vali, S.R., Y.H. Ju, T.N.B. Kaimal and Y.T. Chern. 2005. A process for preparation of food-grade rice bran wax and the determination of its composition. **J. Am. Oil Chem. Soc.** 82(1): 57-64.

Vazquez, J.F.T., J.A.M. Rueda, E.D. Alvarado, M.C. Alonso, M.A. Macias and M.M.G. Chávez. 2007. Thermal and textural properties of oleogels developed by candelilla wax in safflower oil. **J. Am. Oil Chem. Soc.** 84: 989-1000.

Verhe, R., T. Verleyen, V. Van Hoed and W. De Greyt. 2006. Influence of refining of vegetable oils on minor components. **J. Oil Palm Res.** Special issue: 168-179.

Vithanage, C.H., M.J. Grimson and B.G. Smith. 2009. The effect of temperature on the rheology of butter, a spreadable blend and spreads**. J. Texture Stud.** 346-369: 346-369.

Wang M.F., H.Z. Lian, L. Mao, J.P. Zhou, H.J. Gong, B.Y. Qian, Y. Fang and J. Li. 2007. Comparison of various extraction methods for policosanol form rice bran wax and establishment of chromatographic fingerprint of policosanol. **J. Agric. Food. Chem.** 55: 5552-5558.

Wassell, P., G. Bonwick, C.J. Smith, E.A. Roig and N.W.G. Young. 2010. Towards a multidisciplinary approach to structuring in reduced saturated fat-based system-a review. **Int.J. Food Sci. Tech.** 46: 642-655.

Yoon, S.H. and J.S. Rhee. 1982. Composition of waxes from crude rice bran oil. **J. Am. Oil Chem. Soc.** 59(12): 561-572.

Yuki, A., K. Matsuda and A. Nishimura. 1990. Effect of sucrose polyesters on crystallization behaviour of vegetable shortening and margarine fat. **J. Jpn. Oil Chem. Soc.** 39: 236-244.

Zarrouk, W., B. Baccouri, W. Taamalli, A. Trigui, D. Daoud and M. Zarrouk. 2009. oil fatty acid composition of eighteen Mediterranean olive varieties cultivated under the arid conditions of Boughrara (Southern Tunisia). **Grasas Y. Aceites.** 60:498-506

Zetzl, A.K., A.G. Marangoni. and S. Barbut. 2012. Mechanical properties of ethylcellulose oleogels and their potential for saturated fat reduction in frankfurters. **Food Funct.** 3: 327-337

Ziggers, D. 2005. **Oil and fats indispensable in feed.** Available Source: http://www.allaboutfeed.net/oil and fats indispensable in feed, April 14 2014.

Appendix

Statistical analysis

Appendix Table 1 Statistical analysis of free fatty acid ratio in unevaporated fraction (UMD) after molecular distillation at temperature 120 °C, 140 °C and 160 °C

Source	Type III Sum of Squares	df	Mean Square	F	Sig.
Corrected Model	.049[a]	2	.025	43.834	.006
Intercept	.025	1	.025	43.834	.007
trt	.049	2	.025	43.834	.006
Error	.002	3	.001		
Total	.075	6			
Corrected Total	.051	5			

a. R Squared = .967 (Adjusted R Squared = .945), Dependent Variable: free fatty acid

Appendix Table 2 Statistical analysis of monoacylglycerol ratio in unevaporated fraction (UMD) after molecular distillation at temperature 120 °C, 140 °C and 160 °C

Source	Type III Sum of Squares	df	Mean Square	F	Sig.
Corrected Model	.035[a]	2	.017	23.425	.015
Intercept	.400	1	.400	538.436	.000
trt	.035	2	.017	23.425	.015
Error	.002	3	.001		
Total	.437	6			
Corrected Total	.037	5			

a. R Squared = .940 (Adjusted R Squared = .900), Dependent Variable: Monoacylglycerol

Appendix Table 3 Statistical analysis of diacylglycerol ratio in unevaporated fraction (UMD) after molecular distillation at temperature 120 °C, 140 °C and 160 °C

Source	Type III Sum of Squares	df	Mean Square	F	Sig.
Corrected Model	.019[a]	2	.009	48.891	.005
Intercept	.062	1	.062	324.695	.000
trt	.019	2	.009	48.891	.005
Error	.001	3	.000		
Total	.081	6			
Corrected Total	.019	5			

a. R Squared = .970 (Adjusted R Squared = .950), Dependent Variable: Diacylglycerol

Appendix Table 4 Statistical analysis of triacylglycerol ratio in unevaporated fraction (UMD) after molecular distillation at temperature 120 °C, 140 °C and 160 °C

Source	Type III Sum of Squares	df	Mean Square	F	Sig.
Corrected Model	.053[a]	2	.027	464.523	.000
Intercept	1.986	1	1.986	34640.419	.000
trt	.053	2	.027	464.523	.000
Error	.000	3	5.733E-5		
Total	2.039	6			
Corrected Total	.053	5			

a. R Squared = .997 (Adjusted R Squared = .995), Dependent Variable: Triacylglycerol

Appendix Table 5 Statistical analysis of γ-oryzanol content in unevaporated fraction (UMD) after molecular distillation at temperature 120 °C, 140 °C and 160 °C

Source	Type III Sum of Squares	df	Mean Square	F	Sig.
Corrected Model	.148[a]	2	.074	397.870	.000
Intercept	16.733	1	16.733	90022.125	.000
trt	.148	2	.074	397.870	.000
Error	.003	15	.000		
Total	16.884	18			
Corrected Total	.151	17			

a. R Squared = .981 (Adjusted R Squared = .979), Dependent Variable: Gamma oryzanol

Appendix Table 6 Statistical analysis of Tonset (To) of RBO with and without 1% UMD and 1% MDG

Source	Type III Sum of Squares	df	Mean Square	F	Sig.
Corrected Model	13.698[a]	3	4.566	2.987	.096
Intercept	9998.721	1	9998.721	6540.914	.000
trt	13.698	3	4.566	2.987	.096
Error	12.229	8	1.529		
Total	10024.648	12			
Corrected Total	25.927	11			

a. R Squared = .528 (Adjusted R Squared = .351), Dependent Variable: T(onset)

Appendix Table 7 Statistical analysis of Tend (Te) of RBO with and without 1% UMD and 1% MDG

Source	Type III Sum of Squares	df	Mean Square	F	Sig.
Corrected Model	.500[a]	3	.167	.625	.619
Intercept	301.943	1	301.943	1133.559	.000
trt	.500	3	.167	.625	.619
Error	2.131	8	.266		
Total	304.574	12			
Corrected Total	2.631	11			

a. R Squared = .190 (Adjusted R Squared = -.114), Dependent Variable: T(end)

Appendix Table 8 Statistical analysis of solid fat content (SFC) at 15 °C of RBO with and without 1% UMD and 1% MDG

Source	Type III Sum of Squares	df	Mean Square	F	Sig.
Corrected Model	.070[a]	3	.023	11.530	.003
Intercept	7.568	1	7.568	3752.930	.000
trt	.070	3	.023	11.530	.003
Error	.016	8	.002		
Total	7.654	12			
Corrected Total	.086	11			

a. R Squared = .812 (Adjusted R Squared = .742), Dependent Variable: SFC at 15 °C

Appendix Table 9 Statistical analysis of solid fat content (SFC) at 25 °C of RBO with and without 1% UMD and 1% MDG

Source	Type III Sum of Squares	df	Mean Square	F	Sig.
Corrected Model	.054[a]	3	.018	5.953	.020
Intercept	2.960	1	2.960	970.536	.000
trt	.054	3	.018	5.953	.020
Error	.024	8	.003		
Total	3.039	12			
Corrected Total	.079	11			

a. R Squared = .691 (Adjusted R Squared = .575), Dependent Variable: SFC at 25 °C

Appendix Table 10 Statistical analysis of solid fat content (SFC) at 35 °C of RBO with and without 1% UMD and 1% MDG

Source	Type III Sum of Squares	df	Mean Square	F	Sig.
Corrected Model	.001[a]	3	.000	.724	.566
Intercept	.180	1	.180	337.641	.000
trt	.001	3	.000	.724	.566
Error	.004	8	.001		
Total	.186	12			
Corrected Total	.005	11			

a. R Squared = .214 (Adjusted R Squared = -.081), Dependent Variable: SFC1t35

Appendix Table 11 Statistical analysis of apparent viscosity of RBO and RBO-AMF blended at ratio of RBO to AMF of 75:25 with and without 1% MDG and 1% UMD

Source	Type III Sum of Squares	df	Mean Square	F	Sig.
Corrected Model	1075.951[a]	5	215.190	10.476	.000
Intercept	229265.400	1	229265.400	11161.204	.000
trt	1075.951	5	215.190	10.476	.000
Error	616.238	30	20.541		
Total	230957.590	36			
Corrected Total	1692.190	35			

a. R Squared = .636 (Adjusted R Squared = .575), Dependent Variable: viscosity

Appendix Table 12 Statistical of volume of solid fat phase in RBO and RBO-AMF at ratio of 75:25 with and without 1% MDG and 1% UMD after aging at 5°C for 12h and storage at 30°C for 12h

Source	Type III Sum of Squares	df	Mean Square	F	Sig.
Corrected Model	38388.066[a]	5	7677.613	353.381	.000
Intercept	11454.351	1	11454.351	527.215	.000
Trt	38388.066	5	7677.613	353.381	.000
Error	651.784	30	21.726		
Total	50494.201	36			
Corrected Total	39039.851	35			

a. R Squared = .983 (Adjusted R Squared = .981), Dependent Variable:
aged at 5 °C for 12h and storage at 30 °C for 12h

Appendix Table 13 Statistical of volume of solid fat phase in RBO and RBO-AMF at ratio of 75:25 with and without 1% MDG and 1% UMD after aging at 5 °C for 12 h and storage at 30 °C for 24h

Source	Type III Sum of Squares	df	Mean Square	F	Sig.
Corrected Model	41505.321[a]	5	8301.064	1339.809	.000
Intercept	12227.936	1	12227.936	1973.614	.000
Trt	41505.321	5	8301.064	1339.809	.000
Error	185.871	30	6.196		
Total	53919.129	36			
Corrected Total	41691.193	35			

a. R Squared = .996 (Adjusted R Squared = .995), Dependent Variable:
aged at 5 °C for 12h and storage at 30 °C for 24h

Appendix Table 14 Statistical of volume of solid fat phase in RBO and RBO-AMF at ratio of 75:25 with and without 1% MDG and 1% UMD after aging at 5 °C for 24 h and storage at 30 °C for 12h

Source	Type III Sum of Squares	df	Mean Square	F	Sig.
Corrected Model	46024.043[a]	5	9204.809	866.923	.000
Intercept	19652.302	1	19652.302	1850.883	.000
Trt	46024.043	5	9204.809	866.923	.000
Error	318.534	30	10.618		
Total	65994.879	36			
Corrected Total	46342.577	35			

a. R Squared = .993 (Adjusted R Squared = .992), Dependent Variable:
aged at 5 °C for 24h and storage at 30 °C for 12h

Appendix Table 15 Statistical analysis of volume of solid fat phase in RBO and RBO-AMF at ratio of 75:25 with and without 1% MDG and 1% UMD after aging at 5°C for 24 h and storage at 30°C for 24h

Source	Type III Sum of Squares	df	Mean Square	F	Sig.
Corrected Model	42391.730[a]	5	8478.346	866.288	.000
Intercept	16145.514	1	16145.514	1649.692	.000
Trt	42391.730	5	8478.346	866.288	.000
Error	293.610	30	9.787		
Total	58830.854	36			
Corrected Total	42685.340	35			

a. R Squared = .993 (Adjusted R Squared = .992), Dependent Variable: aged at5°C for 24h and storage at 30°C for 24h

Appendix Table 16 Statistical analysis of T(onset) of first peak of RBO and RBO+1.3% RBW with and without 1% MDG and 1% SP

Source	Type III Sum of Squares	df	Mean Square	F	Sig.
Corrected Model	4.879[a]	3	1.626	5.313	.070
Intercept	4387.034	1	4387.034	14330.860	.000
Trt	4.879	3	1.626	5.313	.070
Error	1.224	4	.306		
Total	4393.138	8			
Corrected Total	6.104	7			

a. R Squared = .799 (Adjusted R Squared = .649), Dependent Variable: T(onset)

Appendix Table 17 Statistical analysis of T(peak) of first peak of RBO and RBO+1.3% RBW with and without 1% MDG and 1% SP

Source	Type III Sum of Squares	df	Mean Square	F	Sig.
Corrected Model	1.270[a]	3	.423	2.776	.175
Intercept	1851.361	1	1851.361	12138.084	.000
Trt	1.270	3	.423	2.776	.175
Error	.610	4	.153		
Total	1853.242	8			
Corrected Total	1.881	7			

a. R Squared = .676 (Adjusted R Squared = .432), Dependent Variable: T(peak)

Appendix Table 18 Statistical analysis of T(end)of first peak of RBO and RBO+1.3% RBW with and without 1% MDG and 1% SP

Source	Type III Sum of Squares	df	Mean Square	F	Sig.
Corrected Model	8.225[a]	3	2.742	24.840	.005
Intercept	560.120	1	560.120	5074.704	.000
Trt	8.225	3	2.742	24.840	.005
Error	.441	4	.110		
Total	568.787	8			
Corrected Total	8.667	7			

a. R Squared = .949 (Adjusted R Squared = .911), Dependent Variable: T(end)

Appendix Table 19 Statistical analysis of temperature range of first peak of RBO and RBO+1.3% RBW with and without 1% MDG and 1% SP

Source	Type III Sum of Squares	df	Mean Square	F	Sig.
Corrected Model	2.617[a]	3	.872	7.105	.044
Intercept	8082.926	1	8082.926	65841.975	.000
Trt	2.617	3	.872	7.105	.044
Error	.491	4	.123		
Total	8086.033	8			
Corrected Total	3.108	7			

a. R Squared = .842 (Adjusted R Squared = .723), Dependent Variable: Temperature range

Appendix Table 20 Statistical analysis of delta H of first peak of RBO and RBO+1.3% RBW with and without 1% MDG and 1% SP

Source	Type III Sum of Squares	df	Mean Square	F	Sig.
Corrected Model	3.183[a]	3	1.061	4.039	.105
Intercept	236.314	1	236.314	899.386	.000
Trt	3.183	3	1.061	4.039	.105
Error	1.051	4	.263		
Total	240.548	8			
Corrected Total	4.234	7			

a. R Squared = .752 (Adjusted R Squared = .566), Dependent Variable: Delta H

Appendix Table 21 Statistical analysis of T(onset) of second peak of RBO+1.3% RBW with and without 1% MDG and 1% SP

Source	Type III Sum of Squares	df	Mean Square	F	Sig.
Corrected Model	21.667[a]	3	7.222	271.614	.000
Intercept	1140.557	1	1140.557	42892.579	.000
trt	21.667	3	7.222	271.614	.000
Error	.106	4	.027		
Total	1162.330	8			
Corrected Total	21.774	7			

a. R Squared = .995 (Adjusted R Squared = .991), Dependent Variable: T(onset)

Appendix Table 22 Statistical analysis of T(peak) of second peak of RBO+1.3% RBW with and without 1% MDG and 1% SP

Source	Type III Sum of Squares	df	Mean Square	F	Sig.
Corrected Model	25.878[a]	3	8.626	40.145	.002
Intercept	2141.230	1	2141.230	9965.285	.000
trt	25.878	3	8.626	40.145	.002
Error	.859	4	.215		
Total	2167.967	8			
Corrected Total	26.737	7			

a. R Squared = .968 (Adjusted R Squared = .944), Dependent Variable: T(peak)

Appendix Table 23 Statistical analysis of T(end)of second peak of RBO+1.3% RBW with and without 1% MDG and 1% SP

Source	Type III Sum of Squares	df	Mean Square	F	Sig.
Corrected Model	6.612[a]	3	2.204	22.345	.006
Intercept	5585.082	1	5585.082	56619.863	.000
trt	6.612	3	2.204	22.345	.006
Error	.395	4	.099		
Total	5592.089	8			
Corrected Total	7.007	7			

a. R Squared = .944 (Adjusted R Squared = .901), Dependent Variable: T(end)

Appendix Table 24 Statistical analysis of temperature range of second peak of RBO+1.3% RBW with and without 1% MDG and 1% SP

Source	Type III Sum of Squares	df	Mean Square	F	Sig.
Corrected Model	9.021[a]	3	3.007	32.186	.003
Intercept	1677.827	1	1677.827	17958.931	.000
trt	9.021	3	3.007	32.186	.003
Error	.374	4	.093		
Total	1687.221	8			
Corrected Total	9.395	7			

a. R Squared = .960 (Adjusted R Squared = .930), Dependent Variable: Temperature range

Appendix Table 25 Statistical analysis of delta H second peak of RBO+1.3% RBW with and without 1% MDG and 1% SP

Source	Type III Sum of Squares	df	Mean Square	F	Sig.
Corrected Model	.902[a]	3	.301	18.608	.008
Intercept	30.233	1	30.233	1870.339	.000
trt	.902	3	.301	18.608	.008
Error	.065	4	.016		
Total	31.200	8			
Corrected Total	.967	7			

a. R Squared = .933 (Adjusted R Squared = .883), Dependent Variable: Delta H

Appendix Table 26 Statistical analysis of solid fat content of RBO+1.3% RBW with and without 1% MDG and 1% SP

Source	Type III Sum of Squares	df	Mean Square	F	Sig.
Corrected Model	2.742[a]	3	.914	112.671	.000
Intercept	937.229	1	937.229	115528.938	.000
trt	2.742	3	.914	112.671	.000
Error	.032	4	.008		
Total	940.003	8			
Corrected Total	2.775	7			

a. R Squared = .988 (Adjusted R Squared = .980), Dependent Variable: solid fat content at 20°C

Appendix Table 27 Statistical analysis by cluster analysis of thermal properties of RBO mixed with 0.65% RBW and/or 1.3% RBW with and without 1% MDG and 1% SP

Cluster Membership

Case	4 Clusters	3 Clusters	2 Clusters
1:RBO	1	1	1
2:RBO+1% MDG	1	1	1
3:RBO+1% SP	2	2	2
4:RBO+1% MDG+1% SP	2	2	2
5:RBO+0.65% RBW	3	3	1
6:RBO+1.3% RBW+1% MDG	4	1	1
7:RBO+0.65% RBW+1% SP	2	2	2
8:RBO+1.3% RBW+1% MDG+1% SP	2	2	2
9:RBO+1.3% RBW	3	3	1
10:RBO+0.65% RBW+1% MDG	4	1	1
11:RBO+0.65% RBW+1% SP	2	2	2
12:RBO+1.3% RBW+1% MDG+1% SP	2	2	2

Appendix Table 28 Statistical analysis of temperatureof structure changing from liquid to solid (cooling step) of RBO mixed with 0.65% RBW and/or 1.3% RBW with and without 1% MDG and 1% SP

Source	Type III Sum of Squares	df	Mean Square	F	Sig.
Corrected Model	551.446[a]	11	50.131	597.185	.000
Intercept	838.097	1	838.097	9983.730	.000
TRT	551.446	11	50.131	597.185	.000
Error	1.007	12	.084		
Total	1390.550	24			
Corrected Total	552.453	23			

a. R Squared = .998 (Adjusted R Squared = .997), Dependent Variable: Temperature

Appendix Table 29 Statistical analysis of time of structure changing from liquid to solid(cooling step) of RBO mixed with 0.65% RBW and/or 1.3% RBW with and without 1% MDG and 1% SP

Source	Type III Sum of Squares	df	Mean Square	F	Sig.
Corrected Model	857848.000[a]	11	77986.182	78.260	.000
Intercept	1.719E8	1	1.719E8	172531.514	.000
TRT	857848.000	11	77986.182	78.260	.000
Error	11958.000	12	996.500		
Total	1.728E8	24			
Corrected Total	869806.000	23			

a. R Squared = .986 (Adjusted R Squared = .974), Dependent Variable: Time

Appendix Table 30 Statistical analysis of temperatureof structure changing from solid to liquid (heating step) of RBO mixed with 0.65% RBW and/or 1.3% RBW with and without 1% MDG and 1% SP

Source	Type III Sum of Squares	df	Mean Square	F	Sig.
Corrected Model	2204.473[a]	11	200.407	141.936	.000
Intercept	2695.580	1	2695.580	1909.119	.000
TRT	2204.473	11	200.407	141.936	.000
Error	16.943	12	1.412		
Total	4916.996	24			
Corrected Total	2221.416	23			

a. R Squared = .992 (Adjusted R Squared = .985), Dependent Variable: Temperature

Appendix Table 31 Statistical analysis of time of structure changing from solid to liquid (heating step) of RBO mixed with 0.65% RBW and/or 1.3% RBW with and without 1% MDG and 1% SP

Source	Type III Sum of Squares	df	Mean Square	F	Sig.
Corrected Model	1969573.458[a]	11	179052.133	137.192	.000
Intercept	5.676E8	1	5.676E8	434885.687	.000
TRT	1969573.458	11	179052.133	137.192	.000
Error	15661.500	12	1305.125		
Total	5.696E8	24			
Corrected Total	1985234.958	23			

a. R Squared = .992 (Adjusted R Squared = .985), Dependent Variable: Time

Appendix Table 32 Statistical analysis of oil-holding capacity time of RBO of RBO mixed with 0.65% RBW and/or 1.3% BW with and without 1% MDG and 1% SP

Source	Type III Sum of Squares	df	Mean Square	F	Sig.
Corrected Model	11033463.240[a]	10	1103346.324	2199453.115	.000
Intercept	1445513.044	1	1445513.044	2881541.451	.000
trt	11033463.240	10	1103346.324	2199453.115	.000
Error	27.591	55	.502		
Total	12479003.875	66			
Corrected Total	11033490.831	65			

a. R Squared = 1.000 (Adjusted R Squared = 1.000), Dependent Variable: time

Appendix Table 33 Statistical analysis of % marinade retention of raw marinated pork steak

Source	Type III Sum of Squares	df	Mean Square	F	Sig.
Corrected Model	927.619[a]	3	309.206	52.968	.000
Intercept	56504.856	1	56504.856	9679.429	.000
trt	927.619	3	309.206	52.968	.000
Error	70.051	12	5.838		
Total	57502.526	16			
Corrected Total	997.671	15			

a. R Squared = .930 (Adjusted R Squared = .912), Dependent Variable: retention

Appendix Table 34 Statistical analysis of % weight loss of grilled marinated pork steak

Source	Type III Sum of Squares	df	Mean Square	F	Sig.
Corrected Model	64.302[a]	3	21.434	12.845	.000
Intercept	13617.120	1	13617.120	8160.219	.000
trt	64.302	3	21.434	12.845	.000
Error	20.025	12	1.669		
Total	13701.446	16			
Corrected Total	84.327	15			

a. R Squared = .763 (Adjusted R Squared = .703), Dependent Variable: cooking loss

Appendix Table 35 Statistical analysis of sensory evaluation in appearance characteristic of raw marinated pork steak

Source	Type III Sum of Squares	df	Mean Square	F	Sig.
Corrected Model	197.660[a]	4	49.415	22.050	.000
Intercept	3457.440	1	3457.440	1542.775	.000
trt	197.660	4	49.415	22.050	.000
Error	212.900	95	2.241		
Total	3868.000	100			
Corrected Total	410.560	99			

a. R Squared = .481 (Adjusted R Squared = .460), Dependent Variable: appearance

Appendix Table 36 Statistical analysis of sensory evaluation in odor characteristic of raw marinated pork steak

Source	Type III Sum of Squares	df	Mean Square	F	Sig.
Corrected Model	15.640[a]	4	3.910	2.500	.048
Intercept	4569.760	1	4569.760	2921.448	.000
trt	15.640	4	3.910	2.500	.048
Error	148.600	95	1.564		
Total	4734.000	100			
Corrected Total	164.240	99			

a. R Squared = .095 (Adjusted R Squared = .057), Dependent Variable: odor

Appendix Table 37 Statistical analysis of sensory evaluation in overall liking characteristic of marinated raw pork steak

Source	Type III Sum of Squares	df	Mean Square	F	Sig.
Corrected Model	110.260[a]	4	27.565	17.354	.000
Intercept	3868.840	1	3868.840	2435.651	.000
trt	110.260	4	27.565	17.354	.000
Error	150.900	95	1.588		
Total	4130.000	100			
Corrected Total	261.160	99			

a. R Squared = .422 (Adjusted R Squared = .398), Dependent Variable: overall liking

Appendix Table 38 Statistical analysis of sensory evaluation in appearance characteristic of grilled marinated pork steak

Source	Type III Sum of Squares	df	Mean Square	F	Sig.
Corrected Model	79.860[a]	4	19.965	8.193	.000
Intercept	3504.640	1	3504.640	1438.189	.000
trt	79.860	4	19.965	8.193	.000
Error	231.500	95	2.437		
Total	3816.000	100			
Corrected Total	311.360	99			

a. R Squared = .256 (Adjusted R Squared = .225), Dependent Variable: appearance

Appendix Table 39 Statistical analysis of sensory evaluation in odor of characteristic of grilled marinated pork steak

Source	Type III Sum of Squares	df	Mean Square	F	Sig.
Corrected Model	15.340[a]	4	3.835	2.253	.069
Intercept	4044.960	1	4044.960	2376.445	.000
trt	15.340	4	3.835	2.253	.069
Error	161.700	95	1.702		
Total	4222.000	100			
Corrected Total	177.040	99			

a. R Squared = .087 (Adjusted R Squared = .048), Dependent Variable: odor

Appendix Table 40 Statistical analysis of sensory evaluation in taste characteristic of grilled marinated pork steak

Source	Type III Sum of Squares	df	Mean Square	F	Sig.
Corrected Model	31.240[a]	4	7.810	5.063	.001
Intercept	4369.210	1	4369.210	2832.309	.000
trt	31.240	4	7.810	5.063	.001
Error	146.550	95	1.543		
Total	4547.000	100			
Corrected Total	177.790	99			

a. R Squared = .176 (Adjusted R Squared = .141), Dependent Variable: taste

Appendix Table 41 Statistical analysis of sensory evaluation in juiciness characteristic of grilled marinated pork steak

Source	Type III Sum of Squares	df	Mean Square	F	Sig.
Corrected Model	10.640[a]	4	2.660	1.577	.187
Intercept	4173.160	1	4173.160	2474.720	.000
trt	10.640	4	2.660	1.577	.187
Error	160.200	95	1.686		
Total	4344.000	100			
Corrected Total	170.840	99			

a. R Squared = .062 (Adjusted R Squared = .023), Dependent Variable: juiciness

Appendix Table 42 Statistical analysis of sensory evaluation in overall liking characteristic of grilled marinated pork steak

Source	Type III Sum of Squares	df	Mean Square	F	Sig.
Corrected Model	39.915[a]	4	9.979	6.432	.000
Intercept	4083.210	1	4083.210	2632.095	.000
trt	39.915	4	9.979	6.432	.000
Error	147.375	95	1.551		
Total	4270.500	100			
Corrected Total	187.290	99			

a. R Squared = .213 (Adjusted R Squared = .180), Dependent Variable: overall

CURRICULUM VITAE

NAME : Miss Natchanok Nukit

BIRTH DATE : January 11, 1981

BIRTH PLACE : Bangkok, Thailand

EDUCATION :

YEAR	INSTITUTION	DEGREE/DIPLOMA
2002	Srinakharinwirot University	B.S. (Food Science and Nutrition)
2006	Kasetsart University	M.S.(Agro-Industrial Product Development)
2012	Kasetsart University	Ph.D. candidate (Food Science)

POSITION/TITLE : -

WORK PLACE : School of Culinary Arts, Suan Dusit Rajabhat University

SCHOLARSHIP : Office of the Higher Education Commission 2009-2013